

March 2016

Diffusion of Polymers in Polyelectrolyte Gels

Anand Rahalkar
University of Massachusetts Amherst

Follow this and additional works at: https://scholarworks.umass.edu/dissertations_2

 Part of the [Polymer and Organic Materials Commons](#)

Recommended Citation

Rahalkar, Anand, "Diffusion of Polymers in Polyelectrolyte Gels" (2016). *Doctoral Dissertations*. 598.
https://scholarworks.umass.edu/dissertations_2/598

This Open Access Dissertation is brought to you for free and open access by the Dissertations and Theses at ScholarWorks@UMass Amherst. It has been accepted for inclusion in Doctoral Dissertations by an authorized administrator of ScholarWorks@UMass Amherst. For more information, please contact scholarworks@library.umass.edu.

**DIFFUSION OF POLYMERS
IN POLYELECTROLYTE GELS**

A Dissertation Presented

by

ANAND ARVIND RAHALKAR

Submitted to the Graduate School of the
University of Massachusetts Amherst in partial fulfillment
of the requirements for the degree of

DOCTOR OF PHILOSOPHY

February 2016

Polymer Science & Engineering

© Copyright by Anand Arvind Rahalkar 2016

All Rights Reserved

DIFFUSION OF POLYMERS IN POLYELECTROLYTE GELS

A Dissertation Presented

by

ANAND ARVIND RAHALKAR

Approved as to style and content by:

Murugappan Muthukumar, Chair

David Hoagland, Member

Harry Bermudez, Member

Lori Goldner, Member

David Hoagland, Department Head
Polymer Science & Engineering

ACKNOWLEDGMENTS

I would like to start my acknowledgments with my advisor, Prof. Muthukumar. His knowledge, vision, and enthusiasm to solve scientific problems has been inspiring. He has been very encouraging and supportive in helping me tackle research problems and the freedom to pursue my research in an independent manner has helped me grow as a scientist.

I would like to thank my committee members, Prof. Hoagland, Prof. Bermudez and Prof. Goldner. The committee has been very helpful with their comments and suggestions. Their questions and discussions were extremely insightful and helped in making progress in the project. I would also like to thank Prof. Goldner for her role in mentoring me with FCS instrumentation, measurements and analysis. Her group has also been very helpful in answering any questions I had with the experiments.

My time in the lab would not be as enriching and fruitful as it has been without the Muthu group members. Over the last five years, I have had the pleasure of learning from many fellow graduate students, and post-docs. In particular, I would like to acknowledge and thank Ben, Sunil, Byoung-Jin, Harsh, Sveta and Michael for their teaching, discussion, and criticism of my research. Our discussions have helped me become a better researcher.

Class of 2010 has been wonderful and made learning a fun experience. They made my transition into the U.S. an enjoyable process. I have also been lucky to have great roommates. I have enjoyed watching movies and sports with them. I would also like to acknowledge the softball teams that I have been a part of in the last five years. The teammates have been great fun to play with and the numerous outings with them after the games were really enjoyable.

My time in Amherst would not have been as pleasant as it has been without the music, theater and movies this university offered, especially Indian classical music performances, MMFF in Spring, and UMass theater.

I have been very fortunate to know some very good cooks over the last 5 years, more importantly, they have been very kind in sharing their preparations with me. In particular I would like to thank Dwaipayan, Madhura and Anish for the excellent meals that I have eaten in my time in Amherst. I am also very grateful to Debashish, who helped me with dinners in the last few hectic months of the PhD.

My undergraduate teachers, especially Prof. Mhaske for being a wonderful mentor and encouraging me to pursue higher education. My undergraduate friends for their support and encouragement. As well as, all members of UD10, for many stimulating conversations on a wide variety of topics.

I would also like to thank Madhura, who has been my best friend in my time in Amherst. I have had the pleasure of learning many things from her, from mythology to movies. I have immensely enjoyed the time exploring the New England as well as this country with her.

I am indebted to my family as their unwavering support and encouragement for higher studies has been very important. I want to thank my grandparents for their stories and words of wisdom, my parents for allowing me to pursue my dreams, and my little sister, who has been an inspiration to me.

ABSTRACT

DIFFUSION OF POLYMERS IN POLYELECTROLYTE GELS

FEBRUARY 2016

ANAND ARVIND RAHALKAR

B.Tech., INSTITUTE OF CHEMICAL TECHNOLOGY, MUMBAI

Ph.D., UNIVERSITY OF MASSACHUSETTS AMHERST

Directed by: Professor Murugappan Muthukumar

Polyelectrolyte gels have the ability to undergo volume transitions in response to external stimuli. As a result, they are used in a wide variety of applications such as sensors, actuators, artificial implants, and controlled drug delivery. In addition, diffusion of trapped macromolecules inside gels is of tremendous significance in drug delivery systems. In this thesis, the dynamics of trapped polyelectrolytes in a polyelectrolyte gel is studied using dynamic light scattering technique. The effect of the crosslink density and the charge density of the gel, as well as of solvent quality and salt concentration are investigated. In general, two distinct diffusive modes (fast and slow) are observed in light scattering experiments. We have discovered that the fast mode corresponds to the gel elasticity and the slow mode corresponds to diffusion of trapped polymer. The deduced diffusion coefficient of the trapped polymer obeys an exponential dependence on the volume fraction of the gel, in accordance with the presence of an entropic barrier for polymer diffusion. In addition, we have monitored

the diffusion of a neutral polymer in polyelectrolyte gels using fluorescence correlation spectroscopy. We demonstrate that the polymer diffusion is considerably slowed down by the gel due to the coupling between polymer dynamics and gel dynamics.

TABLE OF CONTENTS

	Page
ACKNOWLEDGMENTS	iv
ABSTRACT	vi
LIST OF TABLES	xi
LIST OF FIGURES	xii
CHAPTER	
1. INTRODUCTION	1
1.1 Gels	1
1.1.1 Relevance to Biology	2
1.1.2 Drug Delivery Systems	4
1.2 Swelling and Volume Phase Transition of Gels	6
1.2.1 Solvent Quality	7
1.2.2 Effect of Charge Density	8
1.3 Light Scattering of Gels	9
1.3.1 Non-ionic Gels	10
1.3.2 Ionic Gels	11
1.4 Diffusion of Probe in Gels	13
1.5 Summary	16
2. GEL CHARACTERIZATION	17
2.1 Introduction	17
2.1.1 Dynamic Light Scattering	18
2.1.2 Data Analysis for Ergodic Systems	22

2.1.2.1	Inverse Laplace Transformation Analysis	22
2.1.2.2	Multi-Exponential Analysis	22
2.1.3	Data Analysis for non-Ergodic Systems	23
2.2	Experimental Setup	26
2.2.1	Gel Synthesis	26
2.2.2	solid state NMR	29
2.2.3	Swelling Ratio	29
2.2.4	Rheology	30
2.2.5	Dynamic Light Scattering	30
2.2.6	Ultraviolet/Visible Spectroscopy	32
2.2.7	Scanning Electron Microscopy	32
2.3	Results and Discussion	32
2.3.1	solid state NMR	32
2.3.2	Swelling Ratio	33
2.3.3	Rheology	39
2.3.4	Dynamic Light Scattering	40
2.3.5	Ultraviolet/Visible Spectroscopy	48
2.3.6	Scanning Electron Microscopy	48
3.	DIFFUSION OF POLYELECTROLYTES IN	
	POLYELECTROLYTE GELS	49
3.1	Introduction	49
3.2	Experimental Setup	51
3.2.1	Gel Synthesis	51
3.2.2	Sample Preparation	52
3.2.2.1	Dynamic Light Scattering	52
3.2.2.2	Rheology	53
3.3	Results and Discussion	53
3.3.1	Light Scattering at High NaCl Concentrations	54
3.3.2	Light Scattering at Low NaCl Concentrations in Water	60
3.3.3	Characterization of Two Modes	62
3.3.3.1	Swelling Ratio	63
3.3.3.2	Rheology	64
3.3.4	Light Scattering at Low NaCl Concentrations in 55% Acetone + 45% Water mixture	66

3.3.4.1	Diffusion Coefficient of Probe in the Gel.....	69
3.3.4.2	Effect of Crosslink Density	70
3.3.4.3	Effect of Charge Density	72
3.3.4.4	Effect of Volume Fraction	73
3.3.4.5	Effect of Sample Preparation	75
3.4	Conclusion	76
4.	DIFFUSION OF POLYMERS IN POLYELECTROLYTE	
	GELS.....	78
4.1	Introduction	78
4.2	Experimental Setup	80
4.3	Data Analysis	82
4.4	Results and Discussion	84
4.5	Conclusion	95
5.	CONCLUSION AND FUTURE WORK	97
5.1	Future Work	99
	APPENDIX: MATERIALS AND SUPPORTING	
	INFORMATION.....	102
	BIBLIOGRAPHY	107

LIST OF TABLES

Table	Page
2.1 Estimation of number of kuhn segments between crosslinks using modified Flory-Rehner theory (Eq. 2.19) and estimating mesh size of the gel in swollen state using Eq. 2.22	37
2.2 Estimation of the mesh size of the gel in NaPSS + 55% acetone + NaCl solution using Eq. 2.23	39
3.1 Comparison of diffusion coefficient from light scattering experiments for the 10C2.7Xl gel in 100 mM NaCl solution, NaPSS in 100 mM NaCl solution and 10C2.7Xl gel + NaPSS in 100 mM NaCl solution	59
3.2 Comparison of diffusion coefficient from light scattering experiments and diffusion coefficient estimated using Eq. 3.3.....	65
A.1 List of materials used in this thesis.	102
A.2 Debye length for given NaCl concentration in 55% Acetone and 45% Water mixture.	104
A.3 Hydrodynamic radius of NaPSS and Dextran for given NaCl concentration in 55% Acetone and 45% Water mixture.	104

LIST OF FIGURES

Figure	Page	
1.1	Different drug release mechanisms for a drug encapsulated in a hydrogel carrier. Figure from Ref. (Peppas et al., 2006). With permission.	5
1.2	Volume phase transition of PAM-PAA gels as a function of salt concentration. Different curves represent different ratios of Acetone concentration in water. As the Acetone concentration of the solvent increases, the amount of salt required for phase transition decreases. The phase transition is continuous for lower Acetone concentrations, but discrete for higher Acetone concentrations . Figure from Ref. (Ohmine and Tanaka, 1982). With permission.	9
2.1	Schematic for the autocorrelation function $g_2(\tau) - 1$ vs. lag time τ	19
2.2	a. (Top) An example of the autocorrelation function $g_1(\tau)$ vs. lag time τ . (Bottom) Plot of Γ vs. q^2 . The slope of the line passing through origin is D as defined in Eq. 2.5.	20
2.3	(Top) Example for the autocorrelation function $g_2(\tau) - 1$ vs. τ . Two distinct diffusive modes are observed. (Bottom) From the plot of Γ vs. q^2 for each mode, the respective diffusion coefficients are obtained.	21
2.4	Reaction scheme of synthesis of Poly(acrylamide-co-sodium acrylate) gel.	29
2.5	ssNMR of the 10C2.7Xl PAM-PAA gel. The chemical shift for acrylamide group is 180 ppm and that for acrylate group is 184 ppm labeled 5 and 6 respectively. The relative ratio of the area under curve of the acrylate and the acrylamide groups is 10%.	33

2.6	Volume transition of 10C2.7Xl PAM-PAA gel in presence of 55% acetone solution at 11 mM NaCl concentration. The gel does not collapse at 11 ml NaCl concentration in presence of water as solution. Inset shows the volume fraction of the gel when the gel is not yet collapsed.	34
2.7	Effect on swelling of gel as a function of NaCl concentration. As more salt is added to the system, the Donnan contribution decreases resulting in deswelling of the gel. Thus the volume fraction (ϕ) increases as more salt is added	36
2.8	Effect on swelling of gel as a function of NaCl concentration in 55% Acetone solution for gels of same charge density (10%) but different crosslink density (2.7% and 3.5%). As more salt is added to the system, the Donnan contribution decreases. Thus the volume fraction (ϕ) increases as more salt is added. Higher crosslink density gel, has higher volume fraction at all NaCl concentrations.	36
2.9	Effect on swelling of gel as a function of NaPSS and NaCl concentration. NaPSS concentration is kept constant at 5 mg/ml (24 mM monomer concentration). As more salt is added to the system, the Donnan contribution decreases resulting in deswelling of the gel. Thus the volume fraction (ϕ) increases as more salt is added	37
2.10	Effect on modulus of gel as a function of NaCl concentration for the same gel (10C2.7Xl). As more salt is added to the system, the gel deswells and its volume fraction increases. Hence adding NaCl, increases the modulus of the gel.	40
2.11	a. Correlation function for the 10C2.7Xl gel + 100 mM NaCl solution. The correlation function is fitted with a single exponential decay. b. The accuracy of the fit can be seen from the residuals. c. The plot of Γ vs. q^2 is shown. The slope of the fit is the diffusion coefficient of the gel.	41
2.12	Correlation function for the 10C2.7Xl gel + 10 mM NaCl solution. The correlation function is fitted with a two exponential decays. The accuracy of the fit can be seen from the residuals.	43
2.13	Diffusion coefficient for the 10C2.7Xl gel + NaCl solution. The diffusion coefficient decreases as NaCl is added to the solution.	44

2.14	The dependence of the friction coefficient with the volume fraction of the gel. Friction coefficient is represented as the ratio G/D from Eq. 2.8.	44
2.15	Correlation function for the 10C2.7Xl gel + 55% acetone + 6 mM NaCl solution. The correlation function is fitted with a two exponential decays. The accuracy of the fit can be seen from the residuals.	46
2.16	Diffusion coefficient for the 10C2.7Xl gel + 55% acetone + NaCl solution and the 10C3.5Xl gel + 55% acetone + NaCl solution. The diffusion coefficient decreases as NaCl is added to the solution. Just before the volume phase transition, the diffusion coefficient of the gel decreases by two orders of magnitude. Higher crosslink density gel collapses at higher salt concentration.	47
2.17	UV-Vis spectra for the PAM-PAA gel. The gel does not absorb in visible region, and has an absorption peak in UV region near 220 nm.	48
2.18	SEM image of 10C2-7Xl PAM-PAA gel. The mesh size range from the image is 40 to 150 nm.	48
3.1	Light scattering data for the NaPSS127k (1 mg/ml) + 100 mM NaCl. (Top) Correlation function with one diffusive mode. Black line corresponds to the correlation function and the red line is the data fitting for single mode; (Middle) Residuals of the single mode data fitting. (Bottom) The diffusion coefficient is calculated from the slope of the linear fit of Γ vs. q^2 plot.	55
3.2	Light scattering data for the 10C2-7Xl gel + NaPSS127k (1 mg/ml) + 100 mM NaCl. (Top) Correlation function with two diffusive modes. Black line corresponds to the correlation function and the red line is the data fitting for two modes; (Middle) Residuals of the two mode data fitting. (Bottom) The diffusion coefficient is calculated from the slope of the linear fit of Γ vs. q^2 plot for both modes. Both modes have a q^2 dependence.	56

3.3 Comparison of correlation function and diffusive modes for the gel and the probe individually and when combined together. The first column represents correlation functions for samples 10C2.7Xl + 100 mM NaCl, NaPSS127k (1 mg/ml) + 100 mM NaCl and 10C2.7Xl + NaPSS127k (1 mg/ml) + 100 mM NaCl respectively. The second and third columns are Γ vs. q^2 plots for the same samples. (First Row) 10C2.7Xl + 100 mM NaCl (left) Correlation function with one diffusive mode. Black line corresponds to the correlation function and the red line is the data fitting for single mode; (right) The diffusion coefficient is calculated from the slope of the linear fit of Γ vs. q^2 plot. (Second Row) NaPSS127k (1 mg/ml) + 100 mM NaCl (left) Correlation function with one diffusive mode. Black line corresponds to the correlation function and the red line is the data fitting for single mode; (right) The diffusion coefficient is calculated from the slope of the linear fit of Γ vs. q^2 plot. (Third Row) 10C2.7Xl + NaPSS127k (1 mg/ml) + 100 mM NaCl (left) Correlation function with two diffusive modes. Black line corresponds to the correlation function and the red line is the data fitting for two modes; (middle and right) The diffusion coefficient is calculated from the slope of the linear fit of Γ vs. q^2 plot for each mode.....58

3.4	<p>Comparison of correlation function and diffusive modes for the gel and the probe individually and when combined together at 10 mM NaCl concentration. The first column represents correlation functions for samples 10C2.7Xl + 10 mM NaCl, NaPSS127k (5 mg/ml) + 10 mM NaCl and 10C2.7Xl + NaPSS127k (5 mg/ml) + 10 mM NaCl respectively. The second and third columns are Γ vs. q^2 plots for the same samples. (First Row) 10C2.7Xl + 10 mM NaCl (left) Correlation function with two modes. Black line corresponds to the correlation function and the red line is the data fitting for two modes; (middle and right) The diffusion coefficient is calculated from the slope of the linear fit of Γ vs. q^2 plot. The second mode does not have a q^2 dependence. (Second Row) NaPSS127k (5 mg/ml) + 10 mM NaCl (left) Correlation function with two diffusive modes. Black line corresponds to the correlation function and the red line is the data fitting for two modes; (middle and right) The diffusion coefficient is calculated from the slope of the linear fit of Γ vs. q^2 plot for each mode. (Third Row) 10C2.7Xl + NaPSS127k (5 mg/ml) + 10 mM NaCl (left) Correlation function with two diffusive modes. Black line corresponds to the correlation function and the red line is the data fitting for three modes; (middle and right) The diffusion coefficient is calculated from the slope of the linear fit of Γ vs. q^2 plot for each mode (Third mode does not have a q^2 dependence is not shown).....</p>	61
3.5	<p>Effect on swelling of gel as a function of NaPSS and NaCl concentration. NaPSS concentration is kept constant at 5 mg/ml (24 mM monomer concentration). As more salt is added to the system, the Donnan potential decreases resulting in deswelling of the gel. Thus the volume fraction (ϕ) increases as more salt is added</p>	63
3.6	<p>Rheology data for the 10C2.7Xl gel + NaPSS127k (5mg/ml) + NaCl.</p>	64

3.7	Comparison of correlation function and diffusive modes for the gel and the probe invidually and when combined together in 55% Acetone + 6 mM NaCl concentration. The first column represents correlation functions for samples 10C2.7Xl + 55% Acetone + 6 mM NaCl, NaPSS127k (5 mg/ml) + 55% Acetone + 6 mM NaCl, and 10C2.7Xl + 55% Acetone + 6 mM NaCl respectively. The second and third columns are Γ vs. q^2 plots for the same samples. (First Row) 10C2.7Xl + 55% Acetone + 6 mM NaCl (left) Correlation function with two modes. Black line corresponds to the correlation function and the red line is the data fitting for two modes; (middle and right) The diffusion coefficient is calculated from the slope of the linear fit of Γ vs. q^2 plot. The second mode does not have a q^2 dependence. (Second Row) NaPSS127k (5 mg/ml) + 55% Acetone + 6 mM NaCl (left) Correlation function with two diffusive modes. Black line corresponds to the correlation function and the red line is the data fitting for two modes; (middle and right) The diffusion coefficient is calculated from the slope of the linear fit of Γ vs. q^2 plot for each mode. (Third Row) 10C2.7Xl + NaPSS127k (5 mg/ml) + 55% Acetone + 6 mM NaCl (left) Correlation function with two diffusive modes. Black line corresponds to the correlation function and the red line is the data fitting for three modes; (middle and right) The diffusion coefficient is calculated from the slope of the linear fit of Γ vs. q^2 plot for each mode (Third mode does not have a q^2 dependence is not shown).	67
3.8	Diffusion coefficient of NaPSS alone in 55% Acetone + NaCl solution. Two diffusive modes are reported.	68
3.9	Diffusion coefficient of the 10C2.7Xl gel in NaPSS + 55% Acetone + NaCl solution. Effect of molecular weight of NaPSS and NaCl concentration of gel diffusion is shown. The gel diffusion coefficient is similar to that in absence of NaPSS.	69
3.10	Diffusion coefficient of NaPSS diffusion in the 10C2.7Xl gel in 55% Acetone + NaCl solution. Effect of molecular weight of NaPSS and NaCl concentration of probe diffusion is shown.	70
3.11	Diffusion coefficient of NaPSS diffusion in the 10C3.5Xl gel in 55% Acetone + NaCl solution. Effect of molecular weight of NaPSS and NaCl concentration of probe diffusion is shown.	71
3.12	Diffusion coefficient of NaPSS diffusion in the 5C2.7Xl gel in 55% Acetone + NaCl solution. Effect of molecular weight of NaPSS and NaCl concentration of probe diffusion is shown.	72

3.13	Diffusion coefficient of NaPSS in the gel in 55% Acetone + NaCl solution normalized by diffusion coefficient of NaPSS in the 55% Acetone + NaCl solution. The normalized diffusion coefficient is linear to volume fraction ϕ in the semi-log plot.	74
3.14	Diffusion coefficient of NaPSS in the gel in 55% Acetone + NaCl solution is compared for two different sample preparation methods. The diffusion coefficients obtained from both methods are reasonably within error.	76
4.1	Schematic of FCS setup. Reproduced with permission from Ref. (Gamari et al., 2014). Copyright 2014, American Association of Physics Teachers.	80
4.2	Fit for the normalized correlation function (black) of Dextran 12k (10 nM) diffusing in water, one parameter (τ) model fit is shown (red). Residuals for the one parameter model, for fitting the correlation function is shown.	83
4.3	Fit for the normalized correlation function using various diffusion models, one parameter (τ), two parameters (τ and α) and four parameters (τ_1 , α_1 , and τ_2 , α_2). Residuals for the four parameter model, for fitting the correlation function is shown. Correlation function of Dextran diffusing in 10C3.5Xl gel in 55% acetone solution and 1 mM NaCl.	84
4.4	Diffusion time (τ) of probe (Dextran) in 10C2.7Xl gel vs. NaCl concentration, in absence of acetone. As the NaCl concentration increases, the diffusion time of the probe in the gel increases.	85
4.5	Stretched exponential parameter (α) for diffusion of Dextran in 10C2.7Xl gel vs. NaCl concentration, in absence of acetone. As the NaCl concentration increases, α remains constant and is near 1. Two parameter model, for the diffusion time (τ) and stretched exponential factor (α) are used as shown in Eq. 4.4.	85

4.6	Comparison of three experiments on the three different samples for the same composition of the gel, solvent and NaCl concentration. (Top) The correlation function is for Dextran diffusing in the 10C3.5Xl gel with 55% acetone and 9 mM NaCl. (Middle) The plots the residuals of the fit for the correlation function shown above. The residual for the fit of the correlation function is represented by the same color. (Bottom) The plot of <i>Residuals/(uncertainty in the data)</i> for the above fits. The lines are represented by the same color as their respective correlation functions in the top figure.	87
4.7	Stretched exponential parameter (α_1) for Dextran diffusion in 10C2.7Xl gel and 10C3.5Xl gel vs. NaCl concentration in presence of 55% Acetone solution. At all NaCl concentration, α_1 remains constant at 1.	88
4.8	Faster diffusion time (τ_1) of probe (Dextran) diffusion in 10C2.7Xl gel and 10C3.5Xl gel vs. NaCl concentration in presence of 55% Acetone solution. Probe diffusion in both the gels is slower than in the solution at all NaCl concentrations. At higher NaCl concentrations, the diffusion time of the probe increases.	89
4.9	Diffusion coefficient for the 10C2.7Xl gel + 55% acetone + NaCl solution and the 10C3.5Xl gel + 55% acetone + NaCl solution. The diffusion coefficient decreases as NaCl is added to the solution. Just before the volume phase transition, the diffusion coefficient of the gel decreases by two orders of magnitude. Higher crosslink density gel collapses at higher salt concentration.	90
4.10	Diffusion coefficient of probe (Dextran) in 10C2.7Xl gel and 10C3.5Xl gel vs. NaCl concentration in presence of 55% Acetone solution. As the NaCl concentration increases, the diffusion coefficient of the probe decreases.	91
4.11	Slower diffusion time (τ_2) of probe (Dextran) diffusion in 10C2.7Xl gel and 10C3.5Xl gel vs. NaCl concentration in presence of 55% Acetone solution. At higher NaCl concentrations, the diffusion time of the probe increases.	92
4.12	Stretched exponential parameter (α_2) for Dextran diffusion in 10C2.7Xl gel and 10C3.5Xl gel vs. NaCl concentration in presence of 55% Acetone solution. α_2 is less than 1 at all NaCl concentration.	93

4.13	Coefficient for the diffusion time (τ_1) as a function of NaCl concentration. Data for 10C2.7Xl gel and 10C3.5Xl gel with 55% acetone and NaCl is shown.	94
A.1	UV-Vis absorbance spectra for the 10C2.7Xl gel + NaPSS. The methyleneblue tagged NaPSS (NaPSS-MB) is present inside the gel.	103
A.2	The effect of equilibration time on the correlation functions obtained from light scattering is shown. The gel was synthesized inside the light scattering tube and NaPSS127k (1 mg/ml) + 100 mM NaCl solution was added to the gel. Black and Green - Equilibrated for two days. Blue - Equilibrated for two weeks. The correlation function shifts and the diffusion coefficient changes as a result.....	105
A.3	Γ vs. q^2 plot for the second mode for DLS of 10C2.7Xl gel + NaPSS + 55% Acetone + 45% Water. (First Row) (Left) NaPSS 16k (Right) NaPSS 30k. (Second Row) (Left) NaPSS 70k (Right) NaPSS 127k.	105
A.4	Γ vs. q^2 plot for the second mode for DLS of 10C3.5Xl gel + NaPSS + 55% Acetone + 45% Water . (First Row) (Left) NaPSS 16k (Right) NaPSS 30k. (Second Row) (Left) NaPSS 70k (Right) NaPSS 127k.	106
A.5	Γ vs. q^2 plot for the second mode for DLS of 5C2.7Xl gel + NaPSS + 55% Acetone + 45% Water. (First Row) (Left) NaPSS 16k (Right) NaPSS 30k. (Second Row) (Left) NaPSS 70k (Right) NaPSS 127k.	106

CHAPTER 1

INTRODUCTION

Gels are ubiquitous in nature and particularly in biological aspects. A gel is a polymer network, which is usually swollen in a solvent. When the gel is swollen in water as a solvent, it is known as a hydrogel. Hydrogels form an important class of gels as they resemble biological systems and have many applications in biological environments. Hydrogels are used in biological applications because of their high water content, biocompatibility and ability to tune the properties as per requirement of application (Lee, and Mooney, 2001). Understanding transport properties of biomacromolecules in these biological materials is important to gain insights into their functioning (Ellis, 2001). Diffusion of polymers in gels have is a vital aspect of controlled drug delivery systems (Gosch and Rigler, 2005; Peppas et al., 2000) as well as other applications such as separation processes etc. In the following discussion, first the gel and its properties are discussed, followed by relevance of gels in biological and drug delivery systems. Later, the swelling of the gel and its light scattering properties (key analytical tool used in this thesis) is discussed. This chapter concludes with discussion of literature for diffusion of polymers in concentrated solutions and gel networks.

1.1 Gels

For a neutral gel, the swelling property arises from favorable interaction with the solvent, and entropy of solvent molecules, while the crosslinks present in the network resist swelling. The gel is a giant single polymer molecule, which does not undergo translational diffusion, however the network strands can have limited move-

ment along its mean position, while the solute inside the gel is free to diffuse. The gel is a viscoelastic material, and usually for chemically crosslinked networks, its elastic component is dominant. If a charged monomer is used in gel synthesis, the gel is known as a polyelectrolyte gel. In polyelectrolyte gels, along with the factors that contribute to gel swelling of a neutral gel, the osmotic pressure of counterion ions contributes to gel swelling. Depending on the nature of the gel, the network can be swollen orders of magnitude compared to its dry state. Polyelectrolyte gels swell more than neutral gels and also undergo a drastic volume transition compared to neutral gel (discussed in section 1.2). This has led to many biomedical applications, such as drug delivery systems and tissue engineering. Hydrogels can undergo volume phase transitions, decreasing the volume of the gel by orders of magnitude, in response to external stimuli such as solvent, temperature, pH, electric field, salt for ionic gels etc. This volume transition can either be continuous over the range of stimuli applied or a discontinuous transition where the gel collapses at a critical stimulus level. As a result, in last few decades, hydrogels have generated huge interest in the scientific community due to the ability to undergo a volume transition when an external stimuli is applied because of their potential applications in various field such as sensors, actuators, artificial biological implants, drug delivery systems etc.

1.1.1 Relevance to Biology

In biology, the gel has many applications as well as many biological systems resemble a gel network. The cell in a simplistic model can be explained as swollen polymer gel inside the cell membrane. The cytoplasm has been explained as a gel, which contains many components such as small molecules, proteins, water and organelles (Luby-Phelps, 1994). The cell responds to external stimuli such as that of ion flow, which depends on the ion concentration inside and outside the cell. In these

processes the Donnan equilibrium is important in controlling the potential across the cell membrane due to concentration difference of the ions. Another important example of an polyelectrolyte gel in biology is vitreous humor. The vitreous humor is a transparent gel inside the eye, which provide mechanical strength and protection to the eye. The vitreous contains collagen fibers and hyaluronic acid macromolecules, making it a complex polyelectrolyte gel (Bishop, 2000). Multiple components contribute to tuning the properties of the gel such as the crosslink density to control the modulus, the swelling of the gel in the solvent controls the volume fraction of the gel and the charge density controls the contribution of ions to osmotic pressure.

In cellular environments, macromolecules often have to diffuse in crowded environments. The cell contains many species such as high concentrations of proteins, nucleic acids and other structures, which influence the diffusion of these macromolecules. It was shown by Marsh and coworkers that although the cytoplasm looks unstructured, with organelles, cytoskeleton and macromolecules distributed inside it, it has different size scales present (from μm size scales to in order of 100 nm size scale (Marsh et al., 2001; Alberts et al., 1994)). It was shown by several researchers that the diffusion of a particle inside the cytoplasm slows down considerably compared diffusion in solution. It was also observed that particles greater than 25 – 30 nm were rendered immobile inside the cytoplasm (Luby-Phelps, D. and F., 1986; Luby-Phelps et al., 1987; Seksek, Biwersi and Verkman, 1997; Arrio-Dupont et al., 2000; Saxton, 1994). These processes are also likely to affect other important cellular functions, such as translocation process, gene therapy (Guthold et al., 1999), signal transductions (Pederson, 2000; Cluzel, Surette and Leibler, 2000), embryogenesis (Crick, 1970) protein assembly and folding etc. Studying such systems is a challenging task that has potential applications in many biological processes. However, it should be noted that the biological systems discussed above have bigger dimensions than the mesh size of

the gels which are discussed in this thesis (mesh size of the gel is discussed in the next chapter). The next discussion of drug delivery systems offers a more relevant size scale to that of the mesh size of the gel in this study.

These complex biological systems have many components present and to fully understand them experimentally is quite difficult. The important physical aspects of these systems, such as the modulus of the network, the charge interaction of species and diffusion properties in them, can be modeled using a simpler synthetic system such as a chemically crosslinked gel. A synthetic gel offers a tool set to control its properties and to replicate these complex biological analogues by controlling the competing forces inside them (entropic, elastic, osmotic and electrostatic). An example of such a synthetic material is a polyelectrolyte gel whose modulus, swelling and charge density can be controlled. The gel can be swollen in water, in a salt water solution or mixture of solvents, depending on the application desired. Monomers and comonomers as well as the amount of crosslinker can be used in various ratios to tune the elastic modulus of the gel, charge density of the gel and consequently the gel swelling. Thus, many researchers have tried to study model systems of polymers in concentrated solutions as well as in gels in order to understand fundamentals of diffusion in constrained environments.

1.1.2 Drug Delivery Systems

In non-cellular systems, diffusion of macromolecules in networks has many applications ranging from chromatography to various separation processes. One of the major applications is improving the efficiency of the drug delivery systems in which the diffusion of the drug to the intended target is in controlled fashion. There are

many mechanisms for drug delivery as shown in Fig. 1.1.

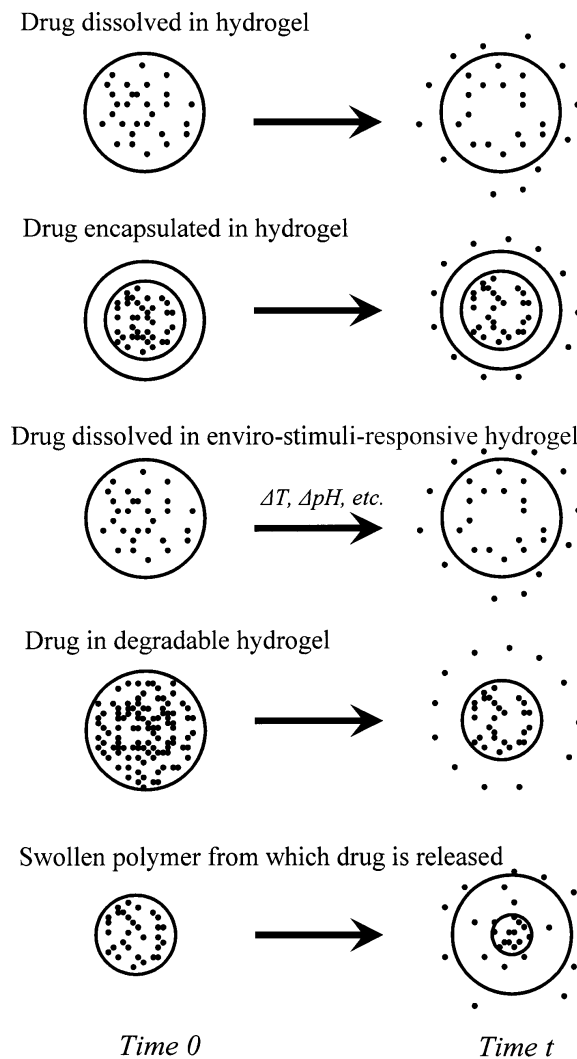


Figure 1.1. Different drug release mechanisms for a drug encapsulated in a hydrogel carrier. Figure from Ref. (Peppas et al., 2006). With permission.

The choice of carrier needs to be selected on the mechanism through which the drug needs to be released. Factors, such as concentration of the drug, the residence time of the carrier and the diffusion constant of the drug through the hydrogel carrier will determine its final dosage. The rate of drug release depends on these facts as well as on the kinetics of gel swelling. Thus it is important to relate the diffusion of probes with the swelling of the gel. In this thesis, the factors affecting the diffusion

constant of polymers in the gels is studied. In most drug delivery systems, the drug will be encapsulated inside the carrier. The carrier, in this case a gel, should have a response to external factors, such as temperature, pH, salt concentration etc. such that when that external stimuli is applied, the gel will expand releasing the captured drug to its intended target (Peppas et al., 2006). Designing such molecules is a difficult task, as the gel carrier needs to be resistant to other external factors which it encounters before the intended target of the drug is reached. Another important aspect of targeted drug delivery is in molecular recognition i.e. the carrier attaches to a specific target based on molecular recognition detectors present in the gel and releases the drug at an active site (Peppas, Hansen and Buri, 1984; Peppas and Sahlin, 1996; Hilt and Byrne, 2004; Byrne, Park and Peppas, 2002). In these systems, the along with drug delivery, bioadhesion is also an important factor. One of the most commonly studied drug delivery carrier is derivatives of Poly N-isopropyl acrylamide (PNIPAM) because of its phase transition (lower critical solution temperature) is near that of human body temperature (37°C), making them an ideal in vivo candidate. Other synthetic hydrogels such as Polyethylene glycol, Polymethacrylate derivatives, Poly(vinyl alcohol), Polyacrylamide etc. have been used recently in drug delivery and biomedical applications.

1.2 Swelling and Volume Phase Transition of Gels

The dynamics of polymers inside the gel is controlled by the local environment of the gel network. The properties of the gel network are dictated by the mesh size, which in turn depends on the extent of the gel swelling. Many factors contribute to gel swelling and deswelling, such as the solvent quality, crosslink density and charge density of the gel, salt concentration for ionic gels etc. In the following sections, the swelling and volume transition of the gel is discussed with respect to these factors.

1.2.1 Solvent Quality

The swelling and volume phase transition of a polymer gel leading to collapse of the gel, is essentially described by balancing the entropic, enthalpic and elastic forces of an uncharged gel and additional component of osmotic pressure of ions for a charged gel. Thus, keeping other parameters constant, the gel can be swollen or shrunk by changing the χ parameter between the gel and the solvent. Depending on the mismatch of the gel and solvent, the gel can undergo a continuous volume phase transition or a discontinuous volume phase transition by changing the amount of cosolvent of the solution. Similarly, keeping the solvent quality fixed, the effective χ parameter can be changed by changing the temperature of the system. The PNIPAM gel, undergoes re-entrant phase transition phenomena, the gel collapses in 33% DMSO and reswells when DMSO is greater than 90% (Ricka and Tanaka, 1984; Katayama, Hirokawa and Tanaka, 1984; Hirokawa and Tanaka, 1984). The concentration of DMSO at which the phase transition occurs can be controlled by changing the crosslink density of the gel. Another non-ionic gel PAM, does not undergo volume phase transition in water-DMSO mixture of any concentration (Ricka and Tanaka, 1984). The difference between these two gels for the same solvent is due to different elastic and enthalpic forces for the gel and its interaction with the solvent (Tanaka, 1978). The exact expression for the osmotic pressure of the gel in equilibrium, is given in next chapter for the Poly(acrylamide-co-acrylic acid) PAM-PAA gel system that is used in this thesis. Tanaka and coworkers also studied effect of solvent composition for charged gels (Katayama, Hirokawa and Tanaka, 1984). The the onset of transition, its re-entrant phenomena as well as the discontinuous nature of transition was observed to depend on the charge density of the gels, temperature of the system and solvent quality. Mccoy et al. also studied the effect of solvent quality on non-ionic as well as ionic gels in presence of salt and observed that PAM-PAA gel undergoes discontinuous volume transition for 55% acetone (water) and in presence of salt concentration, but

the non-ionic PAM gel does not collapse at same salt concentration (McCoy and Muthukumar, 2010).

1.2.2 Effect of Charge Density

Tanaka pioneered the work in establishing volume transition and swelling ratios for ionic and non-ionic gels. He observed that the gels undergo volume phase transition in presence of an unfavorable solvent, and when salt is added to ionic gels. For PAM-PAA gels, the ratio of water-acetone at which the gels collapsed was related to the charge density of the gel. In absence of charges, the gel would undergo a continuous volume transition (Hirotsu, Hirokawa and Tanaka, 1987). Similarly, for ionic charges, the in presence of acetone-water mixtures, the gel will collapse as the salt is added to the solution (McCoy and Muthukumar, 2010), decreasing the effective χ parameter of the gel-solvent interaction. The swelling of the gel can also be controlled by changing the temperature of the system, McCoy et al. observed the effect of temperature on the diffusion coefficient of the PAM-PAA gel (McCoy and Muthukumar, 2010). Another gel system PNIPAM, has also been studied extensively. The gel undergoes a volume phase transition at upon increasing the temperature. The non-ionic as well as ionic gel (PolyN-isopropylacrylamide-Polyacrylic acid (PNIPAM-PAA)) were studied near its volume transition. They observed that the ionic gel has heterogeneous structure while the non-ionic gel has homogeneous structure (Tokuhiko et al., 1991).

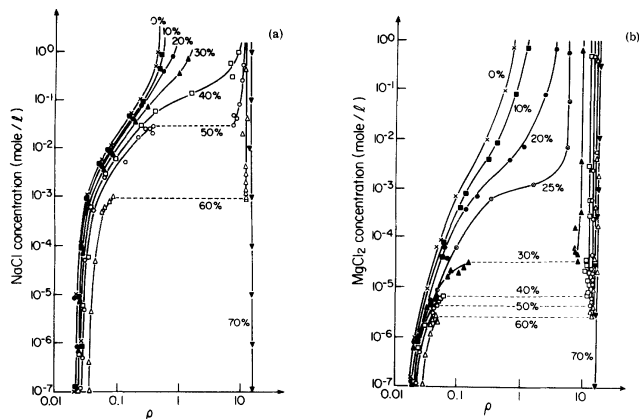


Figure 1.2. Volume phase transition of PAM-PAA gels as a function of salt concentration. Different curves represent different ratios of Acetone concentration in water. As the Acetone concentration of the solvent increases, the amount of salt required for phase transition decreases. The phase transition is continuous for lower Acetone concentrations, but discrete for higher Acetone concentrations. Figure from Ref. (Ohmine and Tanaka, 1982). With permission.

1.3 Light Scattering of Gels

Extensive experiments have been performed to study the dynamic and static structure of the gels using light scattering. The scattering intensity has two contributions: the dynamic component from fluctuations of the gel network and the static component from the gel heterogeneities. Many researchers have related the dynamic component to the osmotic compressibility which relates to the osmotic modulus of the gel (Schosseler, Ilmain and Candau, 1991; Horkay, Hecht and Geissler, 1994; Geissler, Horkay and Hecht, 1991). The scattering arising from the gel heterogeneity results in non-ergodic behavior of the gels. As a result many analysis techniques have been developed for DLS of gels. There is considerable difference in light scattering of ionic and non-ionic gels, primarily due to low volume fractions of ionic gels because of gel swelling. For non-ionic gels, the mesh size is calculated from Stokes-Einstein equa-

tion, while for ionic gels it was shown that this approximation is not valid (McCoy and Muthukumar, 2010).

1.3.1 Non-ionic Gels

Tanaka and coworkers did dynamic light scattering measurements on gels and also provided a detailed theory to interpret the diffusion coefficient results (Tanaka, Hocker and Benedek, 1973). They related the forces due to the displacement vector of a network strand to its modulus and friction coefficient, providing a relationship between the diffusion coefficient of the gel, its bulk modulus and friction coefficient. Even though the gels that they analyzed were non-ergodic in nature, they assumed that only the fluctuating part of the intensity contributed to the dynamic structure factor and analyzed the correlation function using ergodic analysis. They measured the diffusion coefficient of the gel in order of 10^{-7} cm²/s and thus calculated the mesh size using Stokes-Einstein equation, in the range of 2 – 10 nm. In non-ionic gels, using Stokes-Einstein equation to calculate the mesh size is known to give a good approximation. Many other researchers have tried to relate the diffusion coefficient or the mesh size to the concentration of the polymer, and compare it with deGennes prediction of C^* theorem, of $\xi \sim C^{3/4}$ (de Gennes. P. G., 1979; Candau, Bastide and Delsanti, 1982; Hecht and Geissler, 1978; Takebe et al., 1989). Fang and coworkers also studied the relationship of the correlation length and osmotic modulus with the gel crosslinking, the concentration of gel and temperature (Fang, Brown and Konk, 1990).

When the gel is swollen from the prepared state, the mesh expands non-uniformly, creating heterogeneity in the gel (Furukawa et al., 2003). Zhao and Wu, studied the heterogeneity in the PNIPAM and suggested that the heterogeneity correspond to large voids in the gels, which are more dominant when the gel is swollen

(Yue and Chi, 2004). Shibayama and other researchers have also studied poly(N-isopropyl acrylamide) (PNIPAM) (Shibayama and Tanaka, 1995; Shibayama et al., 1996; Shibayama, Shirotani and Shiwa, 2000; Ricka and Tanaka, 1984). The presence of hydrophobic N-isopropyl group creates heterogeneity in the gel, and it undergoes lower critical solution temperature (LCST). Light scattering studies of this gels have reported similar behavior to polyacrylamide gels. Their diffusion coefficient is also reported in the same order of magnitude as PAM gels, suggesting that they have similar mesh size to PAM gels (2 – 10 nm) (Shibayama et al., 1999).

It has been shown that both PNIPAM and PAM gels have heterogeneities (Joosten, McCarthy and Pusey, 1991; Norisuye et al., 2004) and behave as non-ergodic media, and thus different analysis methods have been developed to analyze their light scattering data (Joosten, McCarthy and Pusey, 1991; Pusey and Megen, 1989; Pusey, 1994). These analysis methods describe the non-ergodic nature of the gel, and are used to find the diffusion coefficient of such an system. The methods are discussed in greater detail in the next chapter.

1.3.2 Ionic Gels

Many research groups have studied the structural changes in ionic gels using scattering techniques for the effect of temperature, salt concentration and pH. Tanaka and Shibayama observed a LCST behavior, using swelling measurements by changing the temperature for PNIPAM-PAA gel. The phase transition was reported due to hydrophobic nature of the pendant groups. These gels are heterogeneous in nature, and their microstructure has been studied using neutron scattering. As a result, the local gel concentration fluctuates resulting in different time averaged scattering intensity and ensemble averaged scattering intensity, establishing non-ergodic nature of these gels. The system that we intend on working with is Polyacrylamide-co-poly(acrylic

acid) (PAM-PAA) (or the sodium salt of the acid). PAM-PAA gels behave quite differently compared to the PNIPAM-PAA gels primarily due to the hydrophobic backbone of n-isopropyl acrylamide. It was shown that ionization of polyacrylamide leads to less heterogeneous nature of the gels.

Light scattering of ionic poly(acrylic acid) gels have been studied previously using both dynamic and static light scattering. Static light scattering was used by Schosseler and coworkers to find the osmotic modulus of the gel from scattering intensity at zero q ($q \rightarrow 0$). They also observed that the ratio of osmotic modulus to the shear modulus (measured from rheology) was constant for gels for various salt concentrations at low ionization degree. Dynamic light scattering of these gels was done by Moussaid and coworkers who studied the effect of concentration and degree of ionization on the cooperative diffusion coefficient of the gels and its uncrosslinked solutions. They observed that these gels can be considered as ergodic media as no large scale heterogeneity were observed in light scattering. Neutron scattering measurements also supported this argument of no large scale heterogeneity were present in the these gels. However, the non-ergodic nature of these gels was observed at high crosslink density and at low charge density. This has also been observed by Bansil and others for different gel systems (Bansil and Gupta, 1980; Kizilay and Okay, 2003; Yazici and Okay, 2005). Schosseler and coworkers also measured the effect of ionization degree, salt concentration and polymer concentration on the diffusion coefficient of the gels. Increasing salt concentration decreases the diffusion coefficient of the gels, while increasing the degree of ionization increases the diffusion coefficient (A. Moussaid et al., 1991; Schosseler, Ilmain and Candau, 1991). As the polymer concentration increases due to increasing the crosslink density of the gel, the diffusion coefficient also increases. Such dependence of the diffusion coefficient of the gel on salt concentration, degree of ionization has been reported by Skouri et al. and Mccoy

et al. as well (McCoy and Muthukumar, 2010; Skouri et al., 1995).

1.4 Diffusion of Probe in Gels

The simplest model describing polymer diffusion in a solution is given by Rouse, where hydrodynamic interactions are not present and the viscous drag by the solvent is independent for each monomer bead. The Rouse model describes diffusion coefficient to be inversely related to chain length N as $D \sim N^{-1}$, using the chain connectivity and the bead friction coefficient. This model is not applicable for polymer diffusion in dilute solutions, where hydrodynamic interactions are important. The Zimm dynamics includes the hydrodynamic interactions, which relates the force on one bead and how it affects the force on another bead. In Zimm dynamics, the frictional coefficient which opposes polymer diffusion is proportional to radius of gyration (R_g) of the polymer chain. Thus the diffusion coefficient of the polymer chain is inversely proportional to R_g which implies that $D \sim N^{-\nu}$. With the increase in concentration of the polymer chains in the solvent, such as in a semi-dilute polymer solution, the hydrodynamic interactions are screened and the Rouse dynamics is followed. In this limit, the concentration of the polymer plays an important role in determining the hydrodynamic screening length and consequently the diffusion coefficient. However, in the semi-dilute regime, two diffusion coefficients are used to describe the polymer diffusion. The cooperative diffusion coefficient describes the correlations of neighboring chains. While the tracer diffusion coefficient accounts for the diffusion of a single polymer chain in the system. Both become same in the dilute limit. The cooperative diffusion coefficient, represents the local correlations and, hence, is independent of the molecular weight of the chain. The cooperative diffusion coefficient in a good solvent case is $D_c \sim c^{3/4}$, where c is the concentration of the polymer in the solution. While the tracer diffusion depends on both the molecular weight of the chain as well as

the concentration of the solution, and for a good solvent it scales as $D_t \sim c^{-1/2}N^{-1}$. Ballauff and coworkers, used fluorescence correlation spectroscopy to study diffusion of dye labeled polystyrene chain in a dilute and semi-dilute solution and observed the scaling of $D_s = D_c \sim c^0N^{-3/5}$ and $D_c \sim c^{3/4}N^0$ respectively, in dilute solutions and semi-dilute regime.

In the Rouse model for semi-dilute regime, the polymer chains have not considered to be entangled; Degennes used the reptation model to explain the diffusion of a polymer chain in case of entanglement. In reptation model, the polymer chains are considered to be entangled and these polymer chains form a tube around a polymer chain. The polymer chain diffuses through this tube, and can only move to and fro using its chain ends. It is assumed that the time scale for the tube renewal, i.e., time taken by all polymers chains forming the tube to diffuse and form a new tube, will be longer than the diffusion time of the polymer chain through the tube. Using this model, Degennes proposed the tracer diffusion coefficient would scale with concentration and molecular weight as $D_t \sim c^{-7/4}N^{-2}$. Many researchers (Pajevic, Bansil and Konak, 1991; Wheeler and Lodge, 1989; Pajevic, Bansil and Konak, 1993; Zettl et al., 2009), supported this scaling relation and concluded that the diffusion of polymer chain followed the reptation model. For example, Pajevic et al. observed diffusion of poly(methyl methacrylate) (PMMA) in a PMMA non-ionic gel using DLS, in which the diffusion coefficient of the polymer had a scaling relationship with the molecular weight of the chain with exponent α of 1.8 for $D \sim N^{-\alpha}$. Ballauff and coworkers, have observed the dependence of diffusion as $D_t \sim c^{-7/4}N^{-2}$ in high concentration regime.

Besides the reptation model, other theories based on obstruction effect of the network on diffusion of the solute have been proposed to explain the diffusion of a solute

in a gel (Amsden, 2002; Masaro and Zhu, 1999; Petit et al., 1996). In this theory proposed by Ogston and coworkers, the size of the solute and the size of the network strand are used to estimate the reduced diffusion coefficient (Ogston, Preston and Wells, 1973). Other researchers have used the Ogston model to predict the normalized diffusion coefficient of the probe inside the gel and mesh size of the gel (Johnson et al., 1995, 1996; Basak and Chattopadhyay, 2013). Phillies also proposed a similar model to that of Ogston, where the concentration of the network is used to describe the reduced diffusion coefficient (Phillies, 1986). He proposed the form $D = D_0 \exp(-\alpha c^\beta)$, based on experimental data, where β was usually observed between 0.6-1 (Reina, Bansil and Konak, 1990; Masaro and Zhu, 1999; Liu et al., 2005; Fatin-Rouge et al., 2006; Michelman-Ribeiro et al., 2007). A similar model for decrease in diffusion of the solute in the network, using similar parameters like dry gel content and solute radius is proposed in literature (Cukier, 1984). The objective of the above mentioned theories was to explain the diffusion process in confined environments. Another theory in this context, put forward by Muthukumar and Baumgartner, describes the process of polymer diffusion in confined environments as an entropic barrier process (Muthukumar and Baumgaertner, 1989); the polymer chain is considered to be partitioned in various compartments and the entropic barrier for diffusion from one compartment to another is proportional to size of the polymer and the length of the compartment, i.e., $\Delta F \sim R_g/\xi$. This theory was proposed for systems with greater confinement than that in the reptation model. Experiments of polymer in gels, observed $D \sim N^{-3}$ indicating a greater barrier for polymer diffusion than the reptation model which follows the scaling as $D \sim N^{-2}$. Researchers used entropic barrier model to understand the diffusion of PS in silica glasses, with varying pore sizes (Easwar, 1989; Guo, Langley and Karasz, 1990). Slater and coworkers studied entropic trapping of a polymer chain in a non-periodic array of obstacles using simulations (Slater and Yan Wu, 1995). As the concentration of obstacles increases, the exponent α in $D \sim N^{-\alpha}$ scaling relation

also increases from 1 to 2 and then even further to 2.3, which reflects a close agreement with the mechanism of entropic trappings of polymer chains. Nemoto et al. studied diffusion of polystyrene (PS) in PS-DiBenzyl Pthalate entangled solutions (Nemoto et al., 1989, 1991) and reported the exponent of $\alpha = 2.5$, similarly for the system of polystyrene in polyvinylmethylether (PVME) matrix the exponent is reported as 2.9 compared to 2 of the reptation model (Lodge and Rotstein, 1991).

1.5 Summary

The diffusion of polymers in concentrated solution as well as in gels has been studied by many researchers before. For a more biologically relevant system, the importance of charges in intracellular dynamics as well as in certain drug delivery systems cannot be discounted. This thesis focuses on the effect of diffusion of a polyelectrolyte as well as a neutral polymer inside a charged gel environment. The dynamics and swelling behavior of polyelectrolyte gels have been studied previously. It was observed that the PAM-PAA gel undergoes a collapse transition and the effect of transition on gel dynamics was captured using dynamic light scattering. In this thesis, dynamics of probe molecules, charged and uncharged polymers are investigated with accompanying volume phase transition of the gel in various solvent and salt concentrations. The diffusion of polyelectrolytes in polyelectrolyte gels is measured using dynamic light scattering and the diffusion of neutral polymer in the polyelectrolyte gel is measured using fluorescence correlation spectroscopy.

CHAPTER 2

GEL CHARACTERIZATION

2.1 Introduction

In this thesis, the dynamics of polymer diffusion are discussed in confined environments. Before we discuss this special case, it is necessary to begin with polymer dynamics in solution. Light scattering has been primarily used in this work to study polymer dynamics.

First let us introduce the basics of light scattering and extend our discussion to dynamic light scattering, correlation functions for single and multiple species diffusing in a solution and data analysis of these systems.

In light scattering, a monochromatic and polarized light source is usually used to illuminate a small scattering volume. The incident electromagnetic radiation interacts with a molecule, causing it to scatter electromagnetic radiation as well. The scattered intensity of this radiation is measured by the detectors. Density fluctuations in the scattering volume cause fluctuations in scattering intensity. The time dependence of scattered intensity fluctuations can be analyzed to determine the translational diffusion properties of the molecules, or the time averaged intensity can be analyzed with concentration and scattering vector to determine its radius of gyration, the second virial coefficient of osmotic pressure and molecular weight from the Zimm equation.

2.1.1 Dynamic Light Scattering

Dynamic Light Scattering (DLS) allows us to study translational diffusion of molecules in the system. Using vertically polarized light, translational diffusion can be studied which is the main focus in this study. The variations in scattering intensity are recorded by the detector. Due to the Brownian motion of particles, concentration fluctuations take place in the scattering volume. For dilute solutions, the hydrodynamic size of the particle and the viscosity of the surrounding solvent dictates the diffusion coefficient of the particle. This manifests as variations of in the intensity fluctuations which are collected by the detector.

To find the diffusion coefficient and the hydrodynamic size of the particle, an intensity average correlation function $g_2(\tau)$ (where τ is the lag time) is constructed to find the characteristic relaxation time of the system. The data in this thesis are collected using the ALV-5000 correlator to collect the intensity data in different channels which represents different lag times. The intensity in each channel is correlated as follows for different lag times to construct the intensity correlation function.

$$g_2(\tau) = \frac{\langle I(q, t) I(q, t + \tau) \rangle}{\langle I(q, t)^2 \rangle} \quad (2.1)$$

$$q = \frac{4\pi n}{\lambda} \sin\left(\frac{\theta}{2}\right) \quad (2.2)$$

where g_2 is the intensity correlation function, I is the scattered intensity at a fixed scattering vector (q), and τ is the lag time at which the intensity is correlated. $\langle \rangle$ denotes time averaged intensity. q is the scattering vector given by Eq. 2.2. The incident wavelength is λ , the refractive index of the solution is n , and the angle of detector with the incident beam is θ .

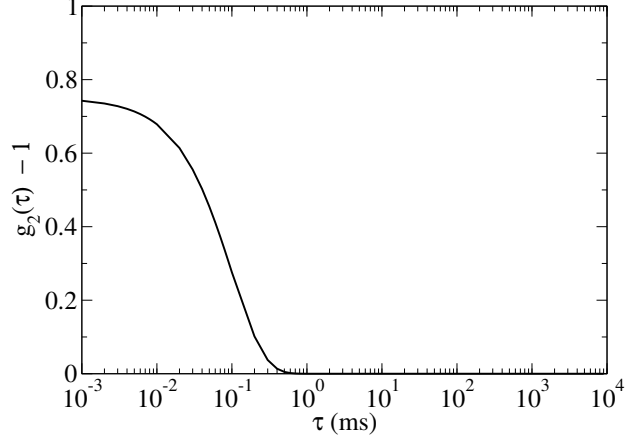


Figure 2.1. Schematic for the autocorrelation function $g_2(\tau) - 1$ vs. lag time τ .

The experimentally measured g_2 is related to the electric field correlation function by the Siegert relationship. The Siegert relationship is only valid for ergodic media. For non-ergodic media, the nature of the relation between intensity and electric field correlation functions is discussed later in section 2.1.3.

For ergodic systems, the intensity correlation function ($g_2(\tau)$) and the electric field correlation function ($g_1(\tau)$) are related by Siegert relationship given by Eq. 2.3

$$g_2(\tau) = \left(1 + \beta |g_1(\tau)|^2\right) \quad (2.3)$$

where β is an experimental parameter based on geometry and design of the apparatus. The electric field correlation function is related to the Brownian diffusion of particles. For an monodisperse sample it is given by an exponential decay, where τ is the characteristic decay time.

$$g_1(\tau) = \exp(-\Gamma\tau) \quad (2.4)$$

From Eq. 2.4, the diffusion coefficient (D) of the sample can be determined from Eq. 2.5

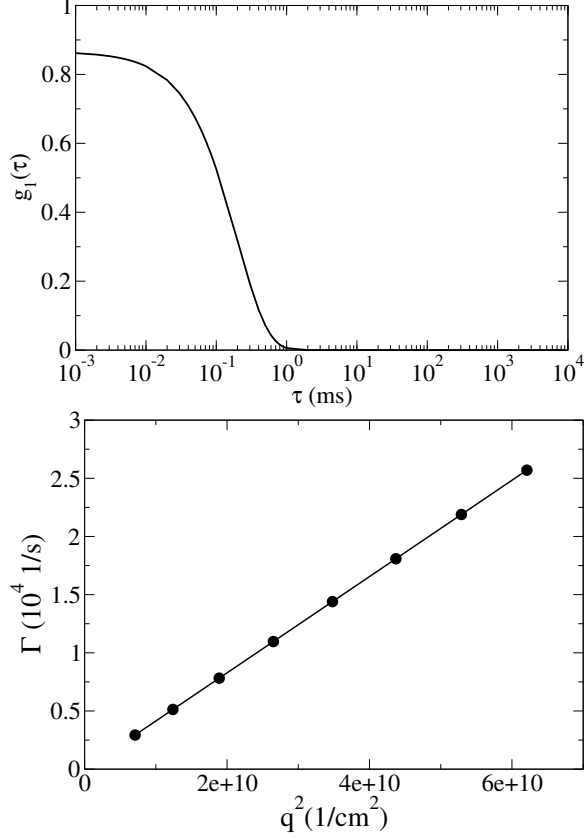


Figure 2.2. a. (Top) An example of the autocorrelation function $g_1(\tau)$ vs. lag time τ . (Bottom) Plot of Γ vs. q^2 . The slope of the line passing through origin is D as defined in Eq. 2.5.

$$\Gamma = Dq^2 \quad (2.5)$$

As shown in Fig. 2.2, the slope of the Γ vs. q^2 is the diffusion coefficient.

From the diffusion coefficient, the hydrodynamic radius can be found using the Stokes-Einstein Eq. 2.6

$$D = \frac{k_B T}{6\pi\eta R_h} \quad (2.6)$$

where k_B is the Boltzmann constant, T is the temperature, η is the viscosity of the solvent, and R_h is the hydrodynamic radius of the diffusing species.

For a system that has multiple components present in it, such as monodisperse particles or a polymer and its aggregates in its solution, a correlation function such shown in Fig. 2.3 is observed.

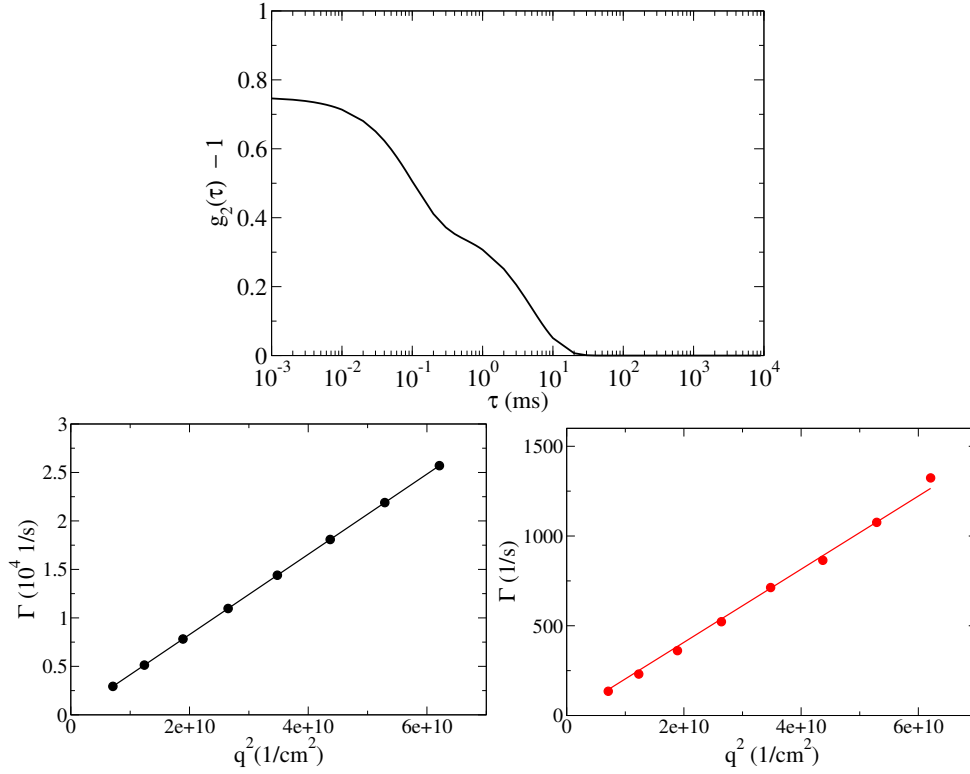


Figure 2.3. (Top) Example for the autocorrelation function $g_2(\tau) - 1$ vs. τ . Two distinct diffusive modes are observed. (Bottom) From the plot of Γ vs. q^2 for each mode, the respective diffusion coefficients are obtained.

Such a correlation function is given by the sum of two exponential decays as shown in Eq. 2.7.

$$g_1(\tau) = A_1 \exp(-\Gamma_1 \tau) + A_2 \exp(-\Gamma_2 \tau) \quad (2.7)$$

where Γ_1 and Γ_2 are the inverse of characteristic decay times of species 1 and 2, respectively. The corresponding diffusion coefficients can be determined by using Eq. 2.5 for Γ_1 vs. q^2 and Γ_2 vs. q^2 respectively as shown in Fig. 2.3.

2.1.2 Data Analysis for Ergodic Systems

2.1.2.1 Inverse Laplace Transformation Analysis

For monodisperse polymer systems, Inverse Laplace Transformation (ILT) is a very popular method. CONTIN is one of the most commonly used method of ILT analysis. CONTIN employs inverse laplace transform to yield a distribution function of characteristic decay times. However for multi-exponential systems as well as non-ergodic systems such as gels (the primary focus of this work), using CONTIN analysis has challenging limitations. In this work, multi-exponential analysis is exclusively used.

2.1.2.2 Multi-Exponential Analysis

The correlation function can be fit to multi exponential functions depending on the number of different size scales diffusing in the solution. As seen from Eq. 2.4, the correlation function can be fit to the exponential function, where the inverse decay time Γ and A are a fitting parameters. For two exponentials, the equation is shown in 2.7, there are four fitting parameters Γ_1 , Γ_2 , A_1 and A_2 .

The data fitting is done using minimization of error between the fit prediction and the data. Two fitting methods are used to analyze and compare the results. The obtained correlation function $(g_2(\tau) - 1)$, was fit using fmincon solver in MATLAB using two-term exponential function as shown in Eqs. 2.7 and 2.3.

The second method of analysis is using a software developed by Dr. Schmidt's lab (details in Ref. (Rausch et al., 2010)). It is important to analyze the data by using multiple exponential fits and ensure the residuals are not biased, that is, they are randomly distributed about the mean of zero and not have systematic fluctuations about its mean. Also, fitting the correlation function with an extra exponential term

should yield same values of atleast two parameters of decay time which is a consistency check to determine the number of characteristic decay modes present in the system. This method has a more user friendly interface, and was used to verify the results obtained from MATLAB analysis.

2.1.3 Data Analysis for non-Ergodic Systems

The theory for dynamic light scattering of Brownian particles and its consequent data analysis has been discussed above. This thesis focuses on light scattering of gels and studying the diffusion of polymer in these gels. Thus it is important to discuss light scattering theory for gels as well. Unfortunately, light scattering of gels cannot be described as an ergodic medium, and thus another theory is necessary to describe the relation between an intensity correlation function to the electric field correlation function. Before we discuss why gels are non-ergodic and what methods are employed to analyze light scattering data, let us discuss the diffusion coefficient for a gel and its significance.

It is also important to realize that the gel network does not undergo Brownian diffusion as in the case of a polymer solution. Thus the question of what diffusion coefficient means for a gel network must be answered. (Tanaka, Hocker and Benedek, 1973) developed a theory to explain the physical meaning of diffusion coefficient for a polymer gel. They related the displacement vector of the network to its longitudinal osmotic modulus (K), shear modulus (μ) and the friction coefficient (f). Thus it is analogous to pressure waves moving through a solid object. By this analogy, it obvious that the diffusion coefficient is proportional to the modulus term and inversely related to friction term as it dampens the wave propagation through the network. The exact expression is given by Eq. 2.8.

$$D = \frac{K + \frac{4}{3}\mu}{f} \quad (2.8)$$

Now we understand the significance of diffusion coefficient of a gel, let us discuss the non-ergodicity of a gel and its light scattering analysis. An ergodic media is one whose time averaged property and ensemble average property is equal. In other words, for light scattering, the particles are allowed to diffuse throughout the system, the system will evolve to explore the configurational space such that the time average intensity will be equal to ensemble averaged intensity. However for a polymer gel, due to presence of crosslinks in the network, the structure of the gel is fixed and hence the chains between crosslinks can only fluctuate about its mean position to a limited extent. Due to this pseudo-fixed position of the scattering elements in the system, the scatterers in this region cannot fully explore the configurational space beyond this region. Thus the ensemble average intensity is not equal to the time average intensity for light scattering gels, due to localization of scatterers in space. Thus gels are defined as non-ergodic media.

Experiments of light scattering of gels are also often described as heterodyne experiment in contrast to a homodyne experiment of a polymer solution. In a homodyne experiment, the total scattering intensity arises from the fluctuating components present in the system, such as a polymer solution. This is similar to an ergodic media. However, in case of gels, the static heterogeneity do not diffuse on the experimental time scales studied and hence, contribute as a static component of the scattering intensity. Thus the scattering intensity is divided in two contributions. First is the time fluctuating component that corresponds to the concentration fluctuations of the gel network, second is the static part which corresponds to static inhomogeneities due to crosslinks in the gel.

There two methods of analysis commonly employed for polymer gels. Non-ergodic analysis is based upon the explanation given above; the gel cannot explore the space due to constraints imposed by crosslinks (Pusey and Megen, 1989; Joosten, McCarthy and Pusey, 1991). While heterodyning concept of analysis utilizes the fact that the scattering intensity is divided in two contributions (Geissler, Horkay and Hecht, 1991; Geissler and Hecht, 1976; Munch et al., 1977; Brown, 1993). Many researchers have used methods of analysis which employ either heterodyne method of analysis or the non-ergodic method of analysis (Geissler, Horkay and Hecht, 1991; Geissler and Hecht, 1976; Munch et al., 1977; Pusey and Megen, 1989; Joosten, McCarthy and Pusey, 1991; Fang and Brown, 1992).

The intensity correlation function for a heterodyning method (Brown, 1993) is related to the electric field correlation function using

$$g_2(\tau) = X^2 (g_1(\tau))^2 + 2X(1 - X) (g_1(\tau)), \quad (2.9)$$

where

$$X = \frac{\langle I(q) \rangle_f}{\langle I(q) \rangle} \quad (2.10)$$

and $\langle I(q) \rangle_f$ is the fluctuating component of the total intensity $\langle I(q) \rangle$

Brown and coworkers used various analysis methods for light scattering of gels to understand the difference in the diffusion coefficients of the gel obtained from different analysis methods (Fang and Brown, 1992). They observed that the values of the diffusion coefficient of the gel are related to the values obtained from different analysis methods by the degree of non-ergodicity or the degree of heterodyning of the gel. It is assumed in the current work that for small change in the crosslink density, and the charge density of the gel, the change in the degree of non-ergodicity of the gel is relatively small. The apparent diffusion coefficient obtained by ergodic analysis

(D_E) for a non-ergodic system, *i.e.* using Eq. 2.4 and the diffusion coefficient obtained by non-ergodic analysis (D_{HT}), *i.e.*, using Eq. 2.10, are proportional to each other by factor X . The ratio of the two diffusion coefficient values is at most a factor of 2, while in most experiments it is between 1 and 2. In case of perfect homodyne experiment, $X = 1$, and thus $D_E = D_{HT}$.

With the above considerations in mind, all experiments are analyzed using the homodyne method of analysis. It is reasonably assumed that the degree of heterodyning does not significantly vary from one gel sample to another sample and thus all reported diffusion coefficients are systematically offset from the heterodyne diffusion coefficient D_{HT} by approximately same ratio.

2.2 Experimental Setup

2.2.1 Gel Synthesis

Poly(acrylamide-co-sodium acrylate) (which will be referred to as PAM-PAA) gel were synthesized using free radical polymerization. All gels were synthesized in water as solvent and at room temperature. The synthesis method was followed as described in literature previously (McCoy and Muthukumar, 2010; Cambrex, N.d.). In our group, the ionic gels were synthesized from polyacrylamide gels from hydrolysis of these gels. But in this thesis they are synthesized using sodium acrylate instead of hydrolysis method to maintain greater control on the charge density of the gel. These gels are defined by three important quantities or parameters.

1. $T\%$, which is the weight of the total monomers and crosslinkers per 100 ml of the gel solution.

$$T\% = \frac{W_{AcAm} + W_{NaAc} + W_{Bis}}{100ml} \quad (2.11)$$

2. $Xl\%$, which is the molar ratio of the crosslinker (Bis) to the total monomers (AcAm and NaAc) in the gel solution.

$$Xl\% = \frac{M_{Bis}}{M_{AcAm} + M_{NaAc} + M_{Bis}} \quad (2.12)$$

3. $C\%$, which is the molar ratio of the charged monomer (NaAc) to the total monomers (AcAm and NaAc) in the gel solution.

$$C\% = \frac{M_{NaAc}}{M_{AcAm} + M_{NaAc}} \quad (2.13)$$

Thus Eqs. 2.11, 2.12 and 2.13 define the chemical composition of the gel. where W = weight of species added to the gel solution, and M = moles of species added to the solution.

For non-ionic gels, as crosslink density increases, the heterogeneity in the gels increases. This increase in heterogeneity has been attributed to clustering of the Bis groups. In this work, three gels are primarily discussed -

1. 10% charge density and 2.7% crosslink density (abbreviated as 10C2.7X1)
2. 10% charge density and 3.5% crosslink density (abbreviated as 10C3.5X1)

3. 5% charge density and 2.7% crosslink density (abbreviated as 5C2.7X1)

Recipe and preparation method for 10C2.7X1 PAM-PAA gel is described below. Other gels are synthesized in similar method. Required amounts of monomers and crosslinkers are taken for necessary charge density and crosslink density.

Millipore water ($18.2M\Omega$) is stirred with 24.6 ml of 40% (w/v) of Acrylamide solution, 6.7 ml of 20% (w/w) of Sodium Acrylate solution, and 33.0 ml of 2% (w/v) of BisAcrylamide solution. The total volume of the solution is 300 ml. Millipore water (235.7 ml) is added to the monomer and crosslinker solution to bring the volume to 300 ml. All the solutions were filtered with 200 nm filter to remove any dust from the pre gel solution. For using the gels for light scattering experiments, it important to filter them and remove dust from samples. This pre-gel solution is bubbled with Nitrogen gas for 15 minutes to remove any dissolved oxygen which can inhibit the reaction. To polymerize the reaction, TEMED ($450 \mu\text{l}$) and Ammonium Persulfate (1.5 ml) is added to the pre-gel solution. The solution is stirred for one minute after addition of the initiator and poured into a tray (1 mm thickness) and casted for two hours at room temperature. The tray is covered with a top plate to prevent wrinkling of the gel. The gel is removed from the tray and cut into pieces. The gel pieces are placed in large millipore water reservoirs to remove any unreacted components and thus ending the reaction. Reaction schemes is shown in Fig. 2.4.

Another method of sample preparation (referred to method B henceforth) was to prepare the same pre-gel solution and filter it into a light scattering tube. This pre-gel solution is also bubbled with Nitrogen gas for 15 minutes to remove any dissolved oxygen which can inhibit the reaction. A concern in the previous method is if impurities present in Nitrogen line are being transferred into the pre-gel solution.

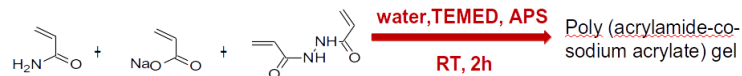


Figure 2.4. Reaction scheme of synthesis of Poly(acrylamide-co-sodium acrylate) gel.

Thus in this method, the pre-gel solution was filtered after the bubbling of Nitrogen gas through the solution. Required amount filtered TEMED and Ammonium Persulfate were added to the light scattering tube. The tube was gently shaken to mix the initiator uniformly in the solution. The reaction was stopped after two hours by adding filtered water to the tube. Filtered water was replaced after every few hours for two days to remove any unreacted monomers.

2.2.2 solid state NMR

The solid state NMR was used to study the composition of the gel. Bruker DSX 300 NMR operating at H frequency of 300 MHz was used to obtain the spectra. The gel sample is freeze dried to remove any water content. The dry gel is powdered and filled in the rotor layer by layer. Few drops of millipore water is added to the dry powder to make sure it is compactly packed in the rotor. A spacer is placed between the cap and the sample to ensure that the sample is held in place during the experiment. Spin rates between 1000 to 1500 RPM were used to spin the sample.

2.2.3 Swelling Ratio

Swelling ratio measurement were performed to determine the volume fraction of the gel as a function of NaCl concentration in water as well as in 45% water and 55% acetone mixture. A piece of gel of known weight is placed in a solution of known salt concentration. The volume of the solution is large enough such that the salt concentration is not affected by the water released from the gel upon shrinking. The weight of the gel is measured after 48 hours when equilibrium has reached. The

volume fraction of the gel in equilibrium in given solution can be determined using Eq. 2.14. To find the volume fraction, the densities of the solvent and polymer are used along with weight of the dry and swollen gel.

$$\phi = \left[1 + \left(\frac{\rho_p}{\rho_s} \right) \left(\frac{m_s}{m_d} \right) - \frac{\rho_p}{\rho_s} \right] \quad (2.14)$$

where ρ_p = density of the polymer

ρ_s = density of the solvent

m_s = weight of the swollen gel

m_d = weight of the dry gel

2.2.4 Rheology

Shear modulus experiments were performed on the gels to measure their shear storage and shear loss modulus. A strain controlled rheometer (ARES TA Instruments) with 40 mm diameter parallel plate was used to measure modulus. The measurements were performed in the viscoelastic region (McCoy and Muthukumar, 2010) by applying a frequency sweep of 0.1 Hz to 1 Hz with shear strain of 0.5%. The frequency sweep was performed in this limited range due to instability at higher frequency and water loss at lower frequencies as has been reported previously (McCoy and Muthukumar, 2010).

2.2.5 Dynamic Light Scattering

Light scattering measurements were performed on the gel samples. The samples were prepared and allowed to equilibrate for atleast two days before experiments were performed. A small piece of swollen gel sample was placed in the light scattering tube and allowed to equilibrate with the solution. In this method of sample preparation, extra care needs to be taken while doing light scattering experiment. Since the entire

tube is not occupied by the gel, care must be taken to ensure the gel is present in the scattering volume. This is experimentally often an arduous task. Thus samples were also prepared in another method, which ensures the gel completely occupies the tube and hence the scattering comes directly from the gel.

Another method of sample preparation was done for gels prepared using method B. The gel synthesized in the light scattering tube was allowed to equilibrate with water for two days, and later replaced with solution (NaCl in water or 55% acetone) for two weeks. It was found that this gel synthesized in the tube required longer time to equilibrate with the supernatant solution. Light scattering was performed both on the gel as well as the supernatant solution to show that state of the gel system and its supernatant solution prior to addition of a probe molecule.

All light scattering experiments were performed on ALV goniometer (ALV, Langen Germany) instrument with ALV-5000/E correlator that has 288 channels. A 2 W argon laser with wavelength $\lambda = 514.5$ nm was used as light source. The power source was adjusted to give good scattering intensity from the samples. All experiments are performed at room temperature. Scattering intensity data was collected from 30° to 120° , which corresponds to scattering wave vector, q , as defined by Eq. 2.15

$$q = \frac{4\pi n}{\lambda} \sin\left(\frac{\theta}{2}\right) \quad (2.15)$$

In this chapter, only the dynamic light scattering studies on the gel are discussed. As has been previously discussed, the static light scattering of the gel needs to distinguish between the static and dynamic contributions of the gel, to relate the $I(q \rightarrow 0)$ to the osmotic compressibility or the osmotic modulus of the gel.

2.2.6 Ultraviolet/Visible Spectroscopy

UV-Vis spectroscopy studies the absorption spectra of the sample in the UV-Vis wavelength region. The UV-Vis spectroscopy was used to study the presence of probe molecules in the gel. The UV-Vis experiments were performed using a Hitachi U3010 UV/visible spectrophotometer with scan region of 200 nm to 700 nm. Experiments were performed in a quartz cuvette with a path length of 2 mm. In this chapter, only the data for gel characterization using UV-Vis spectroscopy is shown. In Appendix, the spectra for presence of the probe along with the gel will be discussed. Quantitative analysis can be performed using Beer-Lambert law, however in this thesis, this is used as a qualitative tool to study the presence probe in the gel, rather than measure amount of probe present inside the gel.

2.2.7 Scanning Electron Microscopy

SEM images of 10% Charge density and 2.7% crosslink density Poly (acrylamide-co-sodiumacrylate) gel swollen in water were taken to determine the mesh size from microscopy technique. The gel was lyophilized to remove the water content of the gel and preserve its mesh structure. Freeze dried gel was immersed in Liquid N₂ and cut to create new surfaces. Sample was sputter coated with gold to make a 2 nm coating layer.

2.3 Results and Discussion

2.3.1 solid state NMR

Using solid state NMR, the ratio of the acrylate groups to the acrylamide groups can be determined. The chemical shifts obtained from the ¹³C ssNMR spectra of the PAM-PAA gel is shown in Fig. 2.5. The sodium acrylate content in the gel compared to acrylamide content is calculated by comparing the relative ratio of the area under

the respective peaks. The chemical shift for acrylamide group is 180 ppm and that for acrylate group is 184 ppm labeled 5 and 6 respectively.

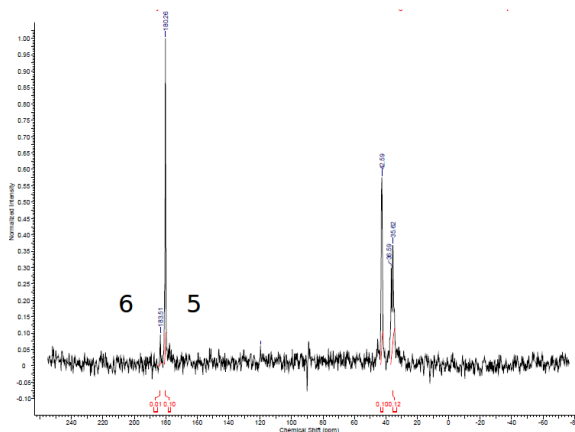


Figure 2.5. ssNMR of the 10C2.7X1 PAM-PAA gel. The chemical shift for acrylamide group is 180 ppm and that for acrylate group is 184 ppm labeled 5 and 6 respectively. The relative ratio of the area under curve of the acrylate and the acrylamide groups is 10%.

2.3.2 Swelling Ratio

The swelling ratio is an important characterization tool, as it is related to many properties of the gel. The molecular weight between crosslinks for a neutral gel is related to the volume fraction ϕ from the Flory-Rehner theory (F-R theory). Degennes also predicted the scaling of volume fraction to osmotic pressure, shear modulus and diffusion coefficient.

It was shown by (Ohmine and Tanaka, 1982) that these gels undergo volume phase transition in presence of unfavorable solvent and at a salt concentration. This result was reproduced previously by (McCoy and Muthukumar, 2010) for the same gel system in our lab.

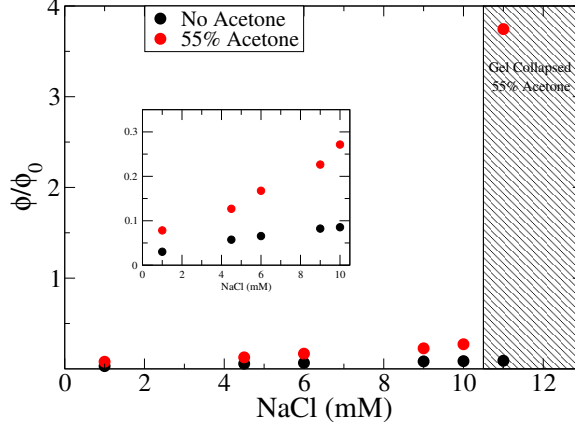


Figure 2.6. Volume transition of 10C2.7X1 PAM-PAA gel in presence of 55% acetone solution at 11 mM NaCl concentration. The gel does not collapse at 11 ml NaCl concentration in presence of water as solution. Inset shows the volume fraction of the gel when the gel is not yet collapsed.

Here the Fig. 2.6 shows the collapse transition for the 10C2.7X1 PAM-PAA gel at 11 mM NaCl concentration in 55% acetone solution, but does not collapse at same NaCl concentration in water. The collapse transition of an ionic gel is explained by the modified F-R theory for ionic gels, which incorporates the Donnan equilibrium contribution for the ionic gels.

The F-R theory balances swelling of the uncharged gel by the elastic forces of the network due to crosslinks. When these two forces are balanced, the network reaches equilibrium. For ionic gels, an additional term of the mobile ions contributes to the total osmotic pressure.

Three terms contribute to the total osmotic pressure of the gel - Osmotic pressure due to mixing (π_{mix})

$$\frac{\pi_{mix}v_1}{k_B T} = -\ln(1 - \phi) - \phi - \chi\phi^2 \quad (2.16)$$

Osmotic pressure due to elasticity of the network (π_{el})

$$\frac{\pi_{el}v_1}{k_B T} = -\frac{1}{N} \left(\alpha_0^2 \phi^{1/3} - \frac{\phi}{2} \right) \quad (2.17)$$

Osmotic pressure due to mobile ions (π_{ion})

$$\frac{\pi_{ion}v_1}{k_B T} = v_1 \left(\sqrt{\alpha^2 \phi^2 + 4c_s^2} - 2c_s \right) \quad (2.18)$$

The expression for the net osmotic pressure is given by addition of Eqs. 2.16, 2.17 and 2.18

$$\frac{\pi v_1}{k_B T} = -\ln(1 - \phi) - \phi - \chi \phi^2 - \frac{1}{N} \left(\alpha_0^2 \phi^{1/3} - \frac{\phi}{2} \right) + v_1 \left(\sqrt{\alpha^2 \phi^2 + 4c_s^2} - 2c_s \right) \quad (2.19)$$

where ϕ = volume fraction of the gel,

χ = interaction parameter between the polymer and solvent,

N = Number of kuhn segments between crosslinks,

α_0 = Reference state of the gel,

α = Degree of ionization,

c_s = Salt concentration of the solution.

In equilibrium, $\pi = 0$. Hence,

$$N = \frac{\left(\alpha_0^2 \phi^{1/3} - \frac{\phi}{2} \right)}{\left(\left(\frac{1}{2} - \chi \right) \phi^2 + \sqrt{\alpha^2 \phi^2 + 4v_1^2 c_s^2} - 2v_1 c_s \right)} \quad (2.20)$$

From the equation for osmotic pressure of the gel, we can find the osmotic modulus of the gel (K_{os})

$$\frac{K_{os}v_1}{k_B T} = \frac{\phi}{1 - \phi} - \left(1 - \frac{1}{2N} + 2\chi\phi \right) \phi - \frac{1}{3N} \alpha_0^2 \phi^{1/3} + \frac{\alpha^2 \phi^2}{\sqrt{\alpha^2 \phi^2 + 4c_s^2}} \quad (2.21)$$

The condition for stability of a gel is $K_{os} > 0$. Thus as the solvent quality becomes poor, the contribution of the term $-2\chi\phi^2$ increases and as we add more salt, the Donnan contribution decreases, and thus results in $K_{os} < 0$, which leads to gel collapse.

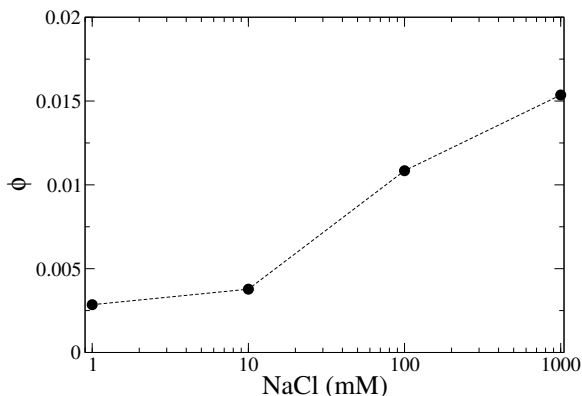


Figure 2.7. Effect on swelling of gel as a function of NaCl concentration. As more salt is added to the system, the Donnan contribution decreases resulting in deswelling of the gel. Thus the volume fraction (ϕ) increases as more salt is added

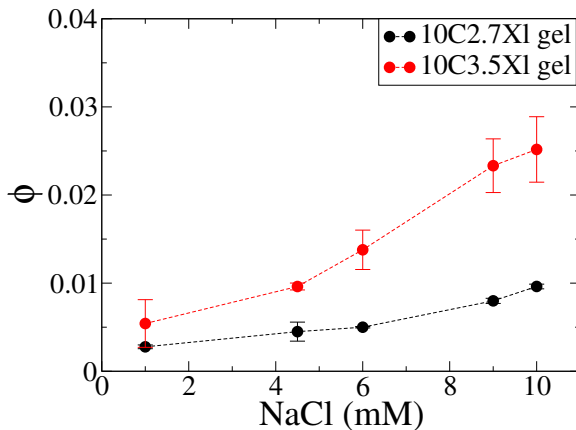


Figure 2.8. Effect on swelling of gel as a function of NaCl concentration in 55% Acetone solution for gels of same charge density (10%) but different crosslink density (2.7% and 3.5%). As more salt is added to the system, the Donnan contribution decreases. Thus the volume fraction (ϕ) increases as more salt is added. Higher crosslink density gel, has higher volume fraction at all NaCl concentrations.

Ionic Gels	10C2.7Xl	10C3.5Xl	5C2.7Xl
ϕ (measured)	0.00106	0.00161	0.00249
α	0.16	0.16	0.08
α_0	0.98	0.98	0.98
N	~ 570	~ 430	~ 600
ξ (nm)	~ 40	~ 32	~ 26

Table 2.1. Estimation of number of kuhn segments between crosslinks using modified Flory-Rehner theory (Eq. 2.19) and estimating mesh size of the gel in swollen state using Eq. 2.22

The number of kuhn segments in the segment between crosslinks is calculated from the Eq. 2.20. However, from the molar ratio of the crosslinker to the monomers, a different theoretical value is expected. Using this value of N, the theoretical mesh size is determined using the end to end distance for a polyelectrolyte chain in no salt limit (Muthukumar, 2011) from Eq. 2.22.

$$\xi = \left(\frac{8}{15\sqrt{6\pi}} \frac{\alpha^2 z_p^2 l_B}{l} \right)^{1/3} Nl \quad (2.22)$$

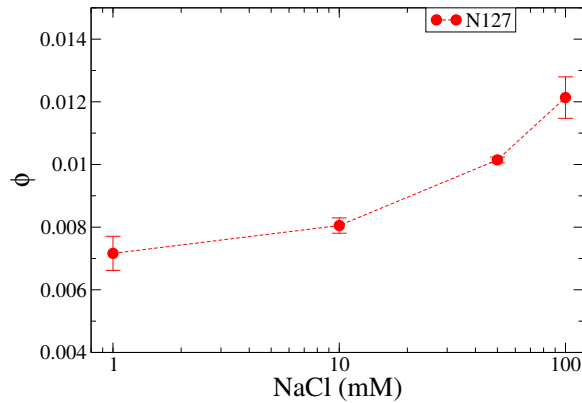


Figure 2.9. Effect on swelling of gel as a function of NaPSS and NaCl concentration. NaPSS concentration is kept constant at 5 mg/ml (24 mM monomer concentration). As more salt is added to the system, the Donnan contribution decreases resulting in deswelling of the gel. Thus the volume fraction (ϕ) increases as more salt is added

Since, NaPSS also charges on its backbone as well as counterions, it acts as salt, in effectively reducing the Donnan potential. As a result the gel deswells even more when NaPSS is present along with NaCl in the solution. This can be seen by comparing the volume fractions of Fig. 2.7 and 3.5.

Using the values for volume fraction ϕ in presence of 55% acetone and NaCl solution, an estimate for mesh size is determined.

To calculate mesh size of the gel in a solution, following approach was used. Suppose there are 'n' mesh each of volume $V_{swollenmesh}$

$$V_{swollenmesh} = \xi_{swollen}^3;$$

$$\text{Total volume of the gel is: } V_{swollengel} = n\xi_{swollen}^3;$$

After we place the gel in a solution of NaPSS, 55% acetone and NaCl, the gel shrinks. But the total number of mesh remain constant (n). If the mesh size reduces to ξ , volume of each mesh is $V_{mesh} = \xi^3$;

$$\text{Total volume of the shrunken gel is: } V_{gel} = n\xi^3;$$

$$\frac{V_{swollengel}}{V_{gel}} = \frac{n\xi_{swollen}^3}{n\xi^3} \quad (2.23)$$

The mesh size of swollen gel has been calculated in Eq. 2.23 and measuring the volume of the gel in swollen state and in equilibrium with the salt solution, we can calculate the mesh size of the gel ξ , after deswelling. The table below summarizes the value of the gel after it is deswollen in the different molecular weights of NaPSS and various NaCl concentrations. All measurements reported are done in presence of 55% acetone and NaCl solution.

The mesh size of the gel does not vary much with the molecular weight of the gel, but decreases when NaCl concentration is increased. This factor is important later, when diffusion of polymers in the gel will be discussed. As the mesh size decreases, the constraints on polymer diffusion are expected to increase, resulting in slower diffusion.

NaCl (mM)	10C2.7Xl - ξ (nm)			
	N16	N30	N70	N127
1	18.2	18.9	17.3	18.3
4.5	16.3	17.2	16.9	16.9
6	16.2	16.2	15.6	15.9
9	15.1	15.9	14.8	15.6
10	13.7	15.0	13.7	14.9

Table 2.2. Estimation of the mesh size of the gel in NaPSS + 55% acetone + NaCl solution using Eq. 2.23

These mesh size estimates will provide us a necessary estimate when compared to the polymer size as to how confined the polymer chains are inside the gel.

2.3.3 Rheology

For chemically crosslinked networks it is typical to observe the modulus to be independent of frequency (Ferry, 1980). Non ionic gels have higher modulus than ionic gels because of higher volume fractions. Using rubber elasticity, Treloar had shown that $G \sim \phi^{1/3}$. And since ϕ is inversely related to molecular weight between crosslinks (N), higher crosslink density gels have higher modulus. Using Treloar's theory for rubber elasticity for swollen networks and substituting the unknown, N from Eq. 2.20, we find the dependence of G vs. N .

$$\frac{G}{RT} = \phi^{1/3} \frac{\left(\left(\frac{1}{2} - \chi \right) \phi^2 + \sqrt{\alpha^2 \phi^2 + 4v_1^2 c_s^2} - 2c_s \right)}{\left(\alpha_0^2 \phi^{1/3} - \frac{\phi}{2} \right)} \quad (2.24)$$

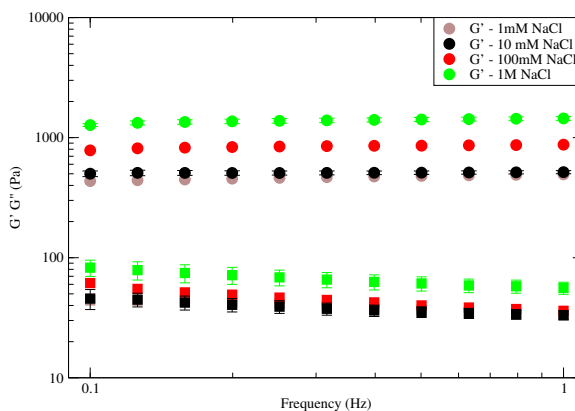


Figure 2.10. Effect on modulus of gel as a function of NaCl concentration for the same gel (10C2.7X1). As more salt is added to the system, the gel deswells and its volume fraction increases. Hence adding NaCl, increases the modulus of the gel.

2.3.4 Dynamic Light Scattering

As has been discussed in data analysis for non-ergodic samples, the correlation functions for the gel samples were analyzed using homodyne method of analysis using multi-exponential fits. The analysis of gels is complicated as modes corresponding to heterogenities in the system also contribute to the scattering intensity and the corresponding intensity correlation function. These modes appear at longer time scales than the characteristic relaxation mode of the gel and does not have q^2 dependence. All correlation functions presented in this work are shown without further normalization. For gels, which are typical of a heterodyne experiment, the amplitude of the intensity correlation function $g_2(\tau)$ is less than that observed for a polymer solution.

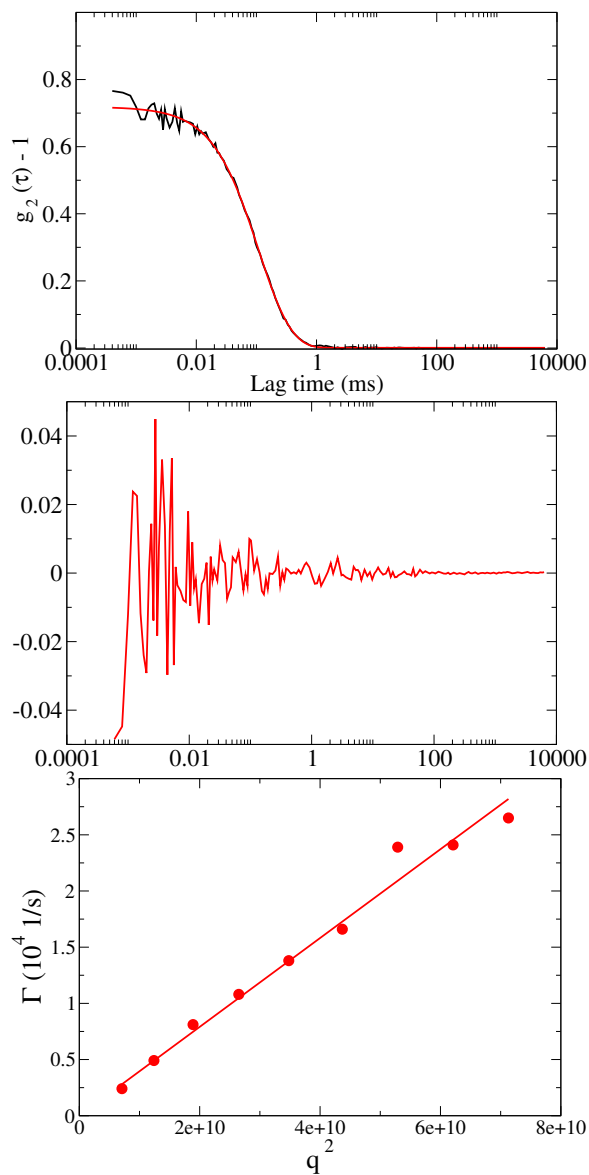


Figure 2.11. a. Correlation function for the 10C2.7Xl gel + 100 mM NaCl solution. The correlation function is fitted with a single exponential decay. b. The accuracy of the fit can be seen from the residuals. c. The plot of Γ vs. q^2 is shown. The slope of the fit is the diffusion coefficient of the gel.

At higher salt concentrations, the gel deswells as the Donnan potential between inside the gel and outside decreases. This also leads to decrease in mesh size of the gel. Thus as the mesh size decreases, the largest mesh size shrinks first, leading to more homogeneous gel structure (this does not mean gel becomes homogeneous, it

becomes more homogeneous compared to its homogeneity without salt). Thus we expect the non- q^2 dependent slow mode which occurs due to heterogeneity to disappear at high salt concentrations.

As seen in the Fig. 2.11, at higher NaCl concentration, the correlation function can be fitted using single exponential decay for the correlation function. It can be seen from the residuals that the fit works well and another exponential function is not required for the fit.

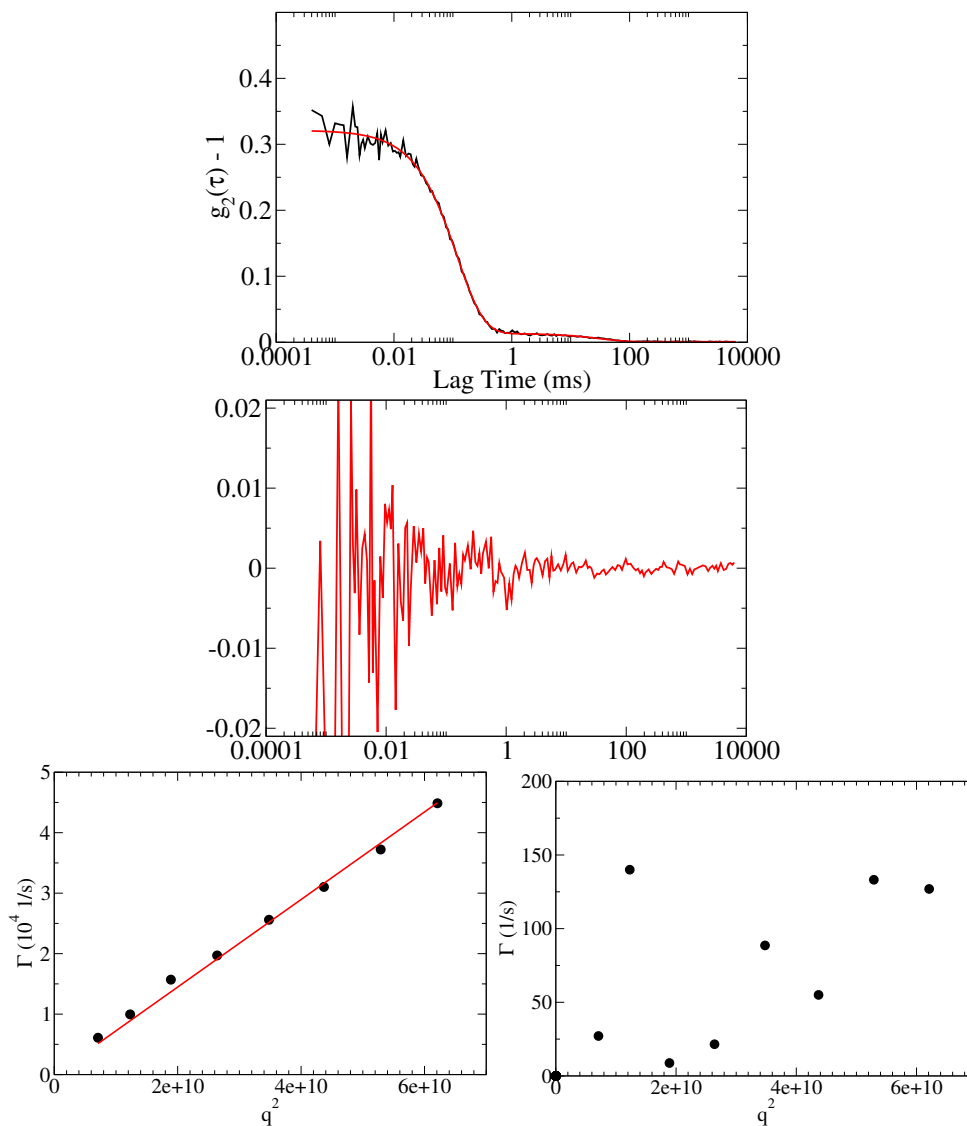


Figure 2.12. Correlation function for the 10C2.7X1 gel + 10 mM NaCl solution. The correlation function is fitted with a two exponential decays. The accuracy of the fit can be seen from the residuals.

As seen in the Fig. 2.12, at lower NaCl concentration, the correlation function needs to be fitted using a two exponential decay for the correlation function. It can be seen from the residuals that the fit works well and another exponential function is not required for the fit. This additional mode is not q^2 dependent as seen from the figure.

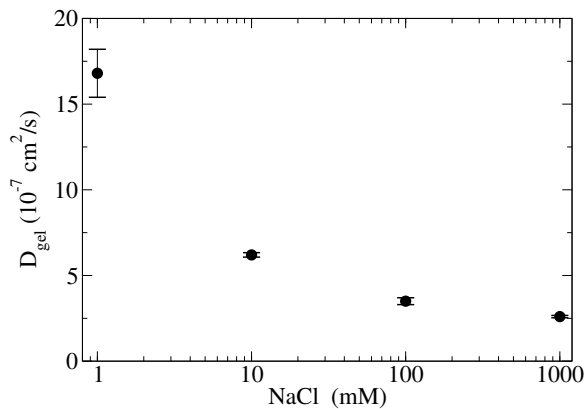


Figure 2.13. Diffusion coefficient for the 10C2.7X1 gel + NaCl solution. The diffusion coefficient decreases as NaCl is added to the solution.

The diffusion coefficient of the gel decreases as NaCl is added to the system. Using values of diffusion coefficient from Fig. 2.13, and the rheology data from Fig. 2.10, a plot of $\ln G/D$ vs. ϕ is plotted in Fig. 2.14. Eq. 2.8, is modified for simplicity to $D G/f$, from the work of Skouri and coworkers (Skouri et al., 1995). The values of ϕ for respective NaCl concentrations are shown in Fig. 2.7.

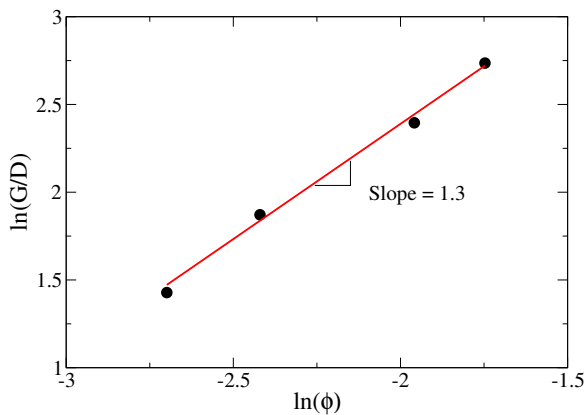


Figure 2.14. The dependence of the friction coefficient with the volume fraction of the gel. Friction coefficient is represented as the ratio G/D from Eq. 2.8.

From Eq. 2.8 and Fig. 2.14, the relation between friction coefficient f and volume fraction ϕ is established for this gel system.

$$f \sim \phi^{1.3} \tag{2.25}$$

Previously, many researchers have used the Stokes-Einstein relationship to obtain an correlation length ξ from the diffusion coefficient of a gel. The approximation is valid for non-ionic gels, but was shown to be invalid for ionic gels by (McCoy and Muthukumar, 2010). Thus we cannot obtain the mesh size of the gels synthesized in this work using the the Stokes-Einstein relation.

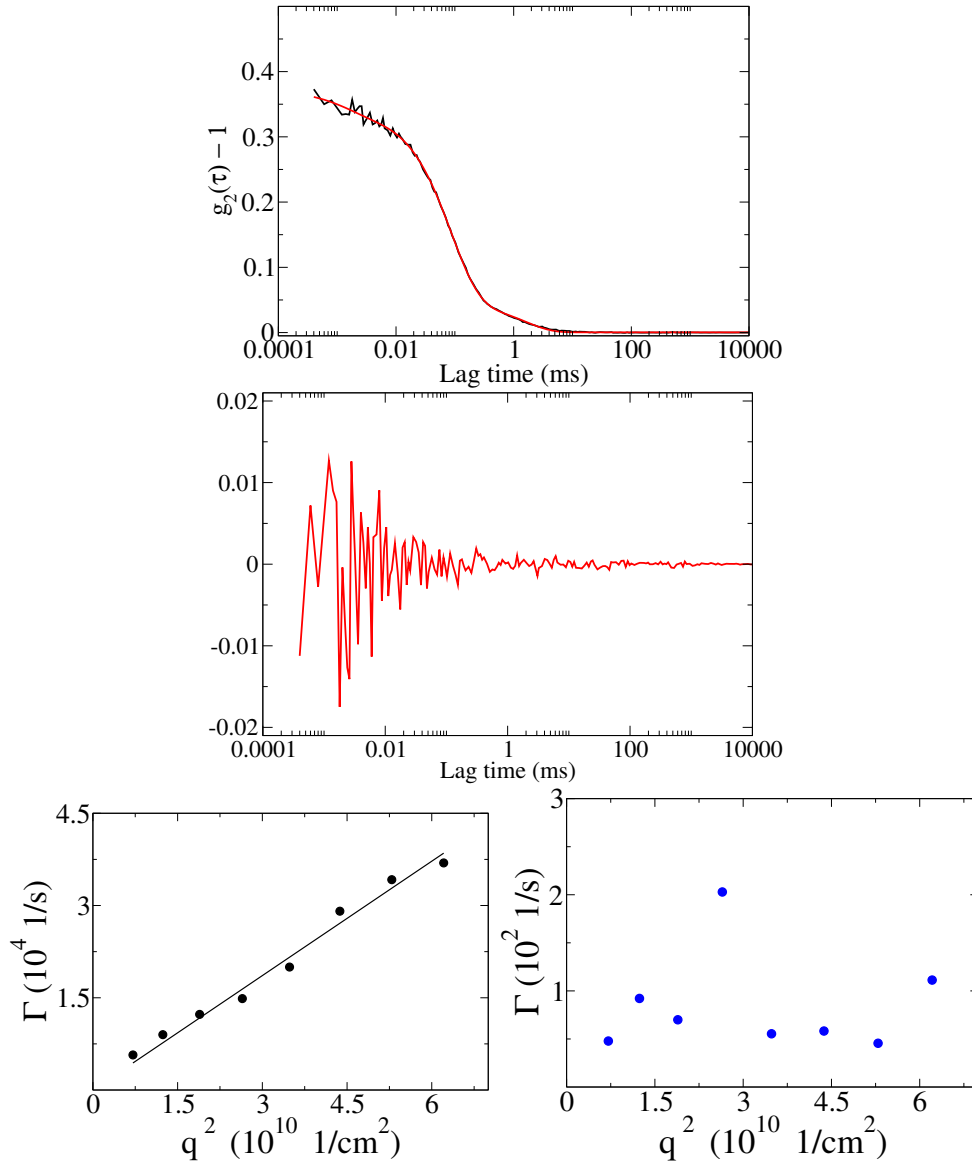


Figure 2.15. Correlation function for the 10C2.7X1 gel + 55% acetone + 6 mM NaCl solution. The correlation function is fitted with a two exponential decays. The accuracy of the fit can be seen from the residuals.

In presence of 55% acetone, the gel undergoes volume phase transition as seen in Fig. 2.8. Acetone being an unfavorable solvent for the gel induces this volume phase transition. The slow mode corresponding to the gel heterogeneity is present in presence of Acetone as seen in the Fig. 2.15. The correlation function needs to be fitted using a two exponential decay for the correlation function. It can be seen from the

residuals that the fit works well and another exponential function is not required for the fit. This additional mode is not q^2 dependent as seen from the figure.

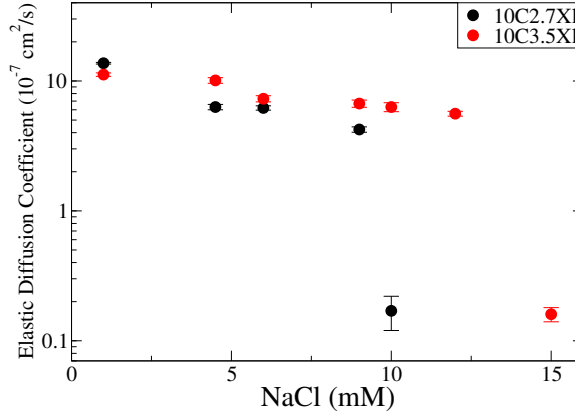


Figure 2.16. Diffusion coefficient for the 10C2.7Xl gel + 55% acetone + NaCl solution and the 10C3.5Xl gel + 55% acetone + NaCl solution. The diffusion coefficient decreases as NaCl is added to the solution. Just before the volume phase transition, the diffusion coefficient of the gel decreases by two orders of magnitude. Higher crosslink density gel collapses at higher salt concentration.

The 10C2.7Xl gel undergoes volume phase transition at 11 mM NaCl concentration as seen in Fig. 2.8. The diffusion coefficient of the gel decreases by about two orders of magnitude just before the volume phase transition of the gel takes place. This was also observed by (McCoy and Muthukumar, 2010) for the same gel system. The authors attributed this to structural changes in the gel prior to the imminent volume phase transition.

2.3.5 Ultraviolet/Visible Spectroscopy

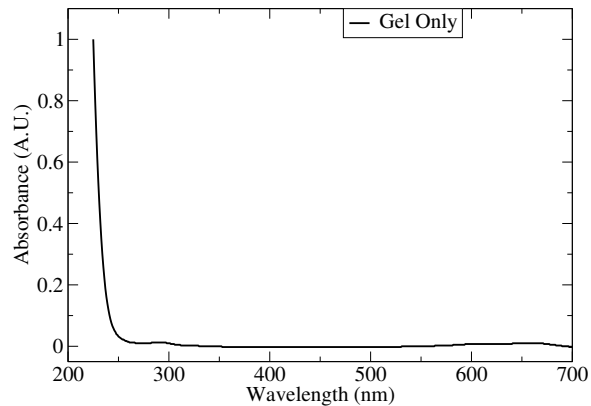


Figure 2.17. UV-Vis spectra for the PAM-PAA gel. The gel does not absorb in visible region, and has an absorption peak in UV region near 220 nm.

The UV-Vis spectra of the gel shown that it does not absorb in the visible region. As a result, a dye-tagged polymer can be studied inside the gel using fluorescence techniques or can be measured in a UV-Vis spectrometer.

2.3.6 Scanning Electron Microscopy

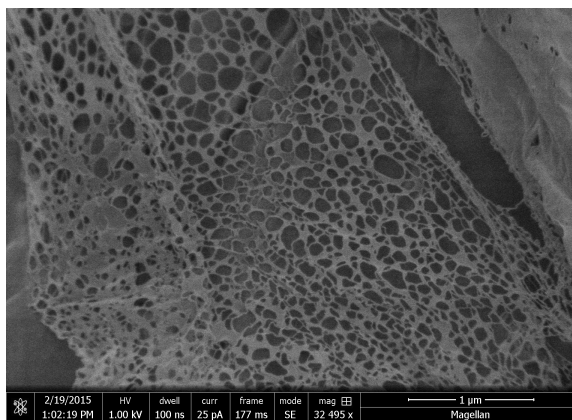


Figure 2.18. SEM image of 10C2-7Xl PAM-PAA gel. The mesh size range from the image is 40 to 150 nm.

The SEM of the gel reveals that the mesh of the gel is similar to that of the mesh size estimated in table 2.3.2.

CHAPTER 3

DIFFUSION OF POLYELECTROLYTES IN POLYELECTROLYTE GELS

3.1 Introduction

In this chapter, the diffusion of polyelectrolyte inside a polyelectrolyte gel is studied using dynamic light scattering. A detailed summary for diffusion of polymers in solutions and in gels has been provided in an earlier chapter. It is briefly summarized here. In dilute solutions, the Zimm dynamics are followed, where the hydrodynamics play an important role in dictating polymer diffusion. When the polymer concentration increases to semi-dilute regime, such that hydrodynamic interactions are screened, the Rouse model is used to describe polymer diffusion. On further increasing the concentration, the reptation model proposed by deGennes is used to explain the diffusion of a polymer chain in an imaginary tube formed by the entangled polymer chains. For diffusion of polymers in gels, other models have been proposed such as Ogston, Phillies etc. which used the concentration of the gel and the size of solute to predict the decrease in diffusion coefficient of the solute inside a gel network (Ogston, Preston and Wells, 1973; Phillies, 1986).

Since polyelectrolytes will be used as probe in this work, it is important to understand the polyelectrolyte dynamics with respect to polymer and salt concentrations. It was shown by many researchers that the polyelectrolytes by itself is an intriguing system in high polyelectrolyte concentrations or low salt concentrations. Two modes are seen when light scattering of a polyelectrolyte solution is done in low salt concentration or high polymer concentration (Drifford and Dalbiez, 1984, 1985; Forster,

Schmidt and Antonietti, 1990; Sedlak, 1996). The fast mode diffusion coefficient in the low salt regime is an order of magnitude higher than the neutral polymer of similar molecular weight while the slow mode diffusion coefficient resembles an aggregate (order of 10^{-8} cm²/s, which corresponds to size in order of 100 nm). The fast mode diffusion coefficient decreases as salt is added to the solution, and resembles that of polymer diffusion in a solution in high salt concentrations (order of 10^{-7} cm²/s which is typical for neutral polymers). The aggregate mode disappears in high salt regime. The fast mode has been attributed to the coupling of dynamics of the counter-ion cloud and the polymer chain in low salt concentration (Muthukumar, 1997; Sedlak, 1999). While the aggregate mode is due to electrostatic interaction which breaks at high salt concentrations. In this chapter, both high and low salt concentrations are used to study polyelectrolyte dynamics in the gel. It is important to note that inside the gel, the aggregate mode is unlikely to be present because of the mesh size of the gel and aggregate size, as well as the electrostatic screening of the aggregate inside the gel.

In this study a crosslinked polyelectrolyte gel is used as a model gel network. Polyacrylamide-co-sodium acrylate gels are used as the matrix to study diffusion of polymers inside these gels. Polyelectrolyte gels undergo volume phase transition in presence of an unfavorable solvent and salt (Ohmine and Tanaka, 1982). The swelling of a polyelectrolyte gel is controlled by the balance of elasticity of gel network, enthalpy of gel and solvent interaction, entropic and osmotic forces of the solvent and the counter-ions. Thus the swelling of the gel can be tuned and controlled by changing various factors of the gel such as charge density, crosslink density, solvent, pH, salt concentration as well as counter-ion valency (Horkay et al., 2002, 2003; Hirotsu, Hirokawa and Tanaka, 1987; Tanaka, 1981; Thiel and Maurer, 1999; Tanaka et al., 1980; English, Tanaka and Edelman, 1997; Ricka and Tanaka, 1984; Tanaka, 1978; English, Tanaka and Edelman, 1997) This change in gel volume, allows us to probe

the effect of mesh size on the diffusion of the probe inside the gel. In this study, three gel systems are synthesized, 10% charge density and 2.7% crosslink density (referred to as 10C2.7Xl) and 10% charge density and 3.5% crosslink density (referred to as 10C3.5Xl) are used to study the effect of crosslink density of the gel. 5% charge density and 2.7% crosslink density (referred to as 5C2.7Xl) is used to study the effect of charge density compared to 10C2.7Xl gel.

These polyelectrolyte gels have been characterized independently for its swelling properties in different solvents and salt concentrations, and corresponding light scattering and rheology measurements have been performed. With the knowledge of these properties of the gel in absence of any polymer chains inside the gel, measurements are made to study the gel properties when polymer chains are present inside the gel. The primary aim of this chapter is to study the diffusion of the polyelectrolyte inside the polyelectrolyte gel using dynamic light scattering. The polymer diffusion is discussed with effects of molecular weight of the probe, crosslink density of the gel, charge density of the gel, salt concentration and solvent. Finally, an attempt is made to identify the regime in which this diffusion takes place (*i.e.* reptation etc.) and determine the mechanism of diffusion in this charged system compared to theories proposed for diffusion of uncharged polymers in uncharged gels.

3.2 Experimental Setup

3.2.1 Gel Synthesis

Gels were synthesized with same procedure as described in previous chapter. Recipe and preparation method for 10C2.7Xl PAM-PAA gel with NaPSS is described below. Other gels are synthesized in similar method. Required amounts of monomers

and crosslinkers are taken for necessary charge density and crosslink density.

Millipore water ($18.2M\Omega$) is stirred with 24.6 ml of 40% (w/v) of Acrylamide solution, 6.7 ml of 20% (w/w) of Sodium Acrylate solution, and 33.0 ml of 2% (w/v) of BisAcrylamide solution and 300 mg of NaPSS was added. The total volume of the solution is 300 ml. Millipore water (235.7 ml) is added to the monomer and crosslinker solution to bring the volume to 300 ml. All the solutions were filtered with 200 nm filter to remove any dust from the pre gel solution. For light scattering experiments, it is important to filter and remove dust from all pre-gel samples. This pre-gel solution is bubbled with Nitrogen gas for 15 minutes to remove any dissolved oxygen which can inhibit the reaction. To polymerize the reaction, TEMED (450 μ l) and Ammonium Persulfate (1.5 ml) is added to the pre-gel solution. The solution is stirred for one minute after addition of the initiator and poured into a tray (1 mm thickness) and casted for two hours at room temperature. The tray is covered with a top plate to prevent wrinkling of the gel. The gel is removed from the tray and cut into pieces. The gel pieces are placed in reservoirs of NaPSS (same concentration as that in gel) and NaCl concentration to equilibrate the gel.

3.2.2 Sample Preparation

3.2.2.1 Dynamic Light Scattering

Samples for light scattering are prepared by two methods. A light scattering tube was thoroughly rinsed with soap water first and then acetone later to remove any dust in the tube. The light scattering samples were prepared by placing a piece of gel (synthesized without NaPSS) inside the tube and excess solution of NaPSS in NaCl (either in water or 55% Acetone + 45% water mixture). The gel was allowed to equilibrate for 48 hours to allow polymer diffuse inside the gel. Light scattering

experiments were performed on this sample. Experiments repeated after two weeks on the same samples ensured that the gel and polymer system had reached equilibrium after two days.

Another method of sample preparation was to prepare the same pre-gel solution (monomers, crosslinker and NaPSS) and synthesizing gel in DLS tube. This pre-gel solution is also bubbled with Nitrogen gas for 15 minutes to remove any dissolved oxygen which can inhibit the reaction. A concern in the previous method is if impurities present in Nitrogen line are being transferred into the pre-gel solution. Thus in this method, the pre-gel solution was filtered after the bubbling of Nitrogen gas through the solution into light scattering tube. Required amount filtered TEMED and Ammonium Persulfate were added to the light scattering tube. The tube was gently shaken to mix the initiator uniformly in the solution. After two hours, filtered solution of NaPSS (same concentration as in gel) and NaCl was added to the tube.

3.2.2.2 Rheology

Rheology experiments were performed with same procedure as described in previous chapter. The samples were synthesized and equilibrated with NaPSS and NaCl solutions as described above.

3.3 Results and Discussion

Light scattering of gel systems is quite complicated and studying diffusion of a probe in these gels, results in even greater complications, especially for interpretation of the data. Thus, this section begins with discussing the simplest case at high salt concentration where the gel heterogeneities are not seen in the intensity correlation function as discussed in previous chapter.

3.3.1 Light Scattering at High NaCl Concentrations

It is important to characterize the probe alone at same NaCl concentration individually to understand the impact on decreased diffusion coefficient of the probe inside the gel. Advantage of using high salt for light scattering of NaPSS is the polyelectrolyte slow mode is absent. This aggregate slow mode is present at low NaCl concentrations and is dependent on the ratio of polymer concentration to the salt concentration in the solution (Forster, Schmidt and Antonietti, 1990; Sedlak and Amis, 1992). Light scattering on a gel and a polyelectrolyte in low salt concentrations is complex due to presence of additional modes from gel as well as NaPSS which make data analysis difficult. Thus using high NaCl concentration, where the gel alone has only one mode (which is q^2 dependent) and the probe alone also has only one mode (which is q^2 dependent), helps in understanding the gel + probe system better.

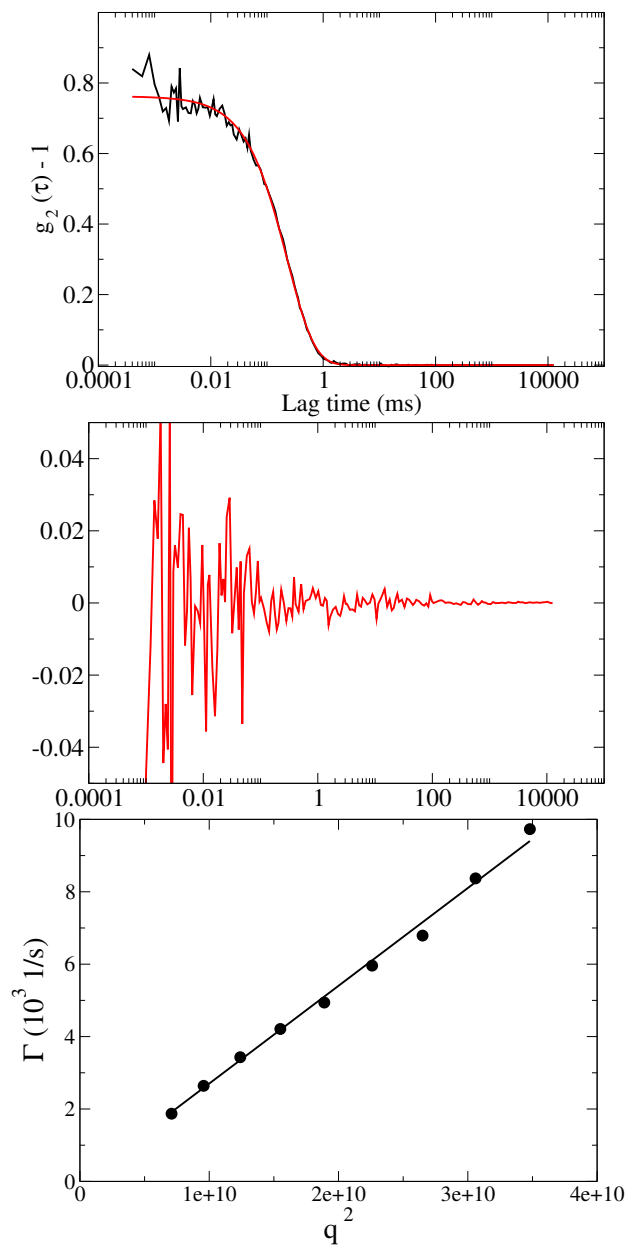


Figure 3.1. Light scattering data for the NaPSS127k (1 mg/ml) + 100 mM NaCl. (Top) Correlation function with one diffusive mode. Black line corresponds to the correlation function and the red line is the data fitting for single mode; (Middle) Residuals of the single mode data fitting. (Bottom) The diffusion coefficient is calculated from the slope of the linear fit of Γ vs. q^2 plot.

One mode is present when light scattering measurement is performed on the polymer alone in in 100 mM NaCl solution as seen in Fig. 3.1. Similarly, the gel alone in 100 mM NaCl solution also has only one mode as has been discussed in detail in pre-

vious chapter. Thus now we discuss light scattering data when the gel and polymer are synthesized together.

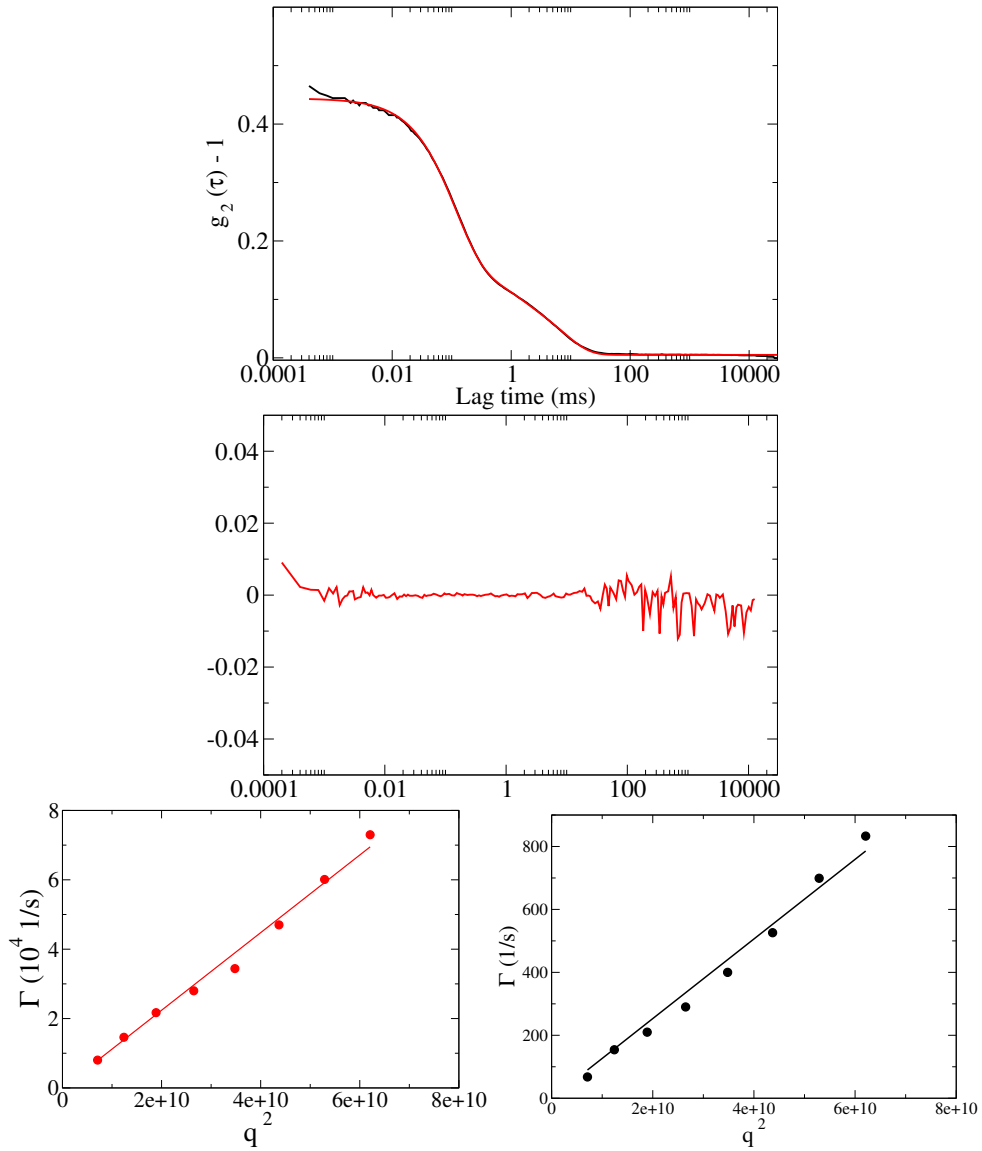


Figure 3.2. Light scattering data for the 10C2-7Xl gel + NaPSS127k (1 mg/ml) + 100 mM NaCl. (Top) Correlation function with two diffusive modes. Black line corresponds to the correlation function and the red line is the data fitting for two modes; (Middle) Residuals of the two mode data fitting. (Bottom) The diffusion coefficient is calculated from the slope of the linear fit of Γ vs. q^2 plot for both modes. Both modes have a q^2 dependence.

Light scattering of the gel + NaPSS reveals that two modes are present when the polymer is added to the gel as seen in Fig. 3.2. Both the polymer as well as the 10C2.7X1 gel in 100 mM NaCl solution show only one mode. Additionally, the the first mode from the gel + NaPSS sample is very similar to the diffusion coefficients of the gel alone, and probe alone as well. Hence, it is important to understand what these two modes represent.

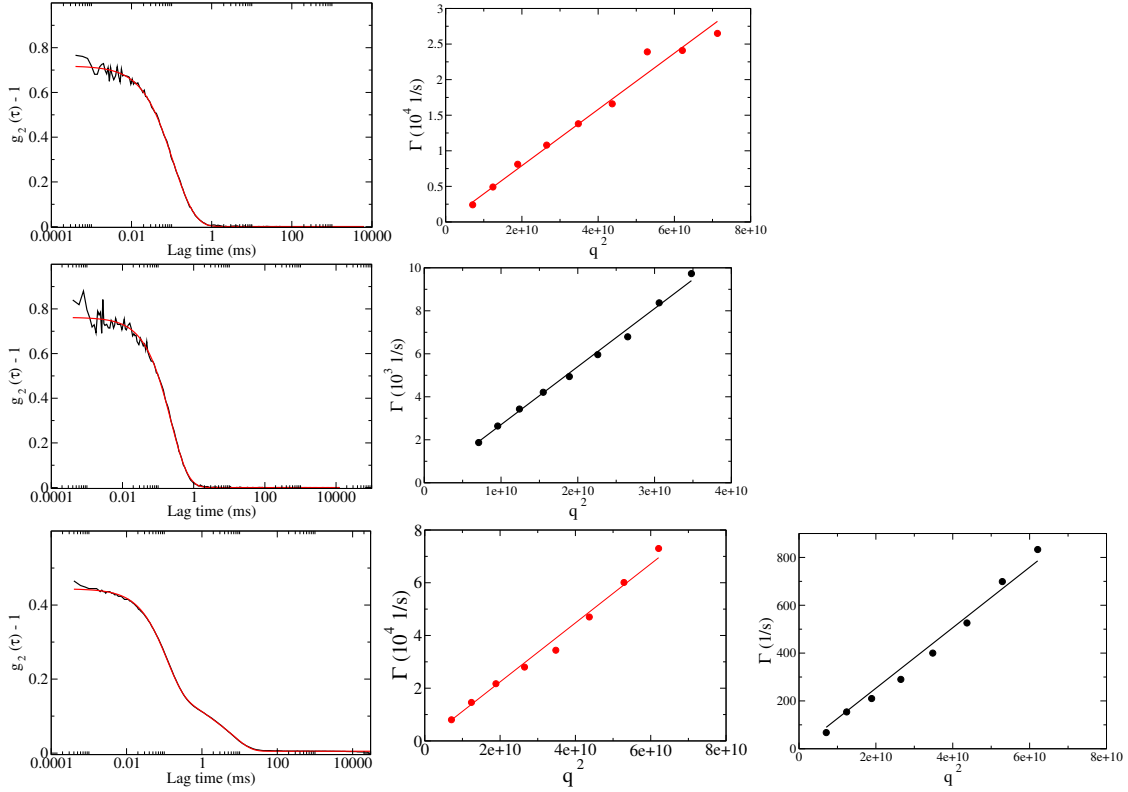


Figure 3.3. Comparison of correlation function and diffusive modes for the gel and the probe individually and when combined together. The first column represents correlation functions for samples 10C2.7X1 + 100 mM NaCl, NaPSS127k (1 mg/ml) + 100 mM NaCl and 10C2.7X1 + NaPSS127k (1 mg/ml) + 100 mM NaCl respectively. The second and third columns are Γ vs. q^2 plots for the same samples. (First Row) 10C2.7X1 + 100 mM NaCl (left) Correlation function with one diffusive mode. Black line corresponds to the correlation function and the red line is the data fitting for single mode; (right) The diffusion coefficient is calculated from the slope of the linear fit of Γ vs. q^2 plot. (Second Row) NaPSS127k (1 mg/ml) + 100 mM NaCl (left) Correlation function with one diffusive mode. Black line corresponds to the correlation function and the red line is the data fitting for single mode; (right) The diffusion coefficient is calculated from the slope of the linear fit of Γ vs. q^2 plot. (Third Row) 10C2.7X1 + NaPSS127k (1 mg/ml) + 100 mM NaCl (left) Correlation function with two diffusive modes. Black line corresponds to the correlation function and the red line is the data fitting for two modes; (middle and right) The diffusion coefficient is calculated from the slope of the linear fit of Γ vs. q^2 plot for each mode.

In Fig. 3.3, the correlation functions of the 10C2.7X1 gel in 100 mM NaCl solution, NaPSS in 100 mM NaCl solution and 10C2.7X1 gel + NaPSS in 100 mM NaCl solution are all compared. An additional mode is present when the polymer is added to

	D_1 (10^{-7} cm ² /s)	D_2 (10^{-7} cm ² /s)
Only Gel	4.5	-
Only NaPSS	2.7	-
Gel + NaPSS	4.1	0.1

Table 3.1. Comparison of diffusion coefficient from light scattering experiments for the 10C2.7Xl gel in 100 mM NaCl solution, NaPSS in 100 mM NaCl solution and 10C2.7Xl gel + NaPSS in 100 mM NaCl solution

the gel. Other researchers have observed an additional mode when a probe molecule was introduced to the gel. As discussed earlier, Shibayama et al. observed only one mode for PNIPAM gels, and on addition of probe to the gel, another diffusive mode at longer time scales was observed, which they attributed to probe diffusion inside the gel (Shibayama et al., 1999). However, in other experiments, multiple modes were observed from the gel alone as is seen in Fig. 3.4, which did not have q^2 dependence. Pajevic and coworkers studied the diffusion of PMMA in PMMA gel, in addition to the modes observed from the gel, they observed an additional mode which they attributed to the probe diffusion (Pajevic, Bansil and Konak, 1991, 1993). It is also important to note the two diffusion coefficients from the gel + NaPSS light scattering data are an order of magnitude apart. The diffusion coefficient of the second mode is an order of magnitude different from the diffusion coefficient of the gel alone or the probe alone as well. As has been observed by others (Shibayama et al., 1999; Lodge and Rotstein, 1991; Pajevic, Bansil and Konak, 1991, 1993). Diffusion coefficients from all three samples are summarized in table 3.1.

One can expect two modes to be present when the gel and polymer are synthesized together. A polymer mode, which is affected due to the presence of the matrix surrounding it, and a gel mode, which may or may not be affected by the polymer chains inside the gel. The gel mode may not be affected since the concentration of

polymer chains in the gel is very small compared to the concentration of the gel. In this particular example, the sample shown in Fig. 3.3 and data from table 3.1, the concentration of gel is 40 mg/ml while that of polymer is 1 mg/ml.

3.3.2 Light Scattering at Low NaCl Concentrations in Water

Light scattering in low NaCl concentrations is complicated because of multiple modes present in the light scattering of the gel alone as well as NaPSS alone. Thus it is difficult to ascertain the modes when light scattering of Gel + NaPSS is performed in low NaCl concentrations.

In low NaCl concentrations in water as solvent, the gel alone sample has two modes. One mode is q^2 dependent while the other mode does not have q^2 dependence. The NaPSS alone sample also has two modes which are both q^2 dependent. The first mode of NaPSS has diffusion coefficient similar to the gel diffusion coefficient and the second mode which is the aggregate mode has diffusion coefficient an order of magnitude smaller (10^{-8} cm²/s). When the gel + NaPSS are synthesized together and equilibrated with NaPSS in 10 mM NaCl solution, the correlation function is compared to that of gel in 10 mM NaCl solution and of NaPSS (5 mg/ml) in 10 mM NaCl solution in Fig. 3.4.

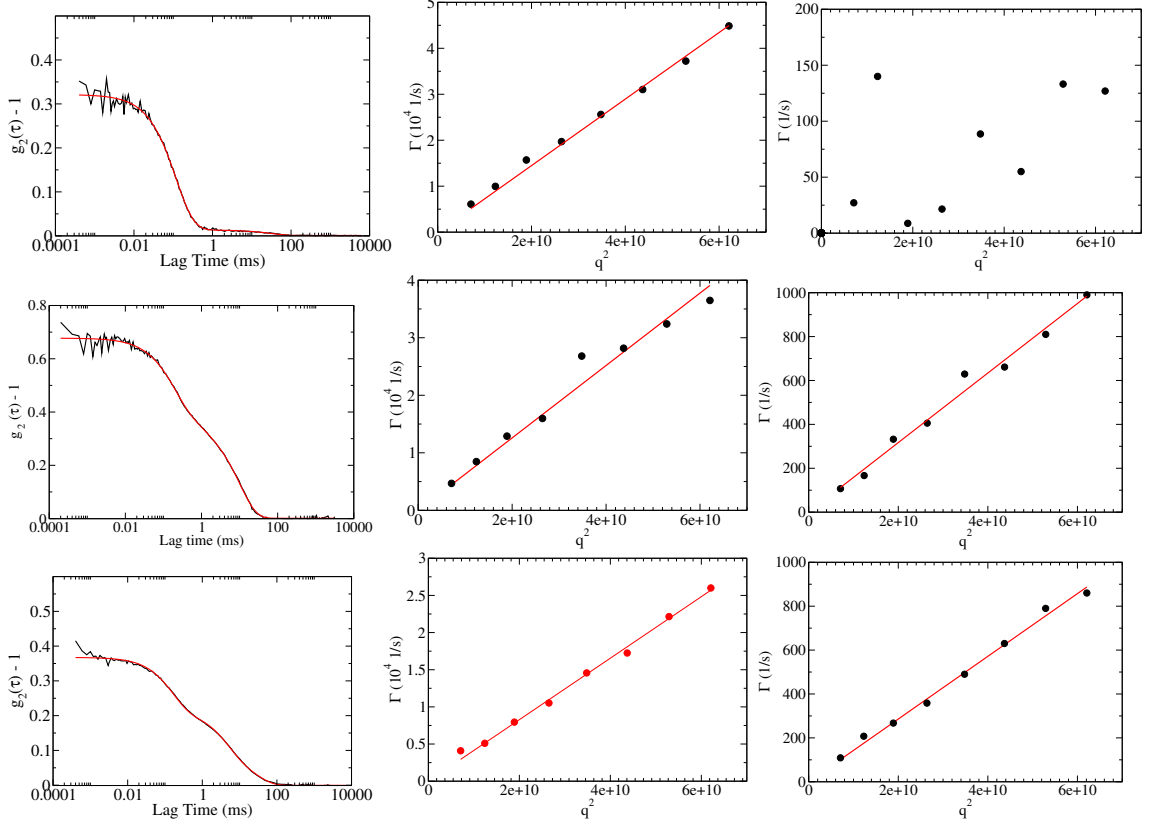


Figure 3.4. Comparison of correlation function and diffusive modes for the gel and the probe individually and when combined together at 10 mM NaCl concentration. The first column represents correlation functions for samples 10C2.7Xl + 10 mM NaCl, NaPSS127k (5 mg/ml) + 10 mM NaCl and 10C2.7Xl + NaPSS127k (5 mg/ml) + 10 mM NaCl respectively. The second and third columns are Γ vs. q^2 plots for the same samples. (First Row) 10C2.7Xl + 10 mM NaCl (left) Correlation function with two modes. Black line corresponds to the correlation function and the red line is the data fitting for two modes; (middle and right) The diffusion coefficient is calculated from the slope of the linear fit of Γ vs. q^2 plot. The second mode does not have a q^2 dependence. (Second Row) NaPSS127k (5 mg/ml) + 10 mM NaCl (left) Correlation function with two diffusive modes. Black line corresponds to the correlation function and the red line is the data fitting for two modes; (middle and right) The diffusion coefficient is calculated from the slope of the linear fit of Γ vs. q^2 plot for each mode. (Third Row) 10C2.7Xl + NaPSS127k (5 mg/ml) + 10 mM NaCl (left) Correlation function with two diffusive modes. Black line corresponds to the correlation function and the red line is the data fitting for three modes; (middle and right) The diffusion coefficient is calculated from the slope of the linear fit of Γ vs. q^2 plot for each mode (Third mode does not have a q^2 dependence is not shown).

From the Fig. 3.4, the gel + NaPSS sample has two modes that are q^2 dependent. The first mode in the gel + NaPSS sample has diffusion coefficient similar to that of the gel alone sample as well as that of the fast mode in NaPSS alone sample. As was discussed in previous section, this mode may correspond to either the gel or the polymer. The second mode of the gel + NaPSS sample has many possibilities as well, it may represent the gel being affected by the polymer chain, or that of polymer chains diffusing in the gel, or that of the aggregate mode inside the gel. From the estimates of mesh size of the gel ($\xi \sim 30$ nm), and the hydrodynamic radius of the aggregate calculated from Stokes-Einstein equation ($R_H \sim 100$ nm), we can assume that the aggregate mode is not present inside the gel. Thus the second mode represents the gel being affected by the polymer or the polymer diffusion inside the gel. Other possibilities for the second mode are discussed in section 3.3.4.

3.3.3 Characterization of Two Modes

In this section, we try to understand what the first mode in light scattering of gel + NaPSS represents. If the mesh size is large enough such that the polymer chain has no constraints on its diffusion, its diffusion coefficient will be similar to that in solution. But from the estimated values of mesh size, we do expect the diffusion coefficient of the probe to decrease inside the gel matrix. The other possibility of the first mode is that of the polymer gel. Since the NaPSS is in such small concentration, the gel diffusion coefficient may not be affected by the polymer chain and thus the diffusion coefficient of the gel in presence and absence of NaPSS remains similar (at least in the same order of magnitude). From previous chapter, it has been discussed based on Tanaka's work, the relationship between the diffusion coefficient of the gel (D), its shear modulus (G) and its friction coefficient ($D \sim G/f$). Also, it was established the scaling of the friction coefficient (f) with the volume fraction (ϕ) is $f \sim \phi^{1.3}$. Next, measurements for volume fraction of the gel in presence of NaPSS

and NaCl solution, and modulus of the gel in presence of NaPSS and NaCl solution are discussed. These measurements will be used to estimate the diffusion coefficient of the gel. The estimated value of gel diffusion coefficient ($D_{estimated}$) can be compared to experimentally measured diffusion coefficient of the first mode ($D_{experimental}$) to determine whether the first mode corresponds to gel or the probe.

3.3.3.1 Swelling Ratio

Swelling ratio measurements of the 10C2.7Xl in NaPSS and NaCl solution are reported. The volume fraction ϕ is used later in Eq. 3.3.

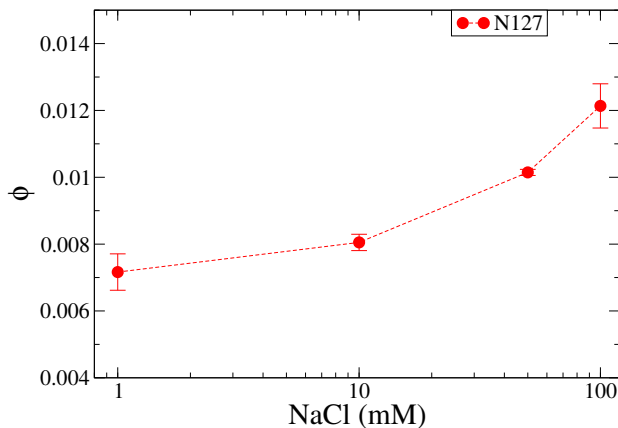


Figure 3.5. Effect on swelling of gel as a function of NaPSS and NaCl concentration. NaPSS concentration is kept constant at 5 mg/ml (24 mM monomer concentration). As more salt is added to the system, the Donnan potential decreases resulting in deswelling of the gel. Thus the volume fraction (ϕ) increases as more salt is added

Since, NaPSS also has charges on its backbone as well as counterions, it acts as salt, in effectively reducing the Donnan potential. As a result the gel deswells even more when NaPSS is present along with NaCl in the solution. This can be seen by comparing the volume fractions of the gel at same NaCl concentration with and without NaPSS.

3.3.3.2 Rheology

Modulus measurements of the 10C2.7Xl in NaPSS and NaCl solution are reported. The modulus G is used later in Eq. 3.3.

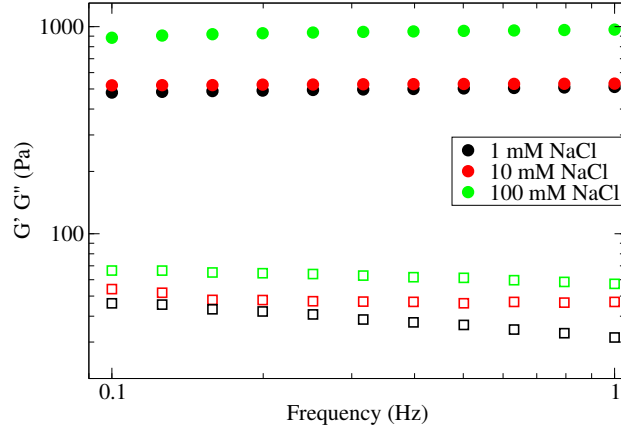


Figure 3.6. Rheology data for the 10C2.7Xl gel + NaPSS127k (5mg/ml) + NaCl.

The modulus of the gel in presence of NaPSS increases compared to in absence of NaPSS at same NaCl concentration. As the volume fraction of the gel increases in presence of NaPSS, the modulus is expected to increase in presence of NaPSS as well.

$$D = \frac{G}{f} \quad (3.1)$$

From Eq. 2.25 from chapter 2, the relationship between the friction coefficient of the gel (f) and the volume fraction (ϕ) was established.

$$f \sim \phi^{1.3} \quad (3.2)$$

Using the values of modulus (G_B) from Fig. 2.10, diffusion coefficient (D_B) from Fig. 2.13 and volume fraction (ϕ_B) from Fig. 2.7 of the gel (at same NaCl concentra-

NaCl (mM)	$D_{experimental}$ (10^{-7} cm ² /s)	$D_{estimated}$ (10^{-7} cm ² /s)
1	6.5	5.6
10	7.1	5.1
100	3.7	4.7

Table 3.2. Comparison of diffusion coefficient from light scattering experiments and diffusion coefficient estimated using Eq. 3.3

tion but without NaPSS) as the reference values, the diffusion coefficient of the gel in presence of NaPSS can be estimated using Eq. 3.3.

$$\frac{D_A}{D_B} = \frac{G_A}{G_B} \left(\frac{\phi_A}{\phi_B} \right)^{1.3} \quad (3.3)$$

The modulus (G_A) from Fig. 3.6 and volume fraction from Fig. 3.5 of the gel (at same NaCl concentration with NaPSS) are used to estimate the diffusion coefficient of the gel (D_A) in presence of NaPSS.

The values of diffusion coefficient reported in table 3.2 for the experimentally measured and the estimated diffusion coefficient are in agreement with each other. The second mode obtained from light scattering of 10C2.7Xl gel + NaPSS + NaCl sample is an order of magnitude smaller ($D \sim 10^{-8}$ cm²/s) than the first mode which is shown in table 3.2. Thus we conclude that the first mode observed in the dynamic light scattering of a gel + NaPSS + NaCl sample corresponds to the gel. The question of second mode will be addressed later in further discussions. It should also be noted that value of D_1 reported in table 3.1 and $D_{experimental}$ in table 3.2, is different for 100 mM NaCl, because of different concentrations of NaPSS used in synthesis of Gel + NaPSS sample.

3.3.4 Light Scattering at Low NaCl Concentrations in 55% Acetone + 45% Water mixture

As was the case in previous section, when low NaCl concentration is used in water as solvent, the gel alone sample has two modes in presence of 55% Acetone and NaCl as well. One mode is q^2 dependent while the other mode does not have a q^2 dependence. The NaPSS alone sample also has two modes which are both q^2 dependent. The first mode has diffusion coefficient similar to the gel diffusion coefficient and the second mode which is the aggregate mode has diffusion coefficient an order of magnitude smaller (10^{-8} cm²/s).

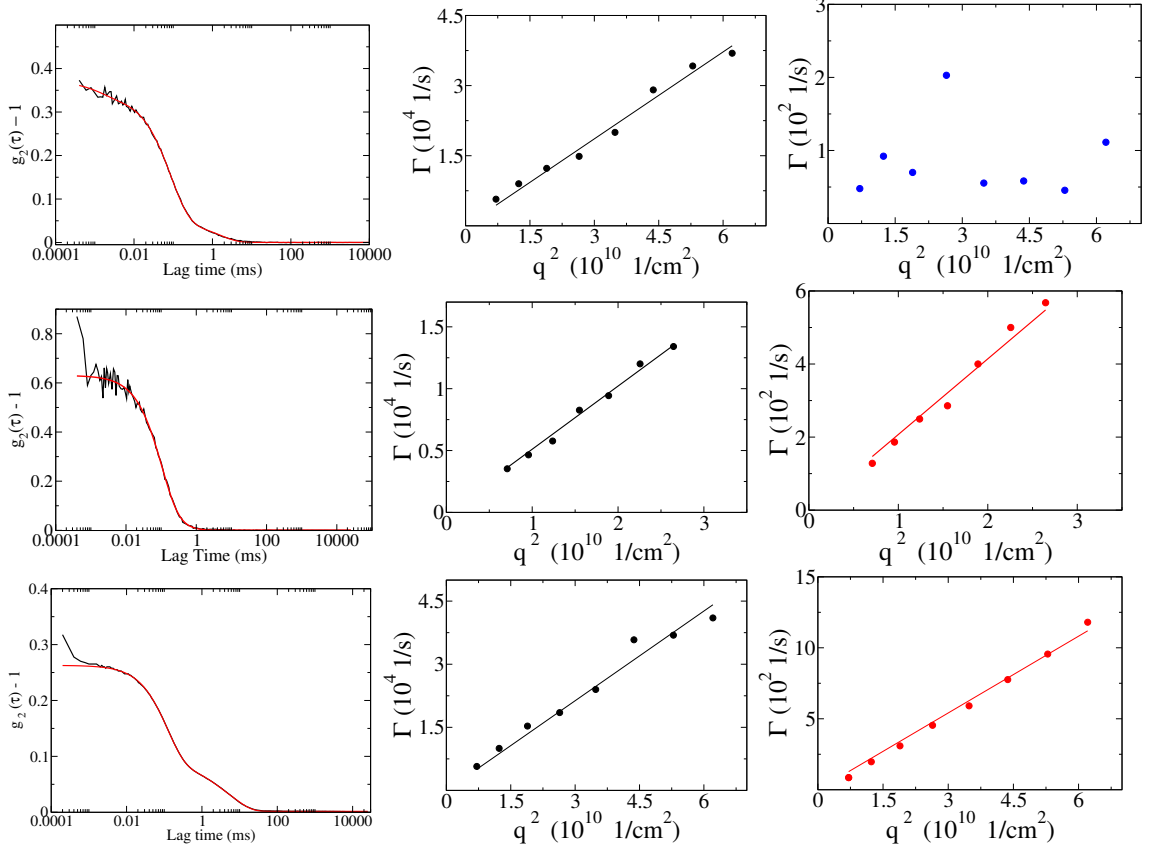


Figure 3.7. Comparison of correlation function and diffusive modes for the gel and the probe individually and when combined together in 55% Acetone + 6 mM NaCl concentration. The first column represents correlation functions for samples 10C2.7X1 + 55% Acetone + 6 mM NaCl, NaPSS127k (5 mg/ml) + 55% Acetone + 6 mM NaCl, and 10C2.7X1 + 55% Acetone + 6 mM NaCl respectively. The second and third columns are Γ vs. q^2 plots for the same samples. (First Row) 10C2.7X1 + 55% Acetone + 6 mM NaCl (left) Correlation function with two modes. Black line corresponds to the correlation function and the red line is the data fitting for two modes; (middle and right) The diffusion coefficient is calculated from the slope of the linear fit of Γ vs. q^2 plot. The second mode does not have a q^2 dependence. (Second Row) NaPSS127k (5 mg/ml) + 55% Acetone + 6 mM NaCl (left) Correlation function with two diffusive modes. Black line corresponds to the correlation function and the red line is the data fitting for two modes; (middle and right) The diffusion coefficient is calculated from the slope of the linear fit of Γ vs. q^2 plot for each mode. (Third Row) 10C2.7X1 + NaPSS127k (5 mg/ml) + 55% Acetone + 6 mM NaCl (left) Correlation function with two diffusive modes. Black line corresponds to the correlation function and the red line is the data fitting for three modes; (middle and right) The diffusion coefficient is calculated from the slope of the linear fit of Γ vs. q^2 plot for each mode (Third mode does not have a q^2 dependence is not shown).

From the Fig. 3.7, the gel + NaPSS sample has two modes that are q^2 dependent. The first mode has diffusion coefficient which is similar to the gel alone sample. As has been established previously, this mode corresponds to the gel. The second mode of the gel + NaPSS sample has two possibilities, either that of polymer chains diffusing in the gel, or that of the aggregate mode inside the gel. From the estimates of mesh size of the gel ($\xi \sim 16$ nm), and the hydrodynamic radius of the aggregate calculated from Stokes-Einstein equation ($R_H \sim 100$ nm), we can assume that the aggregate mode is not present inside the gel. Thus, the diffusion coefficient can be ascertained to polymer diffusion inside the gel. However, it must be noted that other possibilities do exist such as that of heterogeneties inside the gel (which did not have a q^2 dependence) have a q^2 dependence due to electrostatic interactions between the polymer chain and the gel. As will be discussed in coming pages, the effect of crosslink density, charge density and volume fraction of the gel on the diffusion coefficient obtained from the second mode, clearly indicate that the second mode corresponds to the diffusion of the polymer inside the gel. Thus the second mode is described as the probe diffusion inside the gel in further discussions.

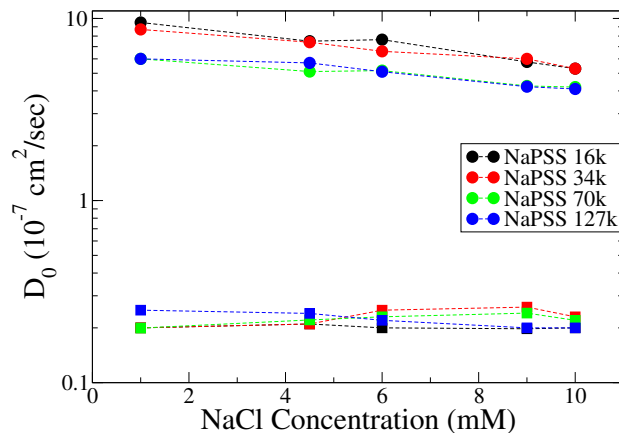


Figure 3.8. Diffusion coefficient of NaPSS alone in 55% Acetone + NaCl solution. Two diffusive modes are reported.

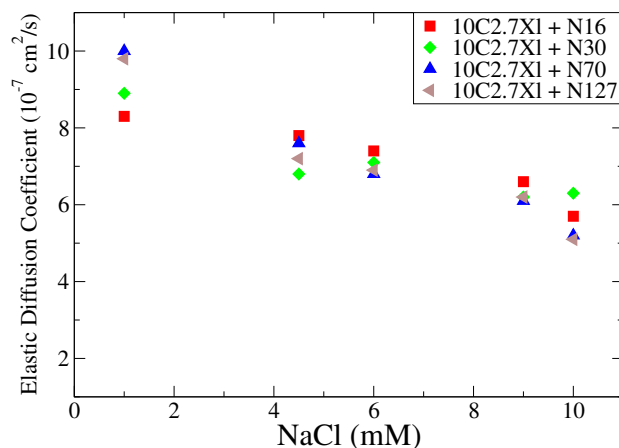


Figure 3.9. Diffusion coefficient of the 10C2.7X1 gel in NaPSS + 55% Acetone + NaCl solution. Effect of molecular weight of NaPSS and NaCl concentration of gel diffusion is shown. The gel diffusion coefficient is similar to that in absence of NaPSS.

The first mode is shown in Fig. 3.9, this mode attributed to the diffusion coefficient of the gel, does not change much compared to the diffusion coefficient of the gel in absence of NaPSS. Also, the diffusion coefficient of the gel does not decrease two orders of magnitude at 10 mM NaCl concentration. In the next section, the diffusion coefficient of the second mode, attributed as the diffusion of the probe inside the gel is reported.

3.3.4.1 Diffusion Coefficient of Probe in the Gel

In this section, the diffusion coefficient from the second mode obtained from light scattering of gel + NaPSS is discussed. The diffusion coefficient of the second mode or probe diffusion coefficient is referred as D_2 is further discussions.

The Fig. 3.10 shows diffusion coefficient of the probe inside the gel as a function of molecular weight of the probe. The probe diffusion inside the gel decreases as NaCl is added, as observed in Fig. 3.10. As NaCl concentration is increased, the gel deswells due to Donnan equilibrium. Thus, addition of NaCl, effectively decreases the mesh size of the gel. Smaller mesh size results in greater hindrance for the diffusion of the

probe, resulting in slower diffusion in the gel matrix.

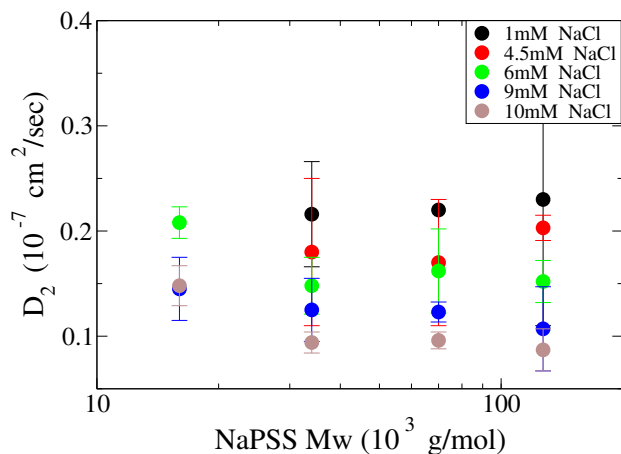


Figure 3.10. Diffusion coefficient of NaPSS diffusion in the 10C2.7Xl gel in 55% Acetone + NaCl solution. Effect of molecular weight of NaPSS and NaCl concentration of probe diffusion is shown.

Effect of molecular weight of the probe on the diffusion coefficient of the probe inside the gel is also shown in the Fig. 3.10. As the molecular weight of the probe increases, probe size increases. For fixed NaCl concentration, the mesh size of a gel remains constant. Thus changing the molecular weight of the probe for fixed NaCl concentration should result in increased levels of confinement for the higher molecular weight probes. One can expect the probe diffusion to decrease because of more confinement on the higher molecular weight probe. But from the Fig. 3.10, as the size of the probe increases, we observe that the diffusion has a weak or negligible dependence on the molecular weight of the probe. Thus we can infer that the 10C2.7Xl gel does not impose strong confinement on the polymer diffusion.

3.3.4.2 Effect of Crosslink Density

To understand the effect of crosslink density on the diffusion of the negatively charged probe in the negatively charged polyelectrolyte gel, a gel of different crosslink

density (3.5%) was synthesized compared to a previous gel of 2.7% crosslink density. Both gels have the same charge density of 10%, to ensure that the electrostatic interaction between the negatively charged polymer chain and the gel matrix backbone which is also negatively charged remains constant.

As the crosslink density of the gel increases, the mesh size decreases for a constant charge density. Thus, 10C3.5Xl has smaller mesh size compared to 10C2.7Xl. The probe diffuses slower in higher crosslink density 10C3.5Xl gel (smaller mesh gel) compared to the 10C2.7Xl gel. The size of the probe compared to mesh size of the gel is important in deciding whether the probe faces any barriers moving through the matrix.

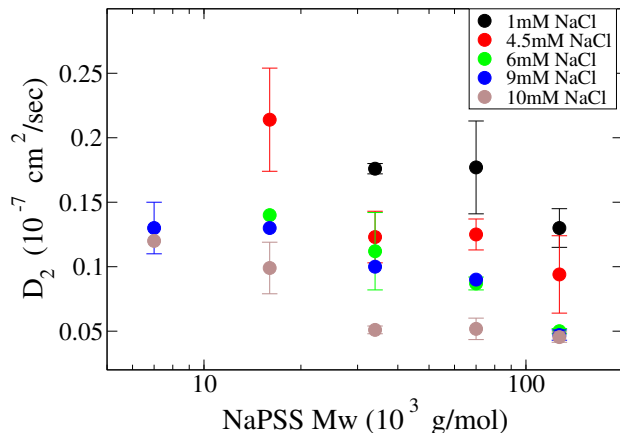


Figure 3.11. Diffusion coefficient of NaPSS diffusion in the 10C3.5Xl gel in 55% Acetone + NaCl solution. Effect of molecular weight of NaPSS and NaCl concentration of probe diffusion is shown.

As seen in the lower crosslink density gel, in the Fig. 3.10, the probe diffusion in the gel does not have a strong dependence on the molecular weight of the probe. But when the crosslink density of the gel is increased, the effect of molecular weight on the probe is seen. This is seen in Fig. 3.11. This may be the case because of the mesh of the 10C2.7Xl gel is not small enough to impose constraints on polymer diffusion

on the gel. But on increasing the crosslink density of the gel, the 10C3.5Xl gel, which has smaller mesh size, imposes sufficient constraints on polymer diffusion that the effect of molecular weight of the probe is observed.

3.3.4.3 Effect of Charge Density

To understand the electrostatic contributions to the diffusion of the negatively charged probe in the negatively charged gel, a gel of different charge density (5%) was synthesized compared to a previous gel of 10% charge density. Both gels have the same crosslink density of 2.7%, to ensure that the molecular weight between crosslinks remains constant. The electrostatic repulsion between the negatively charged polymer chain and the gel matrix backbone which is also negatively charged, could lead to slower diffusion of the probe inside the matrix.

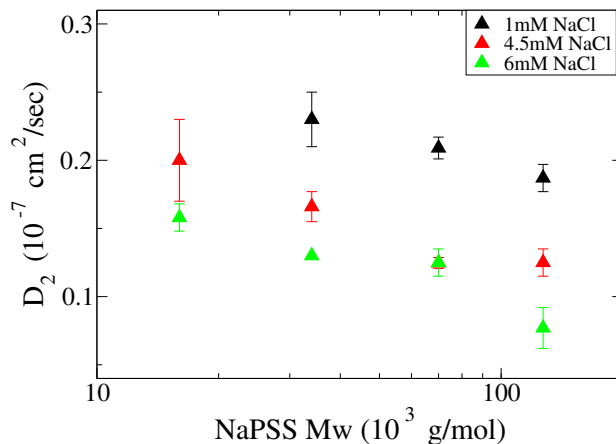


Figure 3.12. Diffusion coefficient of NaPSS diffusion in the 5C2.7Xl gel in 55% Acetone + NaCl solution. Effect of molecular weight of NaPSS and NaCl concentration of probe diffusion is shown.

Either chain entropy or electrostatics or both can contribute to the decrease in the diffusion coefficient of the polymer chain inside the gel mesh. Changing charge density of the gel affects the probe diffusion through two processes; change in mesh

size of the gel due to Donnan equilibrium and change in electrostatic repulsion between the probe and gel matrix (as both are negatively charged). To understand the contribution of electrostatics, the Debye length in the 55% Acetone + NaCl solutions will need to be considered. The Debye length is tabulated in appendix. Comparing the Debye length to the estimated mesh size in earlier chapter, we can expect that the contribution due to electrostatics to be negligible. Thus the mesh size of the gel will play an important role in dictating the diffusion of the polymer chain inside the polymer gel.

The diffusion of NaPSS in 5C2.7Xl is slower than in 10C2.7Xl at all molecular weights of the probe and all NaCl concentrations. As the 5C2.7Xl gel has lower charge density, the gel does not swell as much as 10C2.7Xl. Hence, it has higher dry gel content, resulting in smaller mesh size. Thus we would expect slower diffusion inside the 5C2.7Xl gel compared to 10C2.7Xl gel.

3.3.4.4 Effect of Volume Fraction

Various models have been proposed to explain diffusion of polymers in concentrated solutions or in confined systems. These models are dependent upon the concentration of the polymer-solvent system or that of confinement. When the polymer chains are concentrated such that they entangle, deGennes proposed the reptation model to explain polymer diffusion inside frozen topological environments. The polymer chain is allowed to move to and fro inside an imaginary tube, resulting in scaling form of $D \sim N^{-2}$. Many experiments have supported this scaling argument (Pajevic, Bansil and Konak, 1991; Wheeler and Lodge, 1989; Pajevic, Bansil and Konak, 1993; Zettl et al., 2009), where they concluded that the diffusion process followed the reptation model. Similarly, Ballauff and coworkers, used fluorescence correlation

spectroscopy, to study diffusion of dye labeled polystyrene chain in a semi-dilute solution, where they observed $D \sim N^{-2}$ (Zetzl et al., 2009).

As seen from Figs. 3.10, 3.11 and 3.12, the diffusion coefficient of the probe has a weak dependence on the molecular weight of the probe. Thus it is important to understand the regimes in which the reptation model is applicable and whether the given system can be described in that regime. From the measurements of the hydrodynamic radius (R_H) and the estimated mesh for the gel (ξ), the mesh size is greater than the hydrodynamic radius of the probe by a factor of 3 to 8 ($\xi/R_H = 3 - 8$). Thus the reptation model is not applicable for this system, as the probe which is smaller than the gel mesh, is not confined to a tube as described by the reptation process.

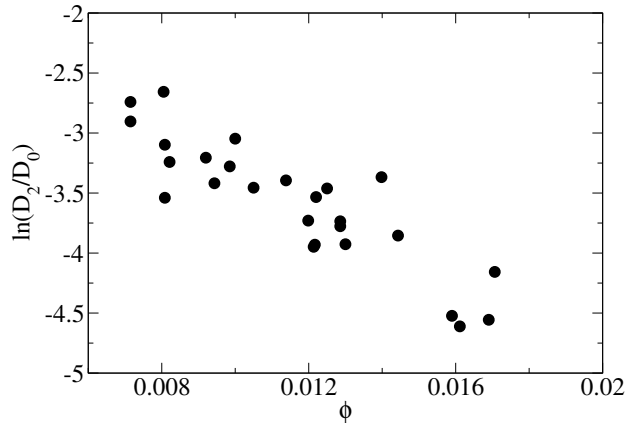


Figure 3.13. Diffusion coefficient of NaPSS in the gel in 55% Acetone + NaCl solution normalized by diffusion coefficient of NaPSS in the 55% Acetone + NaCl solution. The normalized diffusion coefficient is linear to volume fraction ϕ in the semi-log plot.

There are several theories besides the reptation model to explain the diffusion of a solute in a gel (Masaro and Zhu, 1999; Petit et al., 1996). These theories are based on obstruction effect of the network. Ogston et al. used solute size as well as size of the gel network strand to estimate slowing of solute diffusion inside the gel

(Ogston, Preston and Wells, 1973). Similarly, Phillies used a stretched exponential, *i.e.* $D = D_0 \exp(-\alpha c^\beta)$ where α and β are parameters and c represents concentration of the dry gel content in the gel (Phillies, 1986). Many experiments using FCS, to study diffusion of small molecules in swollen gel networks, used the model by Phillies to explain their data (Michelman-Ribeiro et al., 2004; Liu et al., 2005; Fatin-Rouge et al., 2006; Michelman-Ribeiro et al., 2007). These proposed theories try to explain the diffusion process in confined environments.

From Fig. 3.13, we observe that the normalized diffusion coefficient of the NaPSS in the gel can be explained by an equation proposed by Phillies, $D = D_0 \exp(-\alpha\phi)$. The power dependence of $\ln(D/D_0)$ vs. ϕ is not commented because of small range of ϕ that is experimentally accessible.

3.3.4.5 Effect of Sample Preparation

As was discussed earlier, the samples are prepared using two different sample preparation methods to methodically overcome the presence of dust in the gel. The diffusion coefficient of the second mode is reported in the Fig. 3.14. The diffusion of the probe in the gel is not affected by the sample preparation method chosen.

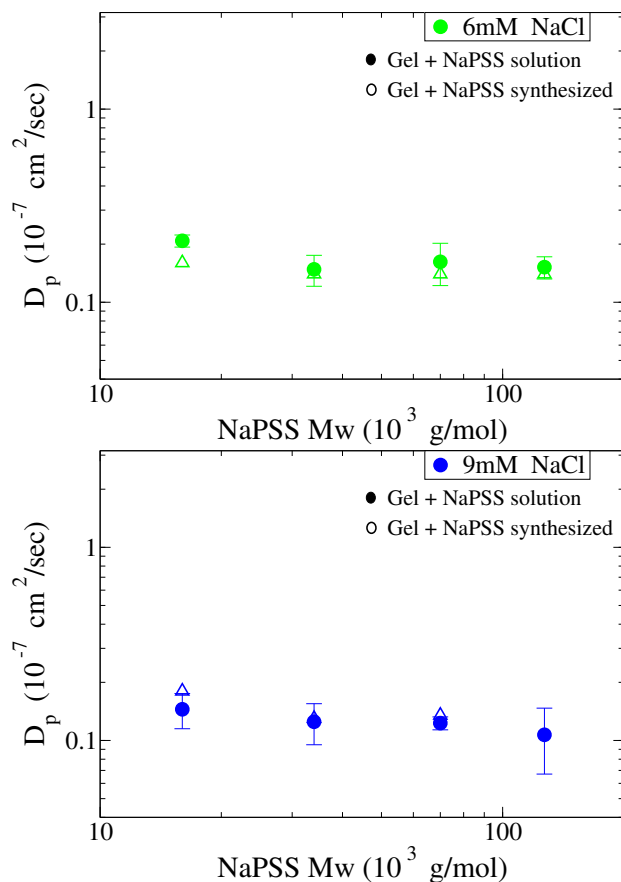


Figure 3.14. Diffusion coefficient of NaPSS in the gel in 55% Acetone + NaCl solution is compared for two different sample preparation methods. The diffusion coefficients obtained from both methods are reasonably within error.

3.4 Conclusion

Diffusion of NaPSS in a polyelectrolyte gel was studied using light scattering to understand the effect of chain confinement and electrostatic interactions on the diffusion of the probe through the matrix. Two diffusive modes were observed in the light scattering experiments. The first mode corresponds to the gel dynamics. The dynamics of the gel are unaffected by the presence of polyelectrolyte chains inside the gel. The second mode is attributed to the diffusion of the polymer inside the gel. The dynamics of the polymer are significantly affected by the gel network. Another interesting conclusion, in contrast to the conclusions for diffusion of an uncharged

probe in the gel matrix (discussed in the next chapter), dynamics of the polymer are not coupled with the gel dynamics *i.e.*, the probe diffusion is not affected near the collapse transition of the gel.

Effect of crosslink density and charge density of the gel were studied on the probe diffusion along with the effect of salt concentration. The probe diffusion constant decreased as the crosslink density of the gel increases due to stronger confinement imposed by smaller mesh size of the gel. Also, we observe that the diffusion of the probe is slower in a lower charge density gel than a higher charge density gel of the same crosslink density because of the reduced mesh size. The mesh size of the gel decreases as the salt concentration is increased. As a result, the probe diffusion coefficient decreases when the salt concentration is increased. It was observed that mesh size relative to the probe size dictates diffusion of the probe inside the gel. In this system, the mesh size is bigger than the polymer chain, thus we do not observe reptation of the chain inside the gel. Instead, the reduced diffusion coefficient of the trapped polymer obeys an exponential dependence on the volume fraction of the gel, in accordance with the presence of an entropic barrier for polymer diffusion. Thus, in our system, the mesh size of the gel governed by the volume fraction of the gel, is an important factor in determining the diffusion of the probe inside the gel compared to the electrostatic interaction between the probe and the matrix.

CHAPTER 4

DIFFUSION OF POLYMERS IN POLYELECTROLYTE GELS

4.1 Introduction

Fluorescence Correlation Spectroscopy (FCS) is a tool to study dynamics of systems from their fluorescence fluctuations. FCS technique is sensitive in very dilute regimes and has single-molecule detection sensitivity. FCS was developed in early 1970s when the principle of working and theory was developed by Elson, Ehrenberg and Rigler. Improvement in detectors, and other electronics along with introduction of confocal volume element to the FCS setup has enabled the improvement of the signal to noise ratio in experiments. Thus FCS studies have a wide range of applications ranging from measuring diffusion coefficient, chemical rates of reactions, concentrations of species, aggregation size and kinetics, and rotational dynamics (Ehrenberg and Rigler, 1974; Elson and Magde, 1974; Magde, Webb and Elson, 1978; Thompson, Lieto and Allen, 2002; Gosch and Rigler, 2005). As a result, the applications of FCS have been extended to many systems, especially polymers and biological systems.

In FCS setup the auto-correlation function is calculated from the intensity of emission of the dye tagged polymer chains diffusing in the detection volume. It has many advantages such as requirement of small volume and low sample concentrations due to its small detection volume (Woll, 2014) . Since FCS technique only detects the intensity of the dye molecule, it can be used to study dynamics of small number of chains in a mixture, depending on their fluorescent labeling (Woll, 2014; Papadakis

et al., 2014; Zettl et al., 2009). These advantages give us an edge in using FCS technique over DLS measurements to find the diffusion of the polymer chain in a gel matrix. In DLS measurements, the gel matrix also contributes to the total scattered intensity along with that of the probe molecule, such contributions are absent in the FCS technique. Hence the FCS technique has been used recently to study dynamics of polymers in concentrated solutions as well as confined systems (Cherdhirankorn et al., 2009; Zettl et al., 2004; Grabowski and Mukhopadhyay, 2008; Zustiak, Boukari and Leach, 2010; Zettl et al., 2009; Michelman-Ribeiro et al., 2007; Zettl, Ballauff and Harnau, 2010).

Various studies have been performed on diffusion of probes in concentrated solutions and gels. Ribeiro and coworkers studied diffusion of a dye molecule in crosslinked PVA gels (Michelman-Ribeiro et al., 2004). Similarly other researchers have studied diffusion of dyes in crosslinked gel networks (Zustiak, Boukari and Leach, 2010; Modesti et al., 2009; Grabowski and Mukhopadhyay, 2008). They observed that as the crosslink density of the gel increases, the probe diffusion decreases. Diffusion of polymers in the gel networks has also been studied by many researchers. Ribeiro and coworkers studied diffusion of Polystyrene latex spheres as well as dye labeled polymers in PVA solutions and observed the effect of gel mesh on probe diffusion (Michelman-Ribeiro et al., 2007; AL-Baradi et al., 2012). In biological systems, Scalettar et. al studied diffusion of DNA in entangled solutions (Scalettar, Hearst and Klein, 1989). Others have studied diffusion of proteins in crowded environments or in cells (Weiss, Hashimoto and Nilsson, 2003; Banks and Fradin, 2005; Zustiak, Nossal and Sackett, 2011), where they observed anomalous diffusion. The anomalous diffusion was attributed to the confinement effects of the cell.

4.2 Experimental Setup

The setup used for fluorescence correlation spectroscopy measurements in this chapter has been described in detail elsewhere (Gamari et al., 2014). A brief summary of the key aspects of the setup is provided here.

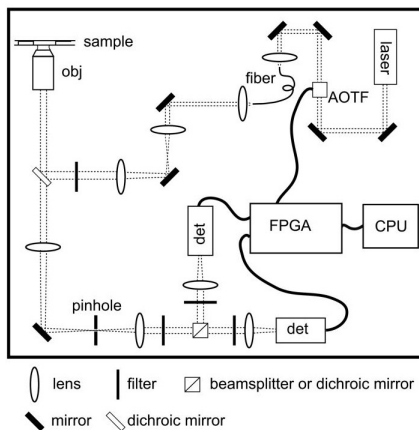


Figure 4.1. Schematic of FCS setup. Reproduced with permission from Ref. (Gamari et al., 2014). Copyright 2014, American Association of Physics Teachers.

In the setup shown above from Ref. (Gamari et al., 2014), the terms are as follows:
Obj: objective lens;
AOTF: acousto-optical tunable filter;
FPGA: field programmable gate array;
det: detector.

The AOTF controls the excitation wavelength and permits fast switching between multiple excitation lines, if required. The FPGA is used to record the arrival times of photons at the detector which are later used to construct the correlation function.

In typical FCS experiment the laser beam is expanded by the lens and then guided to the high numerical aperture objective lens. The objective lens focuses the beam in the sample. Probe molecules are detected if they are present in the detection vol-

ume. The wavelength of the laser corresponds to the excitation wavelength of the dye molecule. Thus the wavelength excites the dye and these molecules then emit a higher wavelength. Emission wavelength from the dye goes back through the objective lens and is allowed to pass to the detector through a dichroic mirror. The dichroic mirror is chosen such that it filters the laser wavelength and allows to pass the emission wavelength. This emission wavelength is guided to the detectors, which record the intensity as function of time.

In fluorescence correlation spectroscopy measurements, like dynamic light scattering, fluctuations in the fluorescent intensity are important. The fluorescent intensity is dependent on the concentration of the molecules present in detection volume which fluctuates in time.

If $I(t)$ is the intensity of fluorescence light at the detector, then the fluorescence intensity correlation function is given by Eq. 4.1.

$$G(\tau) = \frac{I(t)I(t + \tau)}{I(t)^2} \quad (4.1)$$

For a Brownian particle diffusing in the solution, the intensity correlation function can be described by the model in Eq. 4.2.

$$G(t) = 1 + \frac{\frac{1}{N}}{\left(1 + \frac{t}{\tau}\right) \times \left[1 + \left(\frac{R_0}{Z_z}\right)^2 \left(\frac{t}{\tau}\right)\right]} \quad (4.2)$$

where

N = Average number of flourophores in focal volume,

R_0 = Lateral direction of focal volume,

Z_z = Axial direction of focal volume,

τ = Diffusion time,

α = Stretched exponential factor.

Thus, the diffusion coefficient can be calculated from the diffusion time using the Eq. 4.3

$$D = \frac{R_0^2}{4\tau} \quad (4.3)$$

where D = Diffusion coefficient

and R_0 and τ are as defined in Eq. 4.2

In the experiments reported here, a monochromatic laser of wavelength 485 nm is used to excite the Alexa Fluor 488 dye which is attached to a Dextran (M.W. 12 kDa). The focal volume is very small area (1 femtoliter) and typical dye concentration is around 1 nmolar to 10 nmolar. A piece of gel (approximately 3 – 5 mm each side) is immersed in an excess solution of Dextran in water or in a mixture of water (45%) and acetone (55%) with varying NaCl concentrations from 1 mM to 20 mM. It is submersed in the solution for minimum of 48 hours to allow the Dextran molecules to diffuse inside the gel. The gel sample is removed from the Dextran solution and is placed in the sample holder, and the remaining volume is filled with the solution. The sample holder is covered with a film to ensure that the solvent does not evaporate. The sample holder is placed on the microscope stage and focus is adjusted inside the sample. The focus is positioned approximately 30 μm inside the sample. During the duration of the experiment it is important to monitor that the conditions of the gel does not change with time.

4.3 Data Analysis

Equation 4.2 explains events with single diffusion times, such as in the case of dilute polymer solution as shown in Fig. 4.2. Systems that are more complicated

such as that which have two diffusion time scales requires an additional Lorentzian term with parameters of τ_1 and τ_2 .

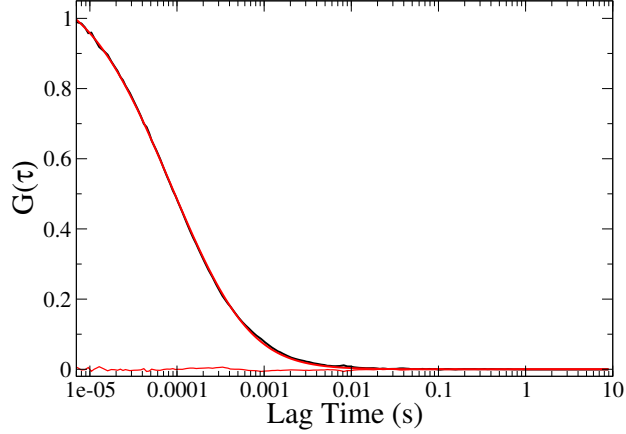


Figure 4.2. Fit for the normalized correlation function (black) of Dextran 12*k* (10 nM) diffusing in water, one parameter (τ) model fit is shown (red). Residuals for the one parameter model, for fitting the correlation function is shown.

Further complications arise when diffusion of polymers in confined environments or in presence of obstacles is studied. Such systems have shown anomalous diffusion behavior. Experiments that have reported anomalous behavior of probe diffusion, used a stretched exponential parameter (α) for the characteristic timescale to explain the diffusion process of the polymer in the gel matrix. The correlation function is accordingly modified as shown

$$G(t) = 1 + \frac{\frac{1}{N}}{\left(1 + \left(\frac{t}{\tau}\right)^\alpha\right) \times \left[1 + \left(\frac{R_0}{Z_z}\right)^2 \left(\left(\frac{t}{\tau}\right)^\alpha\right)\right]} \quad (4.4)$$

The stretched exponential parameter (α), introduces a broad distribution of diffusion time events. When $\alpha < 1$, multiple diffusion time scales are present in the system, with the mean time being reported as τ . Multiple diffusion time scales have been observed for probe diffusion in gel networks, where the variation in mesh size plays an important role in diffusion of the probe. Standard deviation is calculated

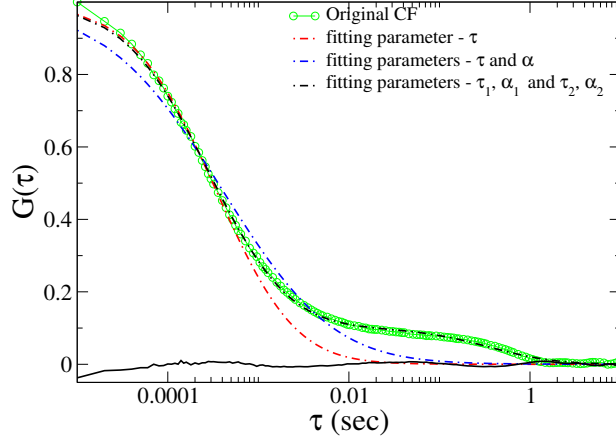


Figure 4.3. Fit for the normalized correlation function using various diffusion models, one parameter (τ), two parameters (τ and α) and four parameters (τ_1 , α_1 , and τ_2 , α_2). Residuals for the four parameter model, for fitting the correlation function is shown. Correlation function of Dextran diffusing in 10C3.5Xl gel in 55% acetone solution and 1 mM NaCl.

from experiments on three different samples for the same conditions. For a system which has two diffusion time scales which may be anomalous in nature, the correlation function is given by

$$G(t) = 1 + \frac{A_1}{\left(1 + \left(\frac{t}{\tau_1}\right)^{\alpha_1}\right) \left[1 + \left(\frac{R_0}{Z_z}\right)^2 \left(\frac{t}{\tau_1}\right)^{\alpha_1}\right]} + \frac{A_2}{\left(1 + \left(\frac{t}{\tau_2}\right)^{\alpha_2}\right) \left[1 + \left(\frac{R_0}{Z_z}\right)^2 \left(\frac{t}{\tau_2}\right)^{\alpha_2}\right]} \quad (4.5)$$

The necessity of the four parameter model can be seen in the Fig. 4.3

4.4 Results and Discussion

We first report results of experiments studying the diffusion of Dextran in the 10C2.7Xl gel. No acetone was used in these experiments, the effect of NaCl concentration on probe diffusion in the gel was studied.

As discussed previously, addition of NaCl to the gel, results in deswelling of the gel due to Donnan equilibrium. Thus with the deswelling of the gel, its mesh size

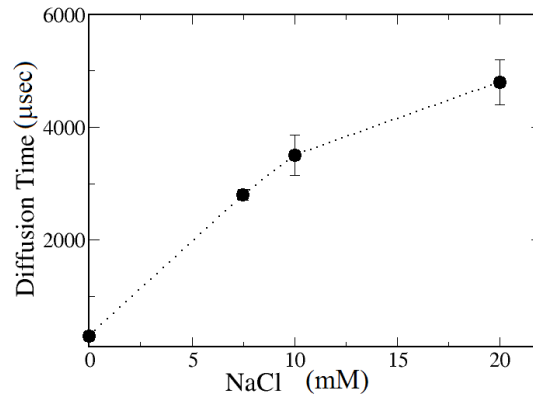


Figure 4.4. Diffusion time (τ) of probe (Dextran) in 10C2.7Xl gel vs. NaCl concentration, in absence of acetone. As the NaCl concentration increases, the diffusion time of the probe in the gel increases.

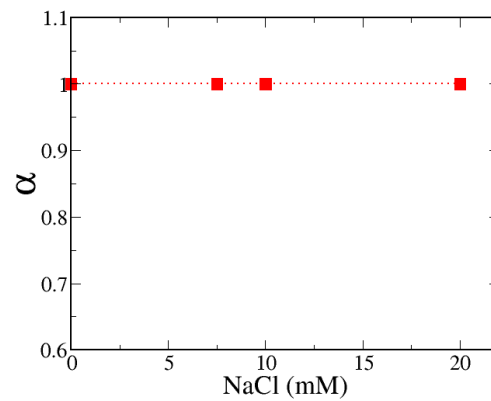


Figure 4.5. Stretched exponential parameter (α) for diffusion of Dextran in 10C2.7Xl gel vs. NaCl concentration, in absence of acetone. As the NaCl concentration increases, α remains constant and is near 1. Two parameter model, for the diffusion time (τ) and stretched exponential factor (α) are used as shown in Eq. 4.4.

also decreases, resulting in more constraints for the probe diffusion. As observed in Fig. 4.4, the diffusion time increases for the probe diffusion as more NaCl is added to the solution due to smaller mesh size of the gel. Diffusion time for Dextran in solution at the same NaCl concentration is $330 \mu\text{sec}$. The diffusion time for the Dextran polymer in the gel is an order of magnitude higher than that in its solution at a same NaCl concentration. The stretched exponential factor $\alpha = 1$ at all NaCl concentrations as seen in Fig. 4.5, indicating that the polymer diffusion process has only one diffusion time scale associated with it. A value of the stretched exponential factor less than unity, *i.e.* $\alpha < 1$, implies that the timescale for diffusion of the polymer chain has a distribution. Diffusion time of the polymer inside the gel can have different time scales depending upon the local environment of the gel. In absence of acetone, a single diffusion time scale for probe diffusion in the gel is observed. However acetone, being an unfavorable solvent for the gel, introduces more heterogeneity in the gel structure. Thus we can expect a broader diffusion time scale for the probe diffusion when acetone is introduced in the system.

Samples of the 10C2.7Xl gel and 10C3.5Xl gel, prepared as discussed previously using solution of Dextran in 55% acetone and varying NaCl concentrations are used in following experiments. The experimental data cannot be explained using the standard model for correlation function (Eq. 4.2) as well as the two parameter model (Eq. 4.4) as seen in Fig. 4.3, a modified correlation function with four fitted parameters (Eq. 4.5) were used. The model that uses the four parameters, two diffusion time scales, and two stretched exponential parameters, will be used to fit the correlation functions henceforth. The effect of adding acetone as solvent on the probe diffusion can be clearly seen in the correlation functions presented in Fig. 4.6

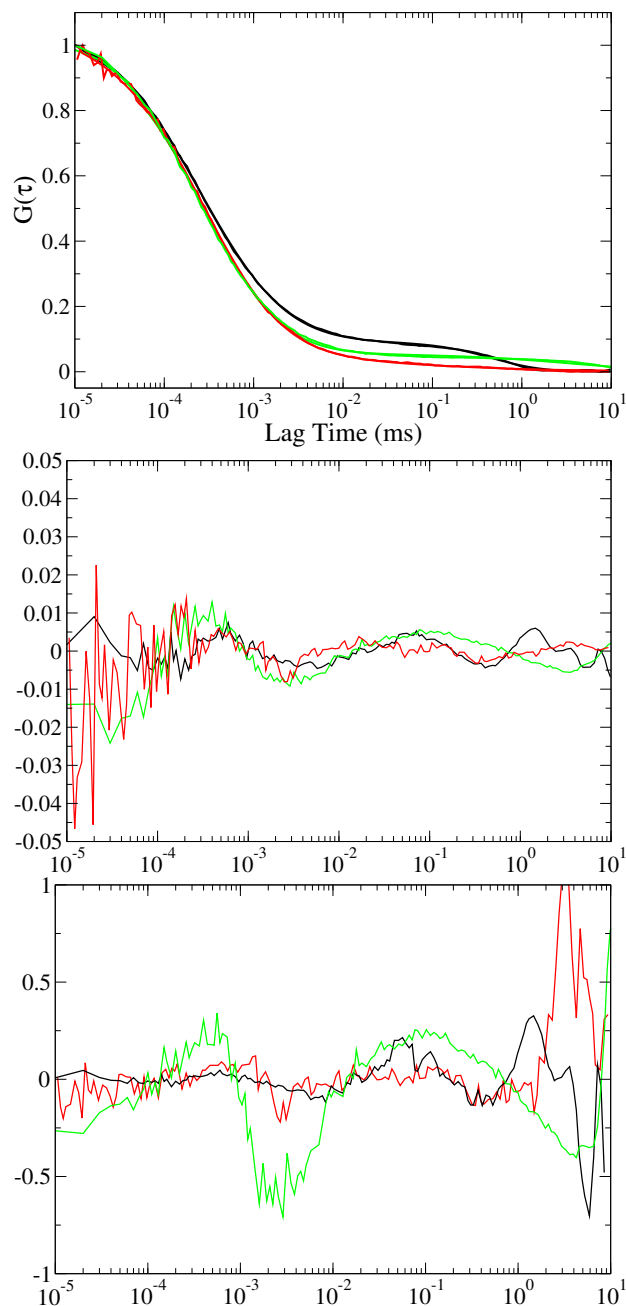


Figure 4.6. Comparison of three experiments on the three different samples for the same composition of the gel, solvent and NaCl concentration. (Top) The correlation function is for Dextran diffusing in the 10C3.5Xl gel with 55% acetone and 9 mM NaCl. (Middle) The plots the residuals of the fit for the correlation function shown above. The residual for the fit of the correlation function is represented by the same color. (Bottom) The plot of $Residuals/(uncertainty\ in\ the\ data)$ for the above fits. The lines are represented by the same color as their respective correlation functions in the top figure.

In Fig. 4.6, the four parameter model gives us the best fit. However, the residuals are not randomly distributed about zero, which indicates the limitations of the model for the given system. Possibly, due to the distribution of time scales, the oscillations in the residuals arise. This can be seen in the residuals plot as well as from the normalized residuals ($Residuals/(uncertainty\ in\ the\ data)$) in the bottom figure in Fig. 4.6. For a good fit, the χ^2_{DOF} should be 1, indicating that the fit is within noise ($\chi^2 = \sum Residuals/(uncertainty\ in\ the\ data)$). For the Fig. 4.6, the value of χ^2 is very small than total number of data points (n), which means the variance on the data is larger than the residuals, possibly due to overestimation of the variance in the correlation function.

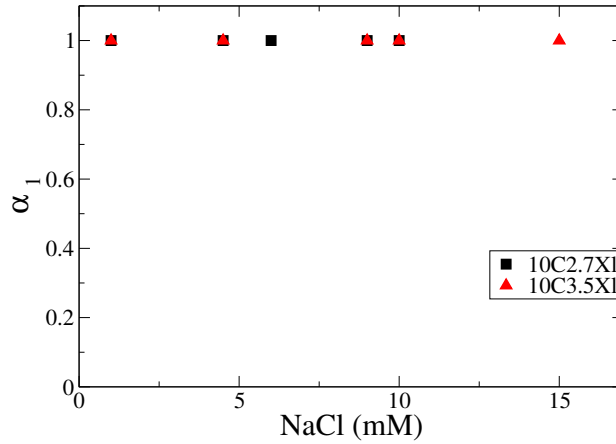


Figure 4.7. Stretched exponential parameter (α_1) for Dextran diffusion in 10C2.7X1 gel and 10C3.5X1 gel vs. NaCl concentration in presence of 55% Acetone solution. At all NaCl concentration, α_1 remains constant at 1.

As shown in Fig. 4.7, stretched exponential parameter α_1 remains constant at 1 at all NaCl concentrations. When $\alpha = 1$, the normal correlation function is recovered, meaning that only one diffusive time scale is present in the system.

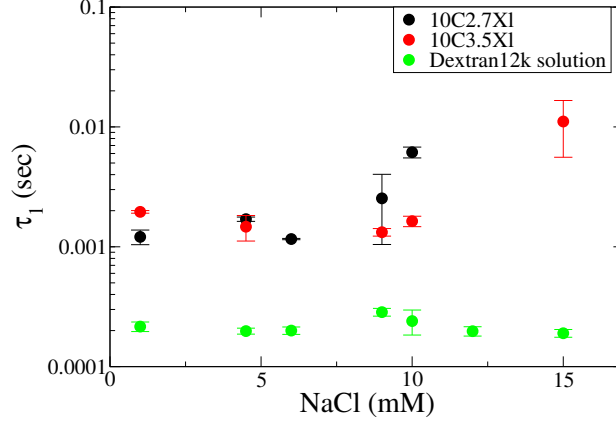


Figure 4.8. Faster diffusion time (τ_1) of probe (Dextran) diffusion in 10C2.7X1 gel and 10C3.5X1 gel vs. NaCl concentration in presence of 55% Acetone solution. Probe diffusion in both the gels is slower than in the solution at all NaCl concentrations. At higher NaCl concentrations, the diffusion time of the probe increases.

As shown in Fig. 4.8 the diffusion time of the polymer chain is greater when diffusing inside a gel as compared to that in the 55% Acetone solution. The polymer chain feels the confinement due to the surrounding gel which introduces fixed obstacles for probe diffusion. However it is interesting to note that the diffusion time remains constant as NaCl concentration is increased from 1 mM to 9 mM, suggesting that even though the gel deswells with the addition of more salt to the solution, the polymer chain does not feel the effect of decreasing mesh size of the gel. For the polymer chain to feel strong confinement in its diffusion inside the gel, the mesh size should be small enough to impose constraints on polymer diffusion. However, for this small molecular weight dextran polymer, the mesh size is still large compared to the polymer chain and hence it does not feel strong confinements from the gel. Diffusion time of the polymer inside the 10C2.7X1 gel at 10 mM NaCl concentration increases almost an order of magnitude. Similarly, inside the 10C3.5X1 gel, the diffusion time of the polymer at 15 mM NaCl concentration increases almost an order of magnitude but remains unchanged at lower salt concentrations. This observation coincides with the decrease in dynamics of both the gels at their respective collapse transitions.

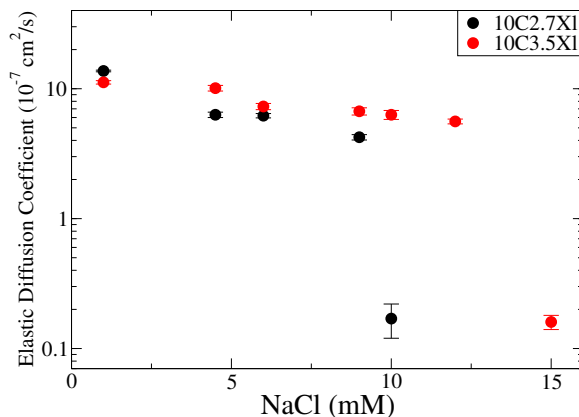


Figure 4.9. Diffusion coefficient for the 10C2.7Xl gel + 55% acetone + NaCl solution and the 10C3.5Xl gel + 55% acetone + NaCl solution. The diffusion coefficient decreases as NaCl is added to the solution. Just before the volume phase transition, the diffusion coefficient of the gel decreases by two orders of magnitude. Higher crosslink density gel collapses at higher salt concentration.

In presence of 55% Acetone solution, the 10C2.7Xl gel undergoes volume phase transition at 11 mM NaCl concentration and The 10C3.5Xl gel undergoes volume phase transition at 16 mM NaCl concentration. As a result, the diffusion coefficient of the gel decreases by about two orders of magnitude just before the volume phase transition of the gel takes place as seen in Fig. 4.9. This was also observed by (McCoy and Muthukumar, 2010) for the same gel system, in which the decrease in gel dynamics was attributed to structural changes in the gel prior to the imminent volume phase transition.

Diffusion time increases in 10C2.7Xl gel at 10 mM NaCl concentration as shown in Fig. 4.8. The estimated mesh size change from 9 mM to 10 mM NaCl concentration, cannot explain this drastic change in diffusion time of the probe inside the gel. Structural changes occur in the gel as its volume transition approaches near the collapse point as indicated by the two orders of magnitude decrease in the diffusion coefficient of these polyelectrolyte gels. This affects the probe diffusion in the gel near its collapse. Similarly in the 10C3.5Xl gel, the diffusion time of the polymer inside the

gel remains constant at lower NaCl concentrations indicating that the effect of mesh size on the polymer diffusion is not pronounced. But at 15 mM NaCl concentration where the collapse transition of the gel is imminent as indicated by the decrease in diffusion coefficient of the gel, the gel dynamics are coupled with the probe diffusion, resulting in slower diffusion of the polymer inside the gel matrix.

For the linear diffusive regime, we can calculate diffusion coefficient using the width of the confocal volume (R_0) is calibrated using a dye of known diffusion constant.

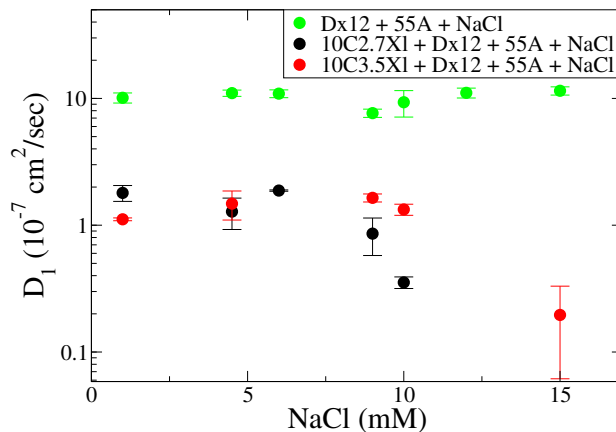


Figure 4.10. Diffusion coefficient of probe (Dextran) in 10C2.7Xl gel and 10C3.5Xl gel vs. NaCl concentration in presence of 55% Acetone solution. As the NaCl concentration increases, the diffusion coefficient of the probe decreases.

Figure 4.10 shows that the diffusion coefficient remains constant at lower NaCl concentrations. Because of the small size of the probe, the polymer chain does not feel the effect of decreasing mesh size of the gel as NaCl concentration increases. Hence its diffusion coefficient in the gel is lower than probe diffusion in solution, but does not decrease with increasing NaCl concentration. However, near the gel collapse, 10 mM NaCl concentration for 10C2.7Xl gel and 15 mM NaCl concentration for 10C3.5Xl gel (Fig. 4.9), the dynamics of the probe molecule are coupled with the gel dynamics, as

a result the diffusion coefficient of the polymer decreases about an order of magnitude near the gel collapse transition.

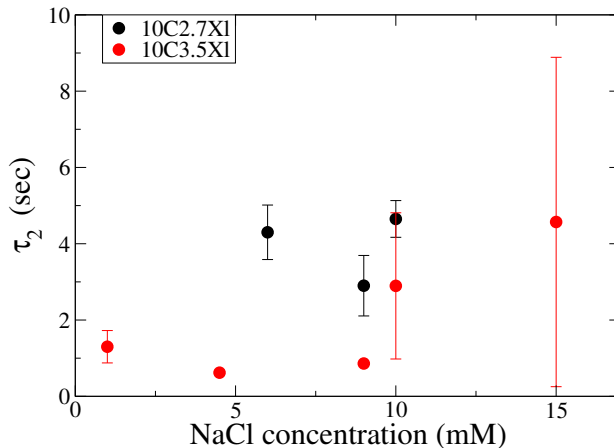


Figure 4.11. Slower diffusion time (τ_2) of probe (Dextran) diffusion in 10C2.7Xl gel and 10C3.5Xl gel vs. NaCl concentration in presence of 55% Acetone solution. At higher NaCl concentrations, the diffusion time of the probe increases.

As seen in Fig. 4.11, the second diffusion time scale is very long compared to the τ_1 diffusion time. This long diffusion time scales indicate either caging of the Dextran molecules inside the gel mesh or can also be possible due to some interactions between the polymer and gel, which are induced by the solvent acetone. Note that in absence of acetone, these long time scales were absent. Thus either the solvent induced interaction causes the Dextran molecule to stay in the focal volume for longer duration or the polymer chain is caged in the gel mesh and escapes the mesh, such that the duration of the event is in 0.1s to a few seconds.

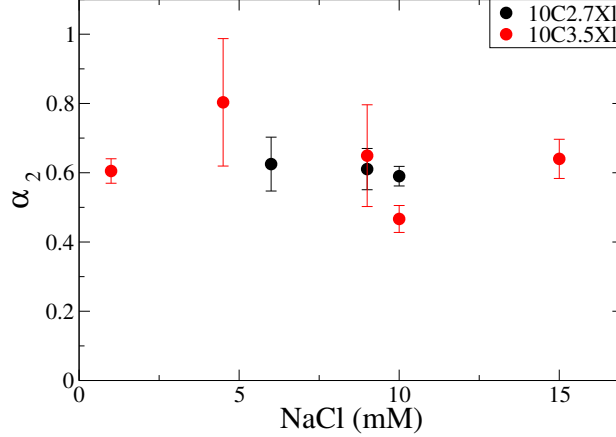


Figure 4.12. Stretched exponential parameter (α_2) for Dextran diffusion in 10C2.7Xl gel and 10C3.5Xl gel vs. NaCl concentration in presence of 55% Acetone solution. α_2 is less than 1 at all NaCl concentration.

The stretched exponential parameter α_2 for the longer probe diffusion time (τ_2) within the uncertainty, is constant with NaCl concentration as observed in Fig. 4.12. When α_2 is less than 1, the stretched exponential function assumes importance, indicating that there are multiple diffusion time scales for the probe diffusion in the gel. We can also relate this data to the mesh size of the gel. At lower NaCl concentrations, the gel mesh is not small enough to introduce sufficient constraints on the probe, hence we observe the stretched exponential coefficient (α_2) of 1 at 1 mM NaCl concentration for the 10C2.7Xl gel. However at higher NaCl concentrations, mesh size decreases and the polymer chain feels more constraints and is possibly trapped in regions of small mesh size. Thus, either sub-diffusive behavior is observed for probe diffusion in the gel or due to the varying and small mesh sizes of the gel, distribution of diffusive time scales which have a distribution is observed. A stretched exponential fit can confirm the presence of several diffusive time scales of the probe in the gel. The exponent values remain almost constant ($\alpha_2 \sim 0.6$), indicating that the τ_2 events in the gel are either of sub-diffusive nature or due to the broad distribution of τ_2 values.

Diffusion of polymers and proteins in cells have also required a stretched exponential fitting parameter for the correlation function fits. When $\alpha < 1$, the process was termed as sub-diffusive due to different levels of confinement offered by the complex morphology of the cell (Weiss, Hashimoto and Nilsson, 2003; Schwille et al., 1999). Thus, three possibilities arise for explaining this result. The polymer chain can be caged inside small mesh structures, resulting in sub-diffusive behavior, or there are interactions between the polymer and gel resulting in sub-diffusive behavior, or the gel has distribution of mesh sizes, which results in distribution of the relaxation time scales, and thus a the stretched exponential parameter $\alpha < 1$ is observed.

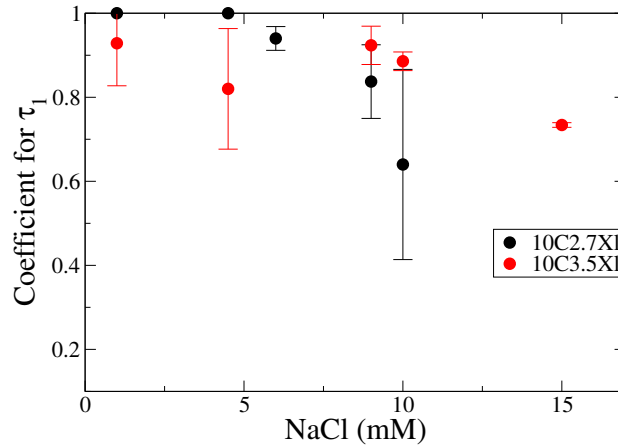


Figure 4.13. Coefficient for the diffusion time (τ_1) as a function of NaCl concentration. Data for 10C2.7Xl gel and 10C3.5Xl gel with 55% acetone and NaCl is shown.

The coefficient (A1) from Eq. 4.5 represents the relative magnitude of the diffusion events corresponding to the two diffusion times (τ_1 and τ_2) is shown in Fig. 4.13. The coefficient for the faster and unique diffusion time event (τ_1), has the coefficient (A1) 0.7 – 1, which means that the τ_1 is the dominant mode and has higher frequency of such events.

In summary, two diffusive time scales are observed, the faster time scale is a diffusive mode which has a narrow distribution, while the slower diffusion time of the probe has diffusion time scale of a few seconds, along with a broad range of distribution of these time scales. The second diffusion time scale observed in the probe diffusion in the gel has a stretched exponential factor of $\alpha < 1$.

4.5 Conclusion

In this chapter, the diffusion of a neutral polymer inside the polyelectrolyte gel was studied using FCS. It was observed that the probe diffusion coefficient decreases inside the gel compared to that in solution, due to the addition of more constraints from the gel network. Effect of salt concentration was studied on the diffusion of the polymer inside the gel in presence of water as well as acetone-water mixtures. Multiple diffusion time scales are observed for diffusion of the probe inside the gel in presence in acetone-water mixture. The first mode of the probe is diffusive in nature. As NaCl concentration is increased, the gel deswells and mesh size decreases. However, the diffusion time of the polymer remains unchanged inside the gel as the mesh size is bigger than the polymer resulting in weak confinement. Near the collapse transition of the gel, where the diffusion coefficient of the gel decreases about two orders of magnitude, the dynamics of the probe are coupled with the gel dynamics. As a result, the diffusion of the polymer inside the gel slows down another order of magnitude at this NaCl concentration.

The second mode is explained with a stretched exponential parameter which indicates either the broad distribution of diffusion time observed or a sub-diffusive behavior. The polymer chain can be caged inside small mesh structures resulting in sub-diffusive behavior, or there are interactions between the polymer and gel resulting

in sub-diffusive behavior, or the gel has distribution of mesh sizes, which results in distribution of the relaxation time scales, and thus the stretched exponential parameter $\alpha < 1$ is observed.

CHAPTER 5

CONCLUSION AND FUTURE WORK

This thesis demonstrates the effect of crosslink density, charge density and the corresponding volume fraction of the gel on the dynamics of polymers in the gels. The effect of external stimuli such as salt concentration and the solvent quality on the gel swelling and its effect on the polymer diffusion inside the gel was studied. This fundamental work to determine the effect of the gel volume fraction on controlling the diffusion of uncharged as well as charged polymers inside the polyelectrolyte gel will help in understanding and designing better controlled drug delivery systems and other biomedical applications.

The dynamics of the gel (in absence of any free polymer chains) were studied for various salt concentrations and different solvents. The measurements from dynamic light scattering were related to other measurements of swelling equilibrium and rheology to establish the relationship of diffusion coefficient, modulus, volume fraction and friction coefficient of the gel, as was established by Tanaka and coworkers (Hirotsu, Hirokawa and Tanaka, 1987). The volume phase transition of the gel and decrease in diffusion coefficient of the gel were also observed in presence of 55% Acetone and NaCl, and the behavior is in accordance with the studies conducted previously on similar gel systems (McCoy and Muthukumar, 2010).

This understanding of the gel was later used in designing the studies to explore the dynamics of polyelectrolytes inside the polyelectrolyte gel. The effects of crosslink

density of the gel and charge density of the gel on the probe dynamics inside the gel were studied. Addition of free polymer chains to the gel resulted in an additional mode in DLS measurements of the sample. The origin of the additional mode is attributed to the polymer diffusion inside the gel. Increasing the crosslink density of the gel decreases the gel mesh size and increases the polymer confinement resulting in slower diffusion constant of the polyelectrolyte. The effect of decreasing the charge density of the gel also resulted in decrease in diffusion coefficient of the gel. This decrease can be explained due to resultant smaller mesh size of the gel due to reduced Donnan potential or can be an effect of decreased electrostatic interaction. The electrostatic interaction can be considered to be negligible, as inferred from the Debye length for the given solvent composition and the salt concentration. The effect of solvent as well as NaCl concentration were studied on the polymer diffusion inside the gel. Addition of NaCl to the system decreases the mesh size of the gel which results in the stronger confinement on the polymer and hence results in slower diffusion coefficient of the polymer inside the gel. Ultimately, it was shown that the dynamics of the trapped polymer obeys an exponential dependence on the volume fraction of the gel, in accordance with the presence of an entropic barrier for polymer diffusion.

It was also noted that the probe diffusion was not affected near the collapse transition of the gel where the diffusion coefficient of the gel decreases two orders of magnitude. The dynamics of the gel are also unaffected by presence of the polyelectrolyte inside the gel.

Diffusion of a neutral probe was studied in the polyelectrolyte gel using FCS. Since in this experiment, only the probe contributes to the emitted intensity, the correlation function has no contribution from the gel. As the crosslink density of the gel increases, the mesh size of the gel decreases. However, no effect was observed

on the diffusion coefficient of the polymer inside the gel on increasing the crosslink density as well as increasing the salt concentration. Due to the large mesh size of the gel compared to the size of the Dextran polymer diffusing inside the gel, the matrix offers weak confinement to polymer diffusion. In addition to one mode corresponding to polymer diffusion inside the gel, a second mode is observed. This second mode only originates in presence of acetone and at high salt concentrations or in higher crosslink density gel. A possible explanation for this mode is caging of the Dextran polymer inside the gel mesh, or the interactions between the gel and the Dextran which results to sticking of the molecule to the gel network resulting in long diffusion time scales. Stretched exponential parameter is used to explain the broad distribution of the diffusion time observed.

Another interesting result was observed. Near the collapse transition of the gel, where the diffusion coefficient of the gel decreases about two orders of magnitude, the dynamics of the probe are coupled with the gel dynamics. As a result, the diffusion of the polymer inside the gel slows down another order of magnitude at the NaCl concentration, where the diffusion coefficient of the gel decreases two orders of magnitude. This observation is in contrast to the conclusion from the studies of diffusion of a charged probe in the gel matrix, in which the effect of gel dynamics near the collapse transition was not observed on the polymer diffusion inside the gel.

5.1 Future Work

In this thesis, the dynamics of polyelectrolyte was studied inside a polyelectrolyte gel. The mesh size of the gel was controlled by changing the salt concentration of the solution. Adding salt to the system, introduces electrostatic screening, and as a result, the effect of electrostatic interactions decreases. The effect of electrostatic interaction can be further investigated by manipulating the electrostatic interactions

between the polyelectrolyte probe and the polyelectrolyte gel. The dynamics can be studied in absence of salt, in which the electrostatic interactions are dominant. Electrostatic interactions between the polymer and the gel will change depending on the concentration of NaPSS in the gel. The electrostatic interaction can also be manipulated by increasing the charge density of the gel. A gel system can be designed such that the mesh size remains smaller than Debye length for the given charges present in the gel. Increase in the charge density also increase the mesh size and thus the mesh size needs to be controlled using other parameters, that does not change the Debye length by considerable magnitude compared to mesh size. Modified Flory-Rehner theory (discussed in chapter 2) can be used to predict the swelling behavior and mesh size of the gel. The partitioning of NaPSS inside the gel in presence of and absence of added salt, can be found using the Donnan equilibrium theory.

A study can be designed to explore the probe diffusion mechanism from the application perspective, as it is the key parameters in understanding physics that governs the diffusion of a polymer chain in a confined environment. This is especially important in drug delivery systems as well as in understanding complex biological processes. Many theories have been put forward to explain the diffusion of neutral polymer chains in constrained environments. The question of what is the most dominating factor dictating polymer dynamics; entropic barriers or reptation of polymer chain etc., can be investigated experimentally. In the current thesis, an attempt is made to find the effect of electrostatics along with confinement effects on polymer dynamics inside a polyelectrolyte gel. However, effect of electrostatic interaction or the confinement due to the gel mesh could not be established distinctly. Thus the effect of electrostatic interactions in diffusion of charged polymers in charged gel networks has not been explicitly investigated yet. This can be experimentally studied by choosing a neutral polymer and a neutral probe and comparing the diffusion co-

efficient of a charged polymer in a charged gel. By careful design of experiments, the volume fraction of the gel can be manipulated such that the entropic effect due to confinement is same for both systems (and the χ parameter also remains same); thus the only difference should arise from electrostatic interactions between the probe and the polymer. Due to difficulties in light scattering, especially for neutral gels, FCS or other contrast scattering techniques might be of more relevance. Recently, synthesis of NaPSS with a dye has been established and thus its dynamics in gel may be compared with dynamics of a Polystyrene attached with a dye inside a gel (Sohn et al., 1996). But it should be recognized that these experimental measurements are very difficult and hence simulations should be performed along with experiments to understand the dynamics better.

APPENDIX

MATERIALS AND SUPPORTING INFORMATION

Materials

Chemical	Company	Catalog Number
Acrylamide (40% w/v)	Amresco	0132
Bisacrylamide (2% w/v)	Amresco	0172
Sodium Acrylate	Sigma Aldrich	408220
Tetramethylethylenediamine	Sigma Aldrich	T22500
Ammonium persulfate	Sigma Aldrich	248614
Sodium Chloride	Thermo Scientific	BP3581
Acetone	Thermo Scientific	A18P-4
NaPSS	Scientific Polymer	620, 621, 622, 624, 872
Dextran-AF488	Invitrogen	D-22910
Methyleneblue	Sigma Aldrich	M9140

Table A.1. List of materials used in this thesis.

UV-Vis Spectroscopy

UV-Vis spectroscopy studies the absorption spectra of the sample in the UV-Vis wavelength region. The UV-Vis spectroscopy was used to study the presence of probe molecules in the gel. The UV-Vis experiments were performed using a Hitachi U3010 UV/visible spectrophotometer with scan region of 200 nm to 700 nm. Experiments were performed in a quartz cuvette with a path length of 2 mm. NaPSS was tagged with methylene blue as per procedure described by Smisek and Hoagland (Smisek and Hoagland, 1989). The NaPSS was stained using methylene blue solution in water (0.01 wt%) which was adjusted to pH 4.0 using glacial acetic acid. The authors also

observed that the polymer and dye bound irreversibly. A gel was immersed in a solution of conjugate of NaPSS + Methyleneblue dye. After 1 week, it was taken out of solution and placed in a cuvette and analyzed in UV-Vis spectrometer.

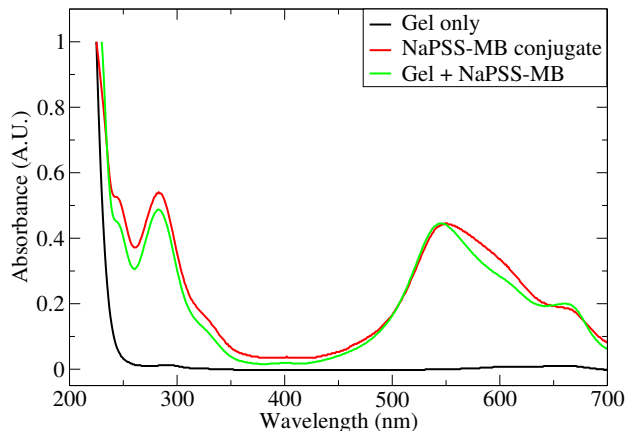


Figure A.1. UV-Vis absorbance spectra for the 10C2.7X1 gel + NaPSS. The methyleneblue tagged NaPSS (NaPSS-MB) is present inside the gel.

The gel does not absorb in the visible region. Tagging of NaPSS with Methyleneblue dye. In the UV-Vis plot below, we can see that the peak of dye shifts from 670 nm (Dye solution) to 548 nm (NaPSS Dye conjugate). From the UV-Vis spectra, of gel + NaPSS-MB sample (no NaCl), the presence of NaPSS-MB conjugate inside the gel can be seen. As described in sample preparation, the outer layer of the gel (2 mm) is removed on either side to ensure that the bulk of the gel is probed using UV-Vis spectroscopy. This confirms presence of NaPSS inside the gel and that NaPSS diffuses from the solution to inside the gel.

Debye length

NaCl (mM)	Debye length (nm)
1	7.2
4.5	3.4
6	2.9
9	2.4
10	2.2

Table A.2. Debye length for given NaCl concentration in 55% Acetone and 45% Water mixture.

Dielectric constant of the mixture is 44.

Hydrodynamic radius of NaPSS and Dextran

Solution - 55% Acetone and 45% Water mixture

NaCl (mM)	N16	N30	N70	N127	Dx12
1	2.3	3.1	3.3	3.6	2.4
4.5	2.9	3.5	4.3	4.1	2.2
6	3.1	3.7	4.8	4.7	2.2
9	3.3	4	5	4.9	3.2
10	3.5	4.3	5.1	5.3	2.6

Table A.3. Hydrodynamic radius of NaPSS and Dextran for given NaCl concentration in 55% Acetone and 45% Water mixture.

Effect of equilibration time

When the gel is synthesized in a light scattering tube, it is important to allow the gel to equilibrate with the solution. The effect of equilibration time on light scattering results can be seen in Fig. A.2.

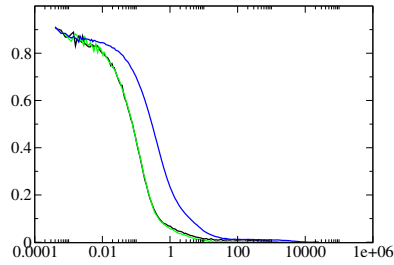


Figure A.2. The effect of equilibration time on the correlation functions obtained from light scattering is shown. The gel was synthesized inside the light scattering tube and NaPSS127k (1 mg/ml) + 100 mM NaCl solution was added to the gel. Black and Green - Equilibrated for two days. Blue - Equilibrated for two weeks. The correlation function shifts and the diffusion coefficient changes as a result.

Γ vs. q^2

10C2.7Xl gel + NaPSS + 55% Acetone + 45% Water

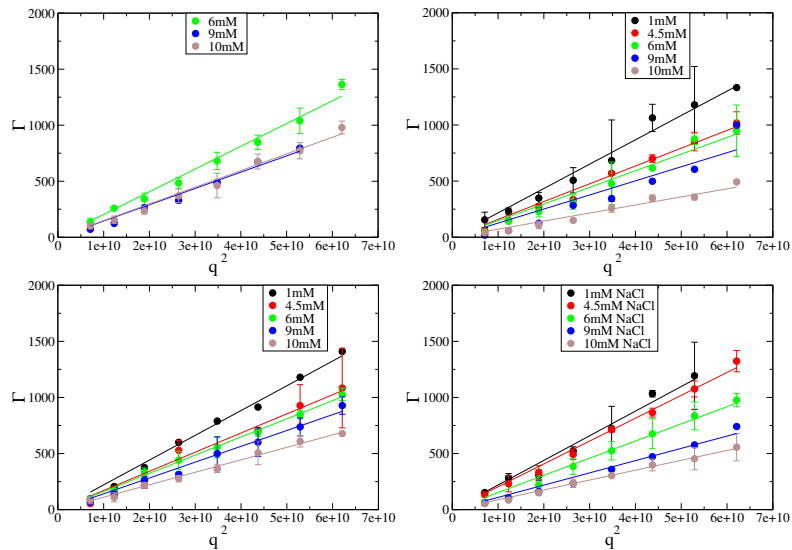


Figure A.3. Γ vs. q^2 plot for the second mode for DLS of 10C2.7Xl gel + NaPSS + 55% Acetone + 45% Water. (First Row) (Left) NaPSS 16k (Right) NaPSS 30k. (Second Row) (Left) NaPSS 70k (Right) NaPSS 127k.

10C3.5Xl gel + NaPSS + 55% Acetone + 45% Water

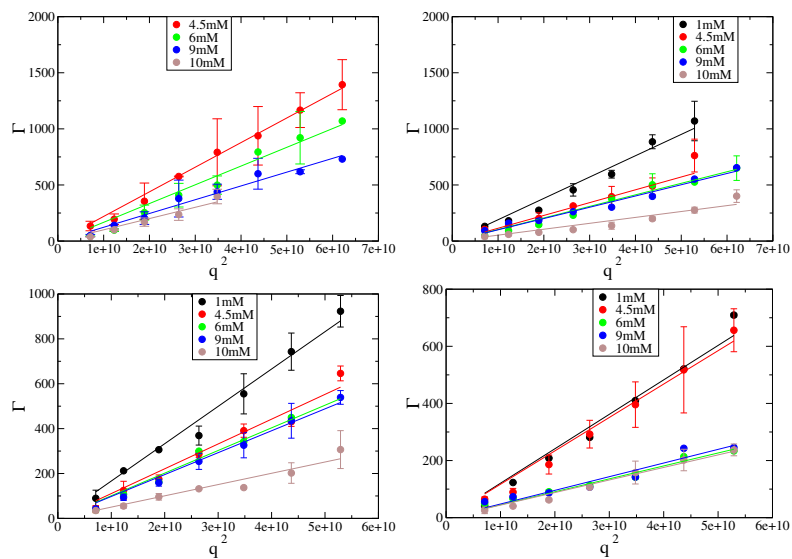


Figure A.4. Γ vs. q^2 plot for the second mode for DLS of 10C3.5Xl gel + NaPSS + 55% Acetone + 45% Water . (First Row) (Left) NaPSS 16k (Right) NaPSS 30k. (Second Row) (Left) NaPSS 70k (Right) NaPSS 127k.

5C2.7Xl gel + NaPSS + 55% Acetone + 45% Water

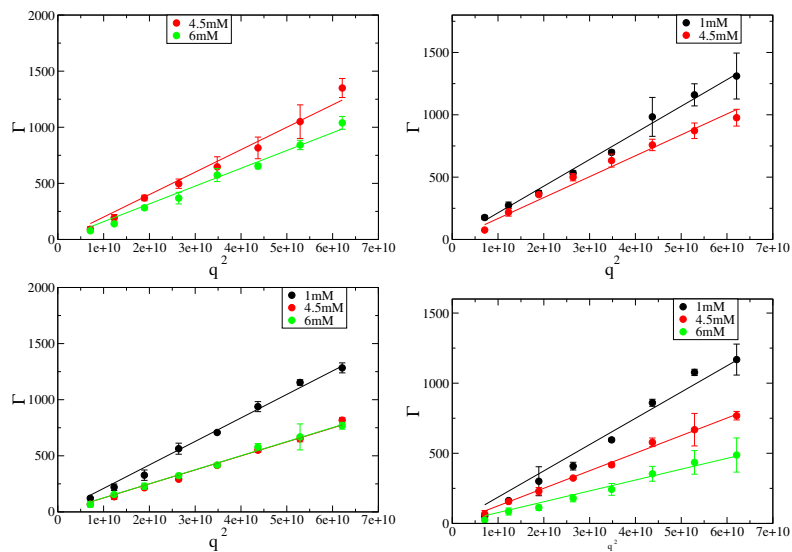


Figure A.5. Γ vs. q^2 plot for the second mode for DLS of 5C2.7Xl gel + NaPSS + 55% Acetone + 45% Water. (First Row) (Left) NaPSS 16k (Right) NaPSS 30k. (Second Row) (Left) NaPSS 70k (Right) NaPSS 127k.

BIBLIOGRAPHY

- A. Moussaid, J. P. Munch, F. Schosseler and S. J. Candau. 1991. "Light scattering study of partially ionized poly(acrylic acid) systems : comparison between gels and solutions." *Journal de Physique II* 1(6):637–650.
- AL-Baradi, Ateyyah M., Matthew Mears, Richard A. L. Jones and Mark Geoghegan. 2012. "Diffusion of dextran within poly(methacrylic acid) hydrogels." *Journal of Polymer Science Part B: Polymer Physics* 50(18):1286–1292.
- Alberts, Bruce, Alexander Johnson, Julian Lewis, Martin Raff, Keith Roberts and Peter Walter. 1994. *Molecular Biology of the Cell*. Garland Science.
- Amsden, Brian. 2002. "Modeling solute diffusion in aqueous polymer solutions." *Polymer* 43(5):1623 – 1630.
- Arrio-Dupont, Martine, Georges Foucault, Monique Vacher, Philippe F. Devaux and Sophie Cribier. 2000. "Translational Diffusion of Globular Proteins in the Cytoplasm of Cultured Muscle Cells." *Biophysical Journal* 78(2):901 – 907.
- Banks, Daniel S. and Ccile Fradin. 2005. "Anomalous Diffusion of Proteins Due to Molecular Crowding." *Biophysical Journal* 89(5):2960 – 2971.
- Bansil, Rama and Manoj K. Gupta. 1980. "Effect of varying crosslinking density on polyacrylamide gels." *Ferroelectrics* 30(1):63–71.
- Basak, Sujit and Krishnananda Chattopadhyay. 2013. "Fluorescence Correlation Spectroscopy Study on the Effects of the Shape and Size of a Protein on Its Diffusion Inside a Crowded Environment." *Langmuir* 29(47):14709–14717.
- Bishop, Paul N. 2000. "Structural macromolecules and supramolecular organisation of the vitreous gel." *Progress in Retinal and Eye Research* 19(3):323 – 344.
- Brown, W. 1993. *Dynamic Light Scattering*. Oxford Press.
- Byrne, Mark E, Kinam Park and Nicholas A Peppas. 2002. "Molecular imprinting within hydrogels." *Advanced Drug Delivery Reviews* 54(1):149 – 161. Recent Developments in Hydrogels.
- Cambrex. N.d. *A Handbook for Gel Electrophoresis*. Cambrex.

- Candau, Sauveur, Jacques Bastide and Michel Delsanti. 1982. Structural, elastic, and dynamic properties of swollen polymer networks. In *Polymer Networks*, ed. Karel Duek. Vol. 44 of *Advances in Polymer Science* Springer Berlin Heidelberg pp. 27–71.
- Cherdhirankorn, Thipphaya, Andreas Best, Kaloian Koynov, Kalina Peneva, Klaus Muellen and George Fytas. 2009. “Diffusion in Polymer Solutions Studied by Fluorescence Correlation Spectroscopy.” *The Journal of Physical Chemistry B* 113(11):3355–3359.
- Cluzel, Philippe, Michael Surette and Stanislas Leibler. 2000. “An Ultrasensitive Bacterial Motor Revealed by Monitoring Signaling Proteins in Single Cells.” *Science* 287(5458):1652–1655.
- Crick, Francis. 1970. “Diffusion in Embryogenesis.” *Nature* 225:420 – 422.
- Cukier, R. I. 1984. “Diffusion of Brownian spheres in semidilute polymer solutions.” *Macromolecules* 17(2):252–255.
- de Gennes. P. G. 1979. *Scaling Concepts in Polymer Physics*. Cornell university press.
- Drifford, Maurice and Jean Pierre Dalbiez. 1984. “Light scattering by dilute solutions of salt-free polyelectrolytes.” *The Journal of Physical Chemistry* 88(22):5368–5375.
- Drifford, Maurice and Jean Pierre Dalbiez. 1985. “Effect of salt on sodium polystyrene sulfonate measured by light scattering.” *Biopolymers* 24(8):1501–1514.
- Easwar, N. 1989. “Diffusion of linear polystyrene in controlled pore glasses. Comparison of experimental data with a theoretical model of entropic barriers.” *Macromolecules* 22(8):3492–3494.
- Ehrenberg, M. and R. Rigler. 1974. “Rotational brownian motion and fluorescence intensify fluctuations.” *Chemical Physics* 4(3):390 – 401.
- Ellis, R. John. 2001. “Macromolecular crowding: an important but neglected aspect of the intracellular environment.” *Current Opinion in Structural Biology* 11(1):114 – 119.
- Elson, Elliot L. and Douglas Magde. 1974. “Fluorescence correlation spectroscopy. I. Conceptual basis and theory.” *Biopolymers* 13(1):1–27.
- English, Anthony E., Toyochi Tanaka and Elazer R. Edelman. 1997. “Equilibrium and non-equilibrium phase transitions in copolymer polyelectrolyte hydrogels.” *The Journal of Chemical Physics* 107(5):1645–1654.
- Fang, Liqi and Wyn Brown. 1992. “Dynamic light scattering by permanent gels: heterodyne and nonergodic medium methods of data evaluation.” *Macromolecules* 25(25):6897–6903.

- Fang, Liqi, Wyn Brown and Cestmir Konk. 1990. “Dynamic properties of polyacrylamide gels and solutions.” *Polymer* 31(10):1960 – 1967.
- Fatin-Rouge, Nicolas, Kevin J. Wilkinson, and Jacques Buffle. 2006. “Combining Small Angle Neutron Scattering (SANS) and Fluorescence Correlation Spectroscopy (FCS) Measurements To Relate Diffusion in Agarose Gels to Structure.” *The Journal of Physical Chemistry B* 110(41):20133–20142.
- Ferry, John D. 1980. *Viscoelastic Properties of Polymers, 3rd Edition*. John Wiley & Sons, Inc.
- Forster, Stephan, Manfred Schmidt and Markus Antonietti. 1990. “Static and dynamic light scattering by aqueous polyelectrolyte solutions: effect of molecular weight, charge density and added salt.” *Polymer* 31(5):781 – 792.
- Furukawa, Hidemitsu, Kazuyuki Horie, Ryunosuke Nozaki and Mamoru Okada. 2003. “Swelling-induced modulation of static and dynamic fluctuations in polyacrylamide gels observed by scanning microscopic light scattering.” *Physical Review E* 68:031406.
- Gamari, B., D. Zhang, R. Buckman, P. Milas, J. Denker, H. Chen, H. Li and L. Goldner. 2014. “Inexpensive electronics and software for photon statistics and correlation spectroscopy.” *American Journal of Physics* 82(7):712–722.
- Geissler, Erik and Anne Marie Hecht. 1976. “Dynamic and static light scattering by aqueous polyacrylamide gels.” *Journal of Chemical Physics* 65:103–108.
- Geissler, Erik, Ferenc Horkay and Anne Marie Hecht. 1991. “Osmotic and scattering properties of chemically crosslinked poly(vinyl alcohol) hydrogels.” *Macromolecules* 24(22):6006–6011.
- Gosch, Michael and Rudolf Rigler. 2005. “Fluorescence correlation spectroscopy of molecular motions and kinetics.” *Advanced Drug Delivery Reviews* 57(1):169 – 190. *Advances in Fluorescence Imaging: Opportunities for Pharmaceutical Science*.
- Grabowski, Christopher A. and Ashis Mukhopadhyay. 2008. “Diffusion of Polystyrene Chains and Fluorescent Dye Molecules in Semidilute and Concentrated Polymer Solutions.” *Macromolecules* 41(16):6191–6194.
- Guo, Yihong, Kenneth H. Langley and Frank E. Karasz. 1990. “Hindered diffusion of polystyrene in controlled pore glasses.” *Macromolecules* 23(7):2022–2027.
- Guthold, Martin, Xingshu Zhu, Claudio Rivetti, Guoliang Yang, Neil H. Thomson, Sandor Kasas, Helen G. Hansma, Bettye Smith, Paul K. Hansma and Carlos Bustamante. 1999. “Direct Observation of One-Dimensional Diffusion and Transcription by *Escherichia coli* {RNA} Polymerase.” *Biophysical Journal* 77(4):2284 – 2294.
- Hecht, Anne Marie and Erik Geissler. 1978. “Dynamic Light-Scattering from Polyacrylamide-Water Gels.” *Journal de Physique* 39:631–638.

- Hilt, J.Zachary and Mark E. Byrne. 2004. "Configurational biomimesis in drug delivery: molecular imprinting of biologically significant molecules." *Advanced Drug Delivery Reviews* 56(11):1599 – 1620.
- Hirokawa, Yoshitsugu and Toyochi Tanaka. 1984. "Volume phase transition in a nonionic gel." *The Journal of Chemical Physics* 81(12):6379–6380.
- Hirotsu, Shunsuke, Yoshitsugu Hirokawa and Toyochi Tanaka. 1987. "Volume phase transitions of ionized Nisopropylacrylamide gels." *The Journal of Chemical Physics* 87(2):1392–1395.
- Horkay, Ferenc, Anne-Marie Hecht and Erik Geissler. 1994. "Small Angle Neutron Scattering in Poly(vinyl alcohol) Hydrogels." *Macromolecules* 27(7):1795–1798.
- Horkay, Ferenc, Anne-Marie Hecht, Isabelle Grillo, Peter J. Basser and Erik Geissler. 2002. "Experimental evidence for two thermodynamic length scales in neutralized polyacrylate gels." *The Journal of Chemical Physics* 117(20):9103–9106.
- Horkay, Ferenc, Peter J. Basser, Anne-Marie Hecht and Erik Geissler. 2003. "Calcium induced volume transition in polyelectrolyte gels." *Macromolecular Symposia* 200(1):21–30.
- Johnson, E.M., D.A. Berk, R.K. Jain and W.M. Deen. 1995. "Diffusion and partitioning of proteins in charged agarose gels." *Biophysical Journal* 68(4):1561 – 1568.
- Johnson, E.M., D.A. Berk, R.K. Jain and W.M. Deen. 1996. "Hindered diffusion in agarose gels: test of effective medium model." *Biophysical Journal* 70(2):1017 – 1023.
- Joosten, Jacques G. H., Jennifer L. McCarthy and Peter N. Pusey. 1991. "Dynamic and Static Light-Scattering by Aqueous Polyacrylamide Gels." *Macromolecules* 24(25):6690–6699.
- Katayama, Seiji, Yoshitsugu Hirokawa and Toyochi Tanaka. 1984. "Reentrant phase transition in acrylamide-derivative copolymer gels." *Macromolecules* 17(12):2641–2643.
- Kizilay, Mine Yener and Oguz Okay. 2003. "Effect of hydrolysis on spatial inhomogeneity in poly(acrylamide) gels of various crosslink densities." *Polymer* 44(18):5239 – 5250.
- Lee, Kuen Yong, and David J. Mooney. 2001. "Hydrogels for Tissue Engineering." *Chemical Reviews* 101(7):1869–1880.
- Liu, Ruigang, Xia Gao, Jrg Adams, and Wilhelm Oppermann. 2005. "A Fluorescence Correlation Spectroscopy Study on the Self-Diffusion of Polystyrene Chains in Dilute and Semidilute Solution." *Macromolecules* 38(21):8845–8849.

- Lodge, T.P. and N.A. Rotstein. 1991. "Tracer diffusion of linear and star polymers in entangled solutions and gels." *Journal of Non-Crystalline Solids* 131133, Part 2:671 – 675. Proceedings of the International Discussion Meetings on Relaxations in Complex Systems.
- Luby-Phelps, Katherine. 1994. "Physical properties of cytoplasm." *Current Opinion in Cell Biology* 6(1):3 – 9.
- Luby-Phelps, Katherine, P. E. Castle, Taylor D. and Lanni F. 1987. "Hindered diffusion of inert tracer particles in the cytoplasm of mouse 3T3 cells." *Proceedings of the National Academy of Sciences* 84(14):49104913.
- Luby-Phelps, Katherine, Taylor D. and Lanni F. 1986. "Probing the structure of cytoplasm." *Current Opinion in Cell Biology* 102(6):2015–2022.
- Magde, Douglas, Watt W. Webb and Elliot L. Elson. 1978. "Fluorescence correlation spectroscopy. III. Uniform translation and laminar flow." *Biopolymers* 17(2):361–376.
- Marsh, Brad J., David N. Mastronarde, Karolyn F. Buttle, Kathryn E. Howell and J. Richard McIntosh. 2001. "Organellar relationships in the Golgi region of the pancreatic beta cell line, HIT-T15, visualized by high resolution electron tomography." *Proceedings of the National Academy of Sciences* 98(5):2399–2406.
- Masaro, L and X.X Zhu. 1999. "Physical models of diffusion for polymer solutions, gels and solids." *Progress in Polymer Science* 24(5):731 – 775.
- McCoy, J. L. and M. Muthukumar. 2010. "Dynamic light scattering studies of ionic and nonionic polymer gels with continuous and discontinuous volume transitions." *Journal of Polymer Science Part B: Polymer Physics* 48(21):2193–2206.
- Michelman-Ribeiro, Ariel, Ferenc Horkay, Ralph Nossal and Hacne Boukari. 2007. "Probe Diffusion in Aqueous Poly(vinyl alcohol) Solutions Studied by Fluorescence Correlation Spectroscopy." *Biomacromolecules* 8(5):1595–1600.
- Michelman-Ribeiro, Ariel, Hacne Boukari, Ralph Nossal, and Ferenc Horkay. 2004. "Structural Changes in Polymer Gels Probed by Fluorescence Correlation Spectroscopy." *Macromolecules* 37(26):10212–10214.
- Modesti, Giorgio, Boris Zimmermann, Michael Borsch, Andreas Herrmann and Kay Saalwachter. 2009. "Diffusion in Model Networks as Studied by NMR and Fluorescence Correlation Spectroscopy." *Macromolecules* 42(13):4681–4689.
- Munch, J. P., P. Lermarechal, S. Candau and J. Herz. 1977. "Light scattering gels." *Journal de Physique* 38:1499.
- Muthukumar, M. 1997. "Dynamics of polyelectrolyte solutions." *Journal of Chemical Physics* 107:2619.

- Muthukumar, M. 2011. *Polymer Translocation*. Taylor & Francis.
- Muthukumar, M. and A. Baumgaertner. 1989. "Effects of entropic barriers on polymer dynamics." *Macromolecules* 22(4):1937–1941.
- Nemoto, Norio, Masahiro Kishine, Tadashi Inoue and Kunihiro Osaki. 1991. "Self-diffusion and viscoelasticity of linear polystyrene in entangled solutions." *Macromolecules* 24(7):1648–1654.
- Nemoto, Norio, Takaharu Kojima, Tadashi Inoue, Masahiro Kishine, Taisei Hirayama and Michio Kurata. 1989. "Self diffusion of polymers in the concentrated regime. Part 2. Self diffusion and tracer-diffusion coefficient and viscosity of concentrated solutions of linear polystyrenes in dibutyl phthalate." *Macromolecules* 22(9):3793–3798.
- Norisuye, Tomohisa, , Qui Tran-Cong-Miyata and Mitsuhiko Shibayama. 2004. "Dynamic Inhomogeneities in Polymer Gels Investigated by Dynamic Light Scattering." *Macromolecules* 37(8):2944–2953.
- Ogston, A. G., B. N. Preston and J. D. Wells. 1973. "On the Transport of Compact Particles Through Solutions of Chain-Polymers." *Proceedings of the Royal Society of London A: Mathematical, Physical and Engineering Sciences* 333(1594):297–316.
- Ohmine, Iwao and Toyochi Tanaka. 1982. "Salt effects on the phase transition of ionic gels." *The Journal of Chemical Physics* 77(11):5725–5729.
- Pajevic, Sinisa, Rama Bansil and Cestmir Konak. 1991. "Diffusion of linear polymer chains in gels." *Journal of Non-Crystalline Solids* 131:630 – 634.
- Pajevic, Sinisa, Rama Bansil and Cestmir Konak. 1993. "Diffusion of linear polymer chains in methyl methacrylate gels." *Macromolecules* 26(2):305–312.
- Papadakis, ChristineM., Peter Koovan, Walter Richtering and Dominik Woll. 2014. "Polymers in focus: fluorescence correlation spectroscopy." *Colloid and Polymer Science* 292(10):2399–2411.
- Pederson, Thoru. 2000. "Diffusional protein transport within the nucleus: a message in the medium." *Nature Cell Biology* 2:E73 – E74.
- Peppas, N.A., J.Z. Hilt, A. Khademhosseini and R. Langer. 2006. "Hydrogels in Biology and Medicine: From Molecular Principles to Bionanotechnology." *Advanced Materials* 18(11):1345–1360.
- Peppas, N.A., P. Bures, W. Leobandung and H. Ichikawa. 2000. "Hydrogels in pharmaceutical formulations." *European Journal of Pharmaceutics and Biopharmaceutics* 50(1):27 – 46.
- Peppas, N.A., P.J. Hansen and P.A. Buri. 1984. "A theory of molecular diffusion in the intestinal mucus." *International Journal of Pharmaceutics* 20(12):107 – 118.

- Peppas, Nikolaos A. and Jennifer J. Sahlin. 1996. "Hydrogels as mucoadhesive and bioadhesive materials: a review." *Biomaterials* 17(16):1553 – 1561.
- Petit, J.-M., B. Roux, X. X. Zhu and P. M. Macdonald. 1996. "A New Physical Model for the Diffusion of Solvents and Solute Probes in Polymer Solutions." *Macromolecules* 29(18):6031–6036.
- Phillies, George D. J. 1986. "Universal scaling equation for self-diffusion by macromolecules in solution." *Macromolecules* 19(9):2367–2376.
- Pusey, P. N. 1994. "Dynamic Light-Scattering by Non-Ergodic Media." *Macromolecular Symposia* 79:17–30.
- Pusey, Peter N. and W. Van Megen. 1989. "Dynamic light scattering by non-ergodic media." *Physica A* 157:704–741.
- Rausch, Kristin, Anika Reuter, Karl Fischer and Manfred Schmidt. 2010. "Evaluation of Nanoparticle Aggregation in Human Blood Serum." *Biomacromolecules* 11(11):2836–2839.
- Reina, J.C., R. Bansil and C. Konak. 1990. "Dynamics of probe particles in polymer solutions and gels." *Polymer* 31(6):1038 – 1044.
- Ricka, J. and Toyochi Tanaka. 1984. "Swelling of ionic gels: quantitative performance of the Donnan theory." *Macromolecules* 17(12):2916–2921.
- Saxton, M.J. 1994. "Anomalous diffusion due to obstacles: a Monte Carlo study." *Biophysical Journal* 66(2, Part 1):394 – 401.
- Scalettar, Bethe A., John E. Hearst and Melvin P. Klein. 1989. "FRAP and FCS studies of self-diffusion and mutual diffusion in entangled DNA solutions." *Macromolecules* 22(12):4550–4559.
- Schosseler, F., F. Ilmain and S. J. Candau. 1991. "Structure and properties of partially neutralized poly(acrylic acid) gels." *Macromolecules* 24(1):225–234.
- Schwille, P., U. Haupts, S. Maiti and W. Webb. 1999. "Molecular dynamics in living cells observed by fluorescence correlation spectroscopy." *Biophysical Journal* 77:2251 – 2265.
- Sedlak, Marian. 1996. "The ionic strength dependence of the structure and dynamics of polyelectrolyte solutions as seen by light scattering: The slow mode dilemma." *The Journal of Chemical Physics* 105(22):10123–10133.
- Sedlak, Marin. 1999. "What Can Be Seen by Static and Dynamic Light Scattering in Polyelectrolyte Solutions and Mixtures?" *Langmuir* 15(12):4045–4051.
- Sedlak, Marin and Eric J. Amis. 1992. "Concentration and molecular weight regime diagram of saltfree polyelectrolyte solutions as studied by light scattering." *The Journal of Chemical Physics* 96(1):826–834.

- Seksek, Olivier, Joachim Biwersi and A.S. Verkman. 1997. "Translational Diffusion of Macromolecule-sized Solutes in Cytoplasm and Nucleus." *The Journal of Cell Biology* 138(1):131–142.
- Shibayama, Mitsuhiro, , Yoshinori Isaka and Yasuhiro Shiwa. 1999. "Dynamics of Probe Particles in Polymer Solutions and Gels." *Macromolecules* 32(21):7086–7092.
- Shibayama, Mitsuhiro, Fumiyoshi Ikkai, Satoshi Inamoto, Shunji Nomura and Charles C. Han. 1996. "pH and salt concentration dependence of the microstructure of poly(Nisopropylacrylamidecoacrylic acid) gels." *The Journal of Chemical Physics* 105(10):4358–4366.
- Shibayama, Mitsuhiro and Toyochi Tanaka. 1995. "Smallangle neutron scattering study on weakly charged poly(Nisopropyl acrylamidecoacrylic acid) copolymer solutions." *The Journal of Chemical Physics* 102(23):9392–9400.
- Shibayama, Mitsuhiro, Yasuhiro Shirotani and Yasuhiro Shiwa. 2000. "Static inhomogeneities and dynamics of swollen and reactor-batch polymer gels." *The Journal of Chemical Physics* 112(1):442–449.
- Skouri, R., F. Schosseler, J. P. Munch and S. J. Candau. 1995. "Swelling and Elastic Properties of Polyelectrolyte Gels." *Macromolecules* 28(1):197–210.
- Slater, Gary W. and Song Yan Wu. 1995. "Reptation, Entropic Trapping, Percolation, and Rouse Dynamics of Polymers in "Random" Environments." *Physical Review Letters* 75:164–167.
- Smisek, David L. and David A. Hoagland. 1989. "Agarose gel electrophoresis of high molecular weight, synthetic polyelectrolytes." *Macromolecules* 22(5):2270–2277.
- Sohn, Daewon, Paul S. Russo, Alfonso Dvila, Drew S. Poche and Mark L. McLaughlin. 1996. "Light Scattering Study of Magnetic Latex Particles and Their Interaction with Polyelectrolytes." *Journal of Colloid and Interface Science* 177(1):31 – 44.
- Takebe, Tomoaki, Kazunari Nawa, Shoji Suehiro and Takeji Hashimoto. 1989. "Quasielastic light scattering studies of swollen and stretched polymer gels." *The Journal of Chemical Physics* 91(7):4360–4368.
- Tanaka, T. 1981. "Gels." *Scientific American* 244(1):124.
- Tanaka, Toyochi. 1978. "Collapse of Gels and the Critical Endpoint." *Physical Review Letters* 40:820–823.
- Tanaka, Toyochi, David Fillmore, Shao-Tang Sun, Izumi Nishio, Gerald Swislow and Arati Shah. 1980. "Phase Transitions in Ionic Gels." *Physical Review Letters* 45:1636–1639.
- Tanaka, Toyochi, Lon O. Hocker and George B. Benedek. 1973. "Spectrum of light scattered from a viscoelastic gel." *The Journal of Chemical Physics* 59(9):5151–5159.

- Thiel, J. and G. Maurer. 1999. "Swelling equilibrium of poly(acrylamide) gels in aqueous salt and polymer solutions." *Fluid Phase Equilibria* 165(2):225–260.
- Thompson, Nancy L, Alena M Lieto and Noah W Allen. 2002. "Recent advances in fluorescence correlation spectroscopy." *Current Opinion in Structural Biology* 12(5):634 – 641.
- Tokuhiro, Tadashi, Takayuki Amiya, Akira Mamada and Toyochi Tanaka. 1991. "NMR study of poly(N-isopropylacrylamide) gels near phase transition." *Macromolecules* 24(10):2936–2943.
- Weiss, Matthias, Hitoshi Hashimoto and Tommy Nilsson. 2003. "Anomalous Protein Diffusion in Living Cells as Seen by Fluorescence Correlation Spectroscopy." *Biophysical Journal* 84(6):4043 – 4052.
- Wheeler, L. M. and T. P. Lodge. 1989. "Tracer diffusion of linear polystyrenes in dilute, semidilute, and concentrated poly(vinyl methyl ether) solutions." *Macromolecules* 22(8):3399–3408.
- Woll, Dominik. 2014. "Fluorescence correlation spectroscopy in polymer science." *RSC Advances* 4:2447–2465.
- Yazici, Ilknur and Oguz Okay. 2005. "Spatial inhomogeneity in poly(acrylic acid) hydrogels." *Polymer* 46(8):2595 – 2602.
- Yue, Zhao and Wu Chi. 2004. "A hybrid polymer gel and its static nonergodicity." *Macromolecular Symposia* 207(1):37–46.
- Zettl, Heiko, Wolfgang Hafner, Alexander Bker, Holger Schmalz, Michael Lanzendrer, Axel H. E. Muller and Georg Krausch. 2004. "Fluorescence Correlation Spectroscopy of Single Dye-Labeled Polymers in Organic Solvents." *Macromolecules* 37(5):1917–1920.
- Zettl, Ute, Matthias Ballauff and Ludger Harnau. 2010. "A fluorescence correlation spectroscopy study of macromolecular tracer diffusion in polymer solutions." *Journal of Physics: Condensed Matter* 22(49):494111.
- Zettl, Ute, Sebastian T. Hoffmann, Felix Koberling, Georg Krausch, Jrg Enderlein, Ludger Harnau and Matthias Ballauff. 2009. "Self-Diffusion and Cooperative Diffusion in Semidilute Polymer Solutions As Measured by Fluorescence Correlation Spectroscopy." *Macromolecules* 42(24):9537–9547.
- Zustiak, Silviya P., Hacene Boukari and Jennie B. Leach. 2010. "Solute diffusion and interactions in cross-linked poly(ethylene glycol) hydrogels studied by Fluorescence Correlation Spectroscopy." *Soft Matter* 6:3609–3618.
- Zustiak, Silviya P., Ralph Nossal and Dan L. Sackett. 2011. "Hindered Diffusion in Polymeric Solutions Studied by Fluorescence Correlation Spectroscopy." *Biophysical Journal* 101(1):255 – 264.